

博士學位論文

**Synthesis and Characterization of Chromium(III),
Nickel(II), and Copper(II) Complexes with Aza- or
Oxaaza-macrocyclic Ligands**



**Department of Chemistry
Graduate School
Cheju National University**

Woo-Hwan Lee

December, 2005

**Aza- 또는 Oxaaza-거대고리 리간드의 크롬(Ⅲ),
니켈(Ⅱ), 구리(Ⅱ) 착물들의 합성 및 물성 연구**

지도교수 : 변 중 철

이 우 환

이 논문을 이학 박사학위 논문으로 제출함.

2005년 12월

이우환의 이학 박사학위 논문을 인준함.

심사위원장 _____
위 원 _____
위 원 _____
위 원 _____
위 원 _____

제주대학교 대학원

2005년 12월

Synthesis and Characterization of Chromium(III), Nickel(II), and Copper(II) Complexes with Aza- or Oxaaza-macrocyclic Ligands

Woo-Hwan Lee

(Supervised by professor Jong-Chul Byun)

A thesis submitted in partial fulfillment of the requirement for the degree
of Doctor of Science.

2005. 12. .

This thesis has been examined and approved.

Date Approved :



Department of Chemistry
Graduate School
Cheju National University

Contents

List of Tables	iv
List of Figures and Schemes	viii
Abstract	xi
I. Introduction	1
II. Experimental section	8
1. Chemicals and Physical Measurements	8
2. Synthesis of Ligand and Complexes	9
1) Cr(III)-tetraaza 14-membered macrocyclic complexes	9
(1) Preparation of <i>cis</i> -[Cr([14]-decane)(<i>o</i> -OOCC ₆ H ₄ OH) ₂]ClO ₄	10
(2) Preparation of the <i>cis</i> -[Cr([14]-decane)(<i>p</i> -OC ₆ H ₄ NO ₂)(OH)]ClO ₄ ·H ₂ O ..	10
2) Binuclear Cu(II)-dioxatetraaza 20-membered macrocyclic complexes	11
(1) Preparation of 2,6-diformyl- <i>p</i> -cresol.	11
(2) Preparation of [Cu ₂ ([20]-DCHDC)Cl ₂] · H ₂ O.	11
(3) [Cu ₂ ([20]-DCHDC)(O ₂ N) ₂] · 6H ₂ O.	13
3) Binuclear Ni(II)-tetraazadioxa 22-membered macrocyclic complexes	13
(1) Preparation of [H ₄ [22]-HMTADO](ClO ₄) ₂ macrocyclic ligand	14
(2) Preparation of [H ₄ [22]-HMTADO](NO ₃) ₂ · H ₂ O crystals	14
(3) Preparation of [Ni ₂ ([22]-HMTADO)(OH ₂) ₂]Cl ₂ · H ₂ O.	16
(4) Preparation of [Ni ₂ ([22]-HMTADO)(μ -O ₂ N)(NO ₂)(OH ₂)].	16
(5) Preparation of [Ni ₂ ([22]-HMTADO)(CN) ₂] · 0.5H ₂ O.	17
3. X-ray Diffraction Measurements	18

1) Cr(III)-tetraaza 14-membered macrocyclic complexes	18
(1) <i>cis</i> -[Cr([14]-decane)(<i>o</i> -OOC ₆ H ₄ OH) ₂]ClO ₄	18
(2) <i>cis</i> -[Cr([14]-decane)(<i>p</i> -OC ₆ H ₄ NO ₂)(OH)]ClO ₄ ·H ₂ O	26
2) Binuclear Cu(II)-tetraazadioxa 20-membered macrocyclic complex	34
(1) [Cu ₂ ([20]-DCHDC)(O ₂ N) ₂] · 6H ₂ O.	34
3) Binuclear Ni(II)-tetraazadioxa 22-membered macrocyclic complexes	39
(1) [H ₄ [22]-HMTADO](NO ₃) ₂ · H ₂ O	39
(2) [Ni ₂ ([22]-HMTADO)(μ -O ₂ N)(NO ₂)(OH ₂)]	47
(3) {[Ni ₆ ([22]-HMTADO) ₃ (CN) ₄][Ni(CN) ₄]·5H ₂ O·8CH ₃ OH} _{<i>n</i>}	55
III. Results and Discussion	65
1. Description of structure and physicochemical properties of Cr(III) -tetraaza 14-membered macrocyclic complexes	65
1) Properties of <i>cis</i> -[Cr([14]-decane)(OH) ₂] ⁺ solution.	65
2) Structure and physicochemical properties of <i>cis</i> -[Cr([14]-decane)(<i>o</i> - OOC ₆ H ₄ OH) ₂]ClO ₄ (I)	68
3) Structure and physicochemical properties of <i>cis</i> -[Cr([14]-decane)(<i>p</i> - OC ₆ H ₄ NO ₂)(OH)]ClO ₄ ·H ₂ O (II)	81
2. Description of structure and physicochemical properties of Cu(II) -dioxatetraaza 20-membered macrocyclic complex	94
1) Structure and physicochemical properties of [Cu ₂ ([20]-DCHDC)(O ₂ N) ₂] · 6H ₂ O (III)	94
3. Description of structure and physicochemical properties of Ni(II)-tetraazadioxa 22-membered macrocyclic complexes	110
1) Structure and physicochemical properties of [H ₄ [22]-HMTADO](NO ₃) ₂ · H ₂ O (IV)	110

2) Structure and physicochemical properties of $[\text{Ni}_2([\text{22}]\text{-HMTADO})(\mu\text{-O}_2\text{N})(\text{NO}_2)(\text{OH}_2)]$ (V)	118
3) Structure and physicochemical properties of $\{[\text{Ni}_6([\text{22}]\text{-HMTADO})_3(\text{CN})_4][\text{Ni}(\text{CN})_4] \cdot 5\text{H}_2\text{O} \cdot 8\text{CH}_3\text{OH}\}_n$ (VI)	134
IV. Conclusion	148
References	157

Abstract(Korean)

Acknowledgment(Korean)



List of Tables

Table 1. Crystal data and structure refinement for <i>cis</i> -[Cr([14]-decane)(<i>o</i> -OOC ₆ H ₄ OH) ₂]-ClO ₄ complex	19
Table 2. Atomic coordinates ($\text{\AA} \times 10^4$) and equivalent isotropic displacement parameters ($\text{\AA}^2 \times 10^3$) for <i>cis</i> -[Cr([14]-decane)(<i>o</i> -OOC ₆ H ₄ OH) ₂]ClO ₄ complex	20
Table 3. Anisotropic displacement parameters ($\text{\AA}^2 \times 10^3$) for <i>cis</i> -[Cr([14]-decane)(<i>o</i> -OOC ₆ H ₄ OH) ₂]ClO ₄ complex	22
Table 4. Hydrogen coordinates ($\text{\AA} \times 10^4$) and isotropic displacement parameters ($\text{\AA}^2 \times 10^3$) for <i>cis</i> -[Cr([14]-decane)(<i>o</i> -OOC ₆ H ₄ OH) ₂]ClO ₄ complex	24
Table 5. Crystal data and structure refinement for <i>cis</i> -[Cr([14]-decane)(<i>p</i> -OC ₆ H ₄ NO ₂)(OH)]ClO ₄ ·H ₂ O complex	27
Table 6. Atomic coordinates ($\text{\AA} \times 10^4$) and equivalent isotropic displacement parameters ($\text{\AA}^2 \times 10^3$) for <i>cis</i> -[Cr([14]-decane)(<i>p</i> -OC ₆ H ₄ NO ₂)(OH)]ClO ₄ ·H ₂ O complex	28
Table 7. Anisotropic displacement parameters ($\text{\AA}^2 \times 10^3$) for <i>cis</i> -[Cr([14]-decane)(<i>p</i> -OC ₆ H ₄ NO ₂)(OH)]ClO ₄ ·H ₂ O complex	30
Table 8. Hydrogen coordinates ($\text{\AA} \times 10^4$) and isotropic displacement parameters ($\text{\AA}^2 \times 10^3$) for <i>cis</i> -[Cr([14]-decane)(<i>p</i> -OC ₆ H ₄ NO ₂)(OH)]ClO ₄ ·H ₂ O complex	32
Table 9. Crystal data and structure refinement for [Cu ₂ ([20]-DCHDC)(O ₂ N) ₂]·6H ₂ O complex	35

Table 10. Atomic coordinates ($\text{\AA} \times 10^4$) and equivalent isotropic displacement parameters ($\text{\AA}^2 \times 10^3$) for $[\text{Cu}_2([\text{20}]\text{-DCHDC})(\text{O}_2\text{N})_2] \cdot 6\text{H}_2\text{O}$ complex	36
Table 11. Anisotropic displacement parameters ($\text{\AA}^2 \times 10^3$) for $[\text{Cu}_2([\text{20}]\text{-DCHDC})(\text{O}_2\text{N})_2] \cdot 6\text{H}_2\text{O}$ complex	37
Table 12. Hydrogen coordinates ($\text{\AA} \times 10^4$) and isotropic displacement parameters ($\text{\AA}^2 \times 10^3$) for $[\text{Cu}_2([\text{20}]\text{-DCHDC})(\text{O}_2\text{N})_2] \cdot 6\text{H}_2\text{O}$ complex	38
Table 13. Crystal data and structure refinement for $[\text{H}_4[\text{22}]\text{-HMTADO}](\text{NO}_3)_2 \cdot \text{H}_2\text{O}$	40
Table 14. Atomic coordinates ($\text{\AA} \times 10^4$) and equivalent isotropic displacement parameters ($\text{\AA}^2 \times 10^3$) for $[\text{H}_4[\text{22}]\text{-HMTADO}](\text{NO}_3)_2 \cdot \text{H}_2\text{O}$	41
Table 15. Anisotropic displacement parameters ($\text{\AA}^2 \times 10^3$) for $[\text{H}_4[\text{22}]\text{-HMTADO}](\text{NO}_3)_2 \cdot \text{H}_2\text{O}$	43
Table 16. Hydrogen coordinates ($\text{\AA} \times 10^4$) and isotropic displacement parameters ($\text{\AA}^2 \times 10^3$) for $[\text{H}_4[\text{22}]\text{-HMTADO}](\text{NO}_3)_2 \cdot \text{H}_2\text{O}$	45
Table 17. Crystal data and structure refinement for $[\text{Ni}_2([\text{22}]\text{-HMTADO})(\mu\text{-O}_2\text{N})(\text{NO}_2)(\text{OH}_2)]$	48
Table 18. Atomic coordinates ($\text{\AA} \times 10^4$) and equivalent isotropic displacement parameters ($\text{\AA}^2 \times 10^3$) for $[\text{Ni}_2([\text{22}]\text{-HMTADO})(\mu\text{-O}_2\text{N})(\text{NO}_2)(\text{OH}_2)]$	49
Table 19. Anisotropic displacement parameters ($\text{\AA}^2 \times 10^3$) for $[\text{Ni}_2([\text{22}]\text{-HMTADO})(\mu\text{-O}_2\text{N})(\text{NO}_2)(\text{OH}_2)]$	51
Table 20. Hydrogen coordinates ($\text{\AA} \times 10^4$) and isotropic displacement parameters ($\text{\AA}^2 \times 10^3$) for $[\text{Ni}_2([\text{22}]\text{-HMTADO})(\mu\text{-O}_2\text{N})(\text{NO}_2)(\text{OH}_2)]$	53
Table 21. Crystal data and structure refinement for $\{[\text{Ni}_6([\text{22}]\text{-HMTADO})_3(\text{CN})_4]$	


-[Ni(CN) ₄]·5H ₂ O· 8CH ₃ OH} _n	56
Table 22. Atomic coordinates (Å×10 ⁴) and equivalent isotropic displacement parameters (Å ² ×10 ³) for {[Ni ₆ ([22]-HMTADO) ₃ (CN) ₄][Ni(CN) ₄]·5H ₂ O·8CH ₃ OH} _n	57
Table 23. Anisotropic displacement parameters (Å ² ×10 ³) for {[Ni ₆ ([22]-HMTADO) ₃ (CN) ₄][Ni(CN) ₄]·5H ₂ O· 8CH ₃ OH} _n	60
Table 24. Hydrogen coordinates (Å×10 ⁴) and isotropic displacement parameters (Å ² ×10 ³) for {[Ni ₆ ([22]-HMTADO) ₃ (CN) ₄][Ni(CN) ₄]·5H ₂ O·8CH ₃ OH} _n	63
Table 25. Electronic transition spectral data of <i>cis</i> -[Cr([14]-decane){O-(<i>o</i> -OOC ₆ H ₄ OH)} ₂] ⁺ , <i>cis</i> -[Cr([14]-decane){O-(<i>p</i> -OC ₆ H ₄ NO ₂)}(OH)] ⁺ , and related Cr(III) complexes	67
Table 26. Bond lengths (Å) for <i>cis</i> -[Cr([14]-decane)(<i>o</i> -OOC ₆ H ₄ OH) ₂]ClO ₄ (I) complex	73
Table 27. Angles (°) for <i>cis</i> -[Cr([14]-decane)(<i>o</i> -OOC ₆ H ₄ OH) ₂]ClO ₄ (I) complex	74
Table 28. Selected bond lengths (Å) and Selected bond angles(°) for hydrogen bond of <i>cis</i> -[Cr([14]-decane)(<i>o</i> -OOC ₆ H ₄ OH) ₂]ClO ₄ (I) complex ...	75
Table 29. Bond lengths (Å) for <i>cis</i> -[Cr([14]-decane)(<i>p</i> -OC ₆ H ₄ NO ₂)(OH)]ClO ₄ ·H ₂ O (II) complex	86
Table 30. Angles (°) for <i>cis</i> -[Cr([14]-decane)(<i>p</i> -OC ₆ H ₄ NO ₂)(OH)]ClO ₄ ·H ₂ O (II) complex	87
Table 31. Selected bond lengths (Å) and Selected bond angles(°) for hydrogen bond of <i>cis</i> -[Cr([14]-decane)(<i>p</i> -OC ₆ H ₄ NO ₂)(OH)]ClO ₄ ·H ₂ O (II) complex	88

Table 32. Bond lengths (Å) for $[\text{Cu}_2([\text{20}]\text{-DCHDC})(\text{O}_2\text{N})_2] \cdot 6\text{H}_2\text{O}$	100
Table 33. Angles [°] for $[\text{Cu}_2([\text{20}]\text{-DCHDC})(\text{O}_2\text{N})_2] \cdot 6\text{H}_2\text{O}$	101
Table 34. Selected bond lengths (Å) and Selected bond angles(°) for hydrogen bond of $[\text{Cu}_2([\text{20}]\text{-DCHDC})(\text{O}_2\text{N})_2] \cdot 6\text{H}_2\text{O}$ complex	102
Table 35. Bond lengths (Å) for $[\text{H}_4[\text{22}]\text{-HMTADO}](\text{NO}_3)_2 \cdot \text{H}_2\text{O}$ (IV)	115
Table 36. Angles [°] for $[\text{H}_4[\text{22}]\text{-HMTADO}](\text{NO}_3)_2 \cdot \text{H}_2\text{O}$ (IV)	116
Table 37. Selected bond lengths (Å) and Selected bond angles(°) for hydrogen bond of $[\text{H}_4[\text{22}]\text{-HMTADO}](\text{NO}_3)_2 \cdot \text{H}_2\text{O}$ (IV) complex	117
Table 38. Bond lengths (Å) for $[\text{Ni}_2([\text{22}]\text{-HMTADO})(\mu\text{-O}_2\text{N})(\text{NO}_2)(\text{OH}_2)] \cdot 12\text{H}_2\text{O}$	124
Table 39. Angles [°] for $[\text{Ni}_2([\text{22}]\text{-HMTADO})(\mu\text{-O}_2\text{N})(\text{NO}_2)(\text{OH}_2)] \cdot 12\text{H}_2\text{O}$	125
Table 40. Selected bond lengths (Å) and Selected bond angles(°) for hydrogen bond of $[\text{Ni}_2([\text{22}]\text{-HMTADO})(\mu\text{-O}_2\text{N})(\text{NO}_2)(\text{OH}_2)] \cdot 12\text{H}_2\text{O}$ complex	127
Table 41. Bond lengths (Å) for $\{[\text{Ni}_6([\text{22}]\text{-HMTADO})_3(\text{CN})_4][\text{Ni}(\text{CN})_4] \cdot 5\text{H}_2\text{O} \cdot 8\text{CH}_3\text{OH}\}_n$	143
Table 42. Angles [°] for $\{[\text{Ni}_6([\text{22}]\text{-HMTADO})_3(\text{CN})_4][\text{Ni}(\text{CN})_4] \cdot 5\text{H}_2\text{O} \cdot 8\text{CH}_3\text{OH}\}_n$	145

List of Figures and Schemes

Figure 1. An ORTEP view of core structure (top view) for the <i>cis</i> -[Cr([14]-decane)(<i>o</i> -OOCC ₆ H ₄ OH) ₂]ClO ₄ (I) complex showing 40% probability thermal ellipsoids and labels for non-H atoms.	69
Figure 2. The molecular packing diagram and hydrogen-bonding scheme of the <i>cis</i> -[Cr([14]-decane)(<i>o</i> -OOCC ₆ H ₄ OH) ₂]ClO ₄ (I) complex.	72
Figure 3. The electronic absorption spectrum of 2.0×10^{-3} M <i>cis</i> -[Cr([14]-decane)(<i>o</i> -OOCC ₆ H ₄ OH) ₂] ⁺ in DMF solution at 298 K.	77
Figure 4. IR spectrum of <i>cis</i> -[Cr([14]-decane)(<i>o</i> -OOCC ₆ H ₄ OH) ₂]ClO ₄ complex. ...	79
Figure 5. The FAB mass spectrum of the <i>cis</i> -[Cr([14]-decane)(<i>o</i> -OOCC ₆ H ₄ OH) ₂]ClO ₄	80
Figure 6. An ORTEP view of core structure (top view) for the <i>cis</i> -[Cr([14]-decane)(<i>p</i> -OC ₆ H ₄ NO ₂)(OH)]ClO ₄ ·H ₂ O (II) complex showing 40% probability thermal ellipsoids and labels for non-H atoms.	82
Figure 7. The molecular packing diagram and hydrogen-bonding scheme of the <i>cis</i> -[Cr([14]-decane)(<i>p</i> -OC ₆ H ₄ NO ₂)(OH)]ClO ₄ ·H ₂ O (II) complex.	85
Figure 8. The electronic absorption spectrum of 2.0×10^{-3} M <i>cis</i> -[Cr([14]-decane)(<i>p</i> -OC ₆ H ₄ NO ₂)(OH)] ⁺ in DMF solution at 298 K.	90
Figure 9. IR spectrum of <i>cis</i> -[Cr([14]-decane)(<i>p</i> -OC ₆ H ₄ NO ₂)(OH)]ClO ₄ ·H ₂ O (II) complex.	92
Figure 10. The FAB mass spectrum of the <i>cis</i> -[Cr([14]-decane)(<i>p</i> -OC ₆ H ₄ NO ₂)(OH)]ClO ₄ ·H ₂ O.	93

Figure 11. Structural representation of asymmetric unit of $[\text{Cu}_2([\text{20}]\text{-DCHDC})\text{-(O}_2\text{N)}_2] \cdot 6\text{H}_2\text{O}$ complex.	94
Figure 12. An ORTEP view of core structure (top view) for the $[\text{Cu}_2([\text{20}]\text{-DCHDC})(\text{O}_2\text{N})_2] \cdot 6\text{H}_2\text{O}$ complex showing 50% probability thermal ellipsoids and labels for non-H atoms.	95
Figure 13. The molecular packing diagram and hydrogen bonding scheme of $[\text{Cu}_2([\text{20}]\text{-DCHDC})(\text{O}_2\text{N})_2] \cdot 6\text{H}_2\text{O}$	98-99
Figure 14. Electronic absorption spectrum of $[\text{Cu}_2([\text{20}]\text{-DCHDC})(\text{O}_2\text{N})_2] \cdot 6\text{H}_2\text{O}$ in methanol ($2.5 \times 10^{-3}\text{M}$).	104
Figure 15. FT-IR spectrum of $[\text{Cu}_2([\text{20}]\text{-DCHDC})(\text{O}_2\text{N})_2] \cdot 6\text{H}_2\text{O}$ complex.	107
Figure 16. FAB mass spectrum of the $[\text{Cu}_2([\text{20}]\text{-DCHDC})(\text{O}_2\text{N})_2] \cdot 6\text{H}_2\text{O}$. ..	109
Figure 17. An ORTEP view of core structure (top view) for the $[\text{H}_4[\text{22}]\text{-HMTADO}](\text{NO}_3)_2 \cdot \text{H}_2\text{O}$ (IV) complex showing 50% probability thermal ellipsoids and labels for non-H atoms.	110-111
Figure 18. The molecular packing diagram and hydrogen bonding scheme of $[\text{H}_4[\text{22}]\text{-HMTADO}](\text{NO}_3)_2 \cdot \text{H}_2\text{O}$ (IV).	114
Figure 19. An ORTEP view of core structure (top view) for the $[\text{Ni}_2([\text{22}]\text{-HMTADO})(\mu\text{-O}_2\text{N})(\text{NO}_2)(\text{OH}_2)]$ complex showing 50% probability thermal ellipsoids and labels for non-H atoms.	119
Figure 20. The molecular packing diagram and hydrogen bonding scheme of $[\text{Ni}_2([\text{22}]\text{-HMTADO})(\mu\text{-O}_2\text{N})(\text{NO}_2)(\text{OH}_2)]$	123
Figure 21. Electronic absorption spectrum of $[\text{Ni}_2([\text{22}]\text{-HMTADO})(\mu\text{-O}_2\text{N})(\text{NO}_2)\text{-(OH}_2)]$ in methanol ($5.0 \times 10^{-3}\text{M}$).	128
Figure 22. FT-IR spectrum of $[\text{Ni}_2([\text{22}]\text{-HMTADO})(\mu\text{-O}_2\text{N})(\text{NO}_2)(\text{OH}_2)]$ complex.	

.....	131
Figure 23. FAB mass spectrum of the $[\text{Ni}_2([\text{22}]\text{-HMTADO})(\mu\text{-O}_2\text{N})(\text{NO}_2)\text{-}(\text{OH}_2)]$	133
Figure 24. Structural representation of asymmetric unit of $\{[\text{Ni}_6([\text{22}]\text{-HMTADO})_3(\text{CN})_4][\text{Ni}(\text{CN})_4]\cdot 5\text{H}_2\text{O}\cdot 8\text{CH}_3\text{OH}\}_n$ (VI) complex.	135
Figure 25. An ORTEP view of core structure (top view) for the $[\text{Ni}_6([\text{22}]\text{-HMTADO})_3(\text{CN})_4][\text{Ni}(\text{CN})_4]$ unit showing 50% probability thermal ellipsoids and labels for non-H atoms.	136
Figure 26. 1D chain structure for $[\text{Ni}_6([\text{22}]\text{-HMTADO})_3(\text{CN})_4]_n$ cation.	137
Figure 27. The graph of the independent part of $\{[\text{Ni}_6([\text{22}]\text{-HMTADO})_3(\text{CN})_4]\text{-}[\text{Ni}(\text{CN})_4]\cdot 5\text{H}_2\text{O}\cdot 8\text{CH}_3\text{OH}\}_n$	142
	
Scheme 1. Synthesis of the Cr(III)-salicylato and <i>p</i> -nitrophenolato tetraaza 14-membered macrocyclic complexes.	9
Scheme 2. Synthesis of the Cu(II)-nitro tetraazadioxa 20-membered macrocyclic complexes.	12
Scheme 3. Synthesis of the Ni(II)-cyano and -nitro tetraazadioxa 22-membered macrocyclic complexes.	15

Abstract

We prepare and isolate (1) Cr(III)-tetraaza 14-membered macrocyclic complexes; *cis*-[Cr([14]-decane)(*o*-OOCC₆H₄OH)₂]ClO₄(**I**), and *cis*-[Cr([14]-decane)](*p*-OC₆H₄NO₂)(OH)]ClO₄·H₂O (**II**), (2) Cu(II)-dioxatetraaza 20-membered macrocyclic complexes; [Cu₂([20]-DCHDC)(O₂N)₂] · 6H₂O (**III**), and (3) Ni(II)-dioxatetraaza 22-membered macrocyclic complexes; [H₄[22]-HMTADO](NO₃)₂ · H₂O (**IV**), [Ni₂([22]-HMTADO)(μ-O₂N)(NO₂)(OH₂)] (**V**), and {[Ni₆(C₂₈H₃₄N₄O₂)₃(CN)₄]-[Ni(CN)₄] · 5H₂O · 8CH₃OH}_{*n*} (**VI**). The crystal structure of (**I**) complex consists of monomeric complex cation of the indicated formula and an uncoordinated perchlorate complex anion. The monomeric cation, [Cr([14]-decane)(*o*-OOCC₆H₄OH)₂]⁺ shows a distorted octahedral environment, where the chromium(III) ion is coordinated by four secondary amines of the macrocycle and the two carboxylate oxygen atoms of the monodentate salicylate ligands in *cis* positions. This configuration is often referred to as the Bosnich type-V stereochemistry. The crystal structure of (**II**) consists of monomeric complex cation of the indicated formula and an uncoordinated perchlorate anion. The monomeric complex cation, [Cr([14]-decane)(*p*-OC₆H₄NO₂)(OH)]⁺ shows a distorted octahedral environment, where the chromium(III) ion is coordinated by four secondary amines of the macrocycle one phenolic oxygen atom of the monodentate *p*-nitrophenolate ligand and one hydroxo oxygen atom in *cis* positions. This configuration is often referred to as the Bosnich type-V stereochemistry. The core structure of binuclear complex(III) is centrosymmetry with each copper(II) ions being six-coordinate with a capped square-pyramidal

geometry concerning with two nitrogen and two oxygen atoms of the binucleating ligand [20]-DCHDC and two oxygen atoms each from the bidentated nitrite ligands at an apical site. The copper ions are displaced by 0.3288 Å from the basal least-squares plane toward nitrite ions. Two nitrite ions attached to two central metal Cu atoms are situated *trans* to each other with respect to the mean molecular plane. The interatomic Cu···Cu separation is 2.9542(8) Å. The crystal structure of this di(hydronitrate) [H₄[22]-HMTADO]·(NO₃)₂·H₂O (**IV**) compound is composed of tetraazadioxa 22-membered macrocycle ([H₄[22]-HMTADO]²⁺), two nitrate ions and one water molecule. Two N₂O₂ sites are vacant, and each azomethine nitrogen atoms is protonated. The tetraazadioxa 22-membered macrocycle ([H₄[22]-HMTADO]²⁺) has C_{2v} symmetry. The dihedral angle between the planes defined by two phenoxide is 16.94(9)°. This means the structure is bent owing to the tetrahedral conformation effect of two dimethyl-propylene at the side. The two dimethyl-propylene moieties are situated eclipsed conformation. In the [H₄[22]-HMTADO]²⁺, two phenoxide planes are shortly. In the green crystals of [Ni₂([22]-HMTADO)(μ-O₂N)(NO₂)(OH₂)] (**V**), the dinegative ([22]-HMTADO)²⁻ accommodates two Ni(II) ions in its N₄O₂ sites in the Ni(1)···Ni(2) separation of 3.013 Å. The structure of title complex shows that the two metal centers are bridged by the two phenoxide oxygens as well as by two oxygens of the coordinated nitrite (O-bonding). Both the metal centers are six-coordinated with irregular octahedral geometry and have N₂O₂ equatorial donors provided by the macrocyclic ligand. The remaining apical position of the Ni(1) center is occupied by a water molecule, while that of another Ni(2) by a nitrite nitrogen (N-bonding). The macrocyclic complex adopts a non-flat structure

(Ni₂N₄O₂) with two octahedral nickel centers bridged by the two phenoxide oxygen atoms. The O(1) and O(2)-phenolic group mean planes of macrocycle are bent 26.52° and 27.11° toward bridged nitrito ligand, respectively, with the basal Ni₂O₂ least-squares plane. The green polymer crystals of {[Ni₆([22]-HMTADO)₃(CN)₄][Ni(CN)₄]·5H₂O·8CH₃OH}_n (**VI**) suitable for X-ray diffraction study which deposited on standing for *ca.* 2 month were crystallized from methanol solution of [Ni₂([22]-HMTADO)(CN)₂]·0.5H₂O complex. The structure of compound (**VI**) is ionic. The unit of title complex contains the polymer [Ni₆([22]-HMTADO)₃(CN)₄]²⁺ cations, [Ni(CN)₄]²⁻ anions, five water molecules, and eight methanol molecules. A novel one-dimensional chain coordination polymer [Ni₆([22]-HMTADO)₃(CN)₄]_n exhibits a novel -(A-B-A')-(A-B-A')- chain array, namely the infinite chain is propagated via alternately five and six-coordinate (A), two five coordinate (B), and five and six-coordinate (A'); centro symmetry of A by B site) sites of bivalent Ni ions.

The dinegative ([22]-HMTADO)²⁻ in (A) site accommodates two Ni(II) ions in its N₄O₂ sites in the Ni(1)···Ni(2) separation of 3.097 Å. The geometry about Ni(1) in the N₂O₂ site is a square-pyramid with a carbon atom of a bridged cyanide at opposite of (B) site. And the geometry about Ni(2) in another N₂O₂ site is an octahedron with a nitrogen atom of two bridged cyanide at the trans positions. The Ni(1) is displaced by 0.569 Å from the basal N₂O₂ least-squares plane towards C(46) (cyanide). The dinegative ([22]-HMTADO)²⁻ in (B) site accommodates two Ni(II) ions in its N₄O₂ sites in the Ni(3)···Ni(3A) (-x+1, -y+1, -z+1) separation of 3.220 Å. The binuclear core structures are centrosymmetric with each Ni(II) ion in the N₂O₂ sites being five-coordinate by square-pyramidal geometry of interactions with

two nitrogen and two oxygen atoms of the binucleating ligand [22]-HMTADO and two carbon atoms each from the bridged cyanide ligands at an apical site. The Ni(3) is displaced by 0.660 Å from the basal N₂O₂ least-squares plane towards C(46) (cyanide). The {Ni(CN)₄²⁻} are exactly planar as required by symmetry.



I. Introduction

Macrocyclic and macroacyclic compounds have attracted increasing interest owing to their role in the understanding of molecular processes occurring in biochemistry, material science, catalysis, encapsulation, activation, transport and separation phenomena, etc..¹⁻⁸ Many ligands have been designed to mimic the function of natural carriers in recognizing and transporting specific metal ions, anions or neutral molecules and in understanding and reproducing the catalytic activity of metallo-enzymes and proteins.¹⁻⁸

There has been considerably interest in the successful application of the modified 1,4,8,11-tetraazacyclotetradecane, cyclam which can be used as models for protein-metal binding site in biological systems⁹⁻¹¹ and as selective reagents of metallic ions.¹²⁻¹⁴ The DNA binding of Cr-macrocyclic complexes is an area of great interest and activity, since these cleavage reagents can potentially be used for cancer therapy or as restriction nucleases.¹⁵⁻¹⁷

In these studies Schiff bases have been extensively employed and a large variety of planar macrocyclic and macroacyclic ligands have been synthesized to ascertain correctly the role of the different donor atoms, their relative position, the number and size of the chelating rings formed, the flexibility and the shape of the coordinating moiety on the selective binding of charged or neutral species.¹⁸⁻²⁰

The evolution of these Schiff bases has produced macrobicyclic ligands obtained in one-step multiple condensation reactions^{8,18,19} the cyclic [2+3] Schiff base condensation represents the extension of the [2+2] macrocyclic

coordination systems into the third dimension. In addition to the use in the field of molecular recognition, catalysis and transport, these cage molecules are promising in the stabilization of particular species. The nature and disposition of donor atoms in the rigid cage may enhance the stability of unusual oxidation states in the coordinated transition metal ion, while encapsulation may protect normally labile substrate species. This combination of characteristics will eventually permit moisture sensitive chemistry to be carried out in the protected cavity under room temperature and atmospheric pressure.

For the macrocycles the hole size represents an additional parameter which may influence greatly the ability to discriminate among the different charged or neutral species to be recognized while for the macrocyclic systems interesting properties may arise from their higher flexibility. These ligands have been primarily designed to form 1:1 complexes. The progressive enlargement of the coordinating moiety allowed studies aimed at a deep understanding of physico-chemical properties arising from the simultaneous presence of two or more metal ion in close proximity within the same coordinating moiety.

Attempts to construct *in vitro* systems that mimic the catalytic activity of enzymes have produced increasing attention to compounds that contain cavities of sufficient diameter and depth to form host-guest complexes, such complexes constituting the first intermediate in enzyme model processes.

A wide variety of different compounds (i.e. cavitands, calixarenes, polyporphyrins, polydentate Schiff bases, polyaza, poly-oxamacropolycycles) have been designed to throw light on these problems. Cavitands¹⁸ and

calixarenes²¹⁻³⁹, widely used since the clarification of the phenol-formaldehyde condensation reaction involved in their systems, represent two examples of macrocyclic systems with an enhanced capability to form stable inclusion complexes with both charged and neutral molecules and to act, after suitable functionalization both at upper and lower rings, as selective catalysts. They corroborate the possibility to design bifunctional or polyfunctional ligands capable to secure contemporary cations and anions at the different functionalities and to insert two- or more equal or different metal ions at suitable distances into their coordinating cavities.

In the past, the major interest was towards the most appropriate synthetic procedures for the preparation of dinuclear complexes and their physico-chemical properties in consequence of the close proximity of two metal ions. In particular the preparation of complexes containing two transition metal ions separated by distances of 3-6 Å is of considerable interest. At these distances, no direct interaction between the metal ions is expected, yet a substrate could interact simultaneously with both ions, and it has been shown that pairs of metal ions at suitable distance and/or with an appropriate structure can mediate certain chemical reactions either better than, or in different manner to isolated centers. Thanks to their peculiar properties, these entities offer the necessary tool for a correct molecular understanding of activation, transport and separation of specific molecules with different complexity, of the selective recognition of neutral or charged species, of the modification of appropriate surfaces, etc. They are currently proposed as essential components in the preparation of suitable devices based on specific molecular assembly.

Starting from simple dinucleating ligands, very complex planar or tridimensional cyclic or acyclic systems have been proposed and prepared using self assembling procedures, recognition processes, template effect, etc. Thus polytopic, polyfunctional or polymeric systems, containing also lateral groups bearing additional coordinating functions, redox active groups (as ferrocene), or IR active groups (as $\text{Cr}(\text{CO})_3$) have been prepared and studied in detail. Also the use of particular complexes as ligands for further complexation has been successfully used.^{5,18,19}

The ability of the specific ligand to bind, in appropriate coordination sites, different metal ions is the basic principle for the design of dinucleating or polynucleating ligands.

Many excellent papers have been published during the last two decades on the preparation and properties of dinuclear complexes and the most relevant results have also been reviewed.^{1-8,18-20,40-49} In particular, attention was devoted to their correlation with the active site of metallo-enzymes and metallo-proteins containing dinuclear metallo entities in order to elucidate the factors that determine the reversible binding and activation of O_2 in various natural oxygen transport systems and mono- and di-oxygenases and to mimic their activity.^{1-8,18-20,40-49} Macrocyclic and macroacyclic ligands have also been used for the generation of compounds with specific spectroscopic and magnetic properties. Complexes containing magnetic metal centers may exhibit magnetic properties which are not simply the sum of those of the individual ions surrounded by their nearest neighbour ligands. These properties result from both the nature and the magnitude of the interactions between the metal ions within the molecular unit.

Using compartmental ligands, binuclear complexes have been synthesized, where the two metal centers, if paramagnetic, interact with each other through the bridging donor atoms of the ligands in a ferromagnetic or antiferromagnetic way. By changing the type of the ligand, the distance between the two chambers and/or the paramagnetic centers, it is possible to vary considerably the magnetic interaction and, with particular complexes, ferromagnetic interactions have been observed. Thus these complexes may be good building blocks for the preparation of molecular magnets.

Complexes in which a single ligand organizes more than two metal centers into some predetermined arrangement, giving rise to unique behaviour, have been also designed, synthesized and fully characterized.

In these studies Schiff bases deserve a relevant role for several reasons⁵⁰:

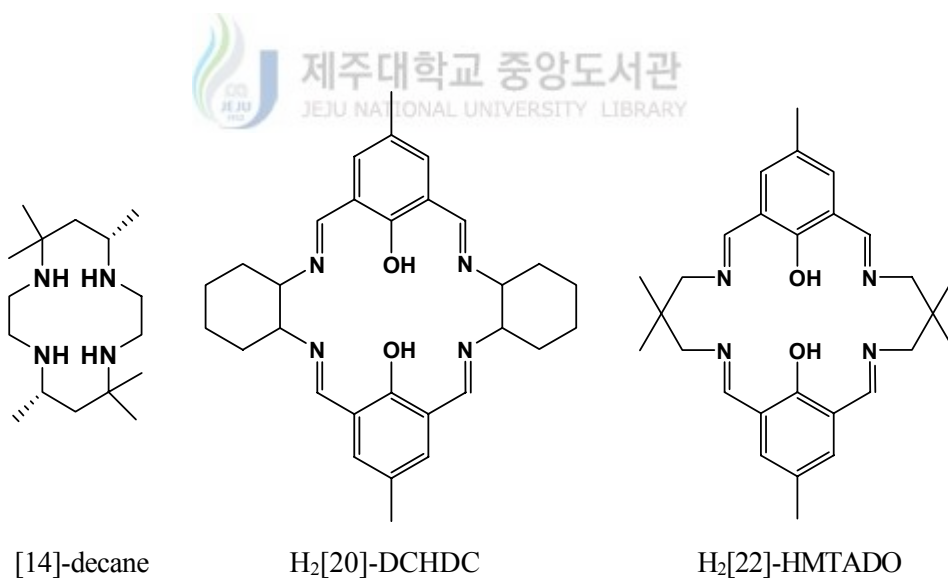
- (a) They can be obtained by simple self-condensation of suitable formyl- or keto- and primary amine-precursors. Multiple self-condensation processes give rise to complex planar or tridimensional compounds in one step.
- (b) They generally can contain additional donor groups (O, N, S, P, etc.) and this makes them good candidates for metal ion complexation and for mimicking biological systems.
- (c) Alternatively they can be obtained by template effect, this procedure directly gives the designed complexes. Moreover, these complexes can undergo transmetallation reactions when reacted with a different metal salt; this synthetic procedure allows the formation of not otherwise accessible complexes. Template and transmetallation reactions quite often

give rise to the designed complexes in high yield and in a satisfactory purity grade.

- (d) They can be functionalized by inserting appropriate groups in the aliphatic and/or aromatic chains of the formyl- or keto- and amine-precursors.
- (e) They can give rise to reductive decomplexation reactions when treated with appropriate reductants with the consequent formation of the corresponding polyamine derivatives less sensitive to hydrolysis and more flexible. These reduced compounds contain NH groups which may be further functionalized by appropriate synthetic procedures.
- (f) The use of particular Schiff bases can exhibit unusual complexation; for instance helicates derivatives have been obtained with imine derivatives containing appropriate chains and/or suitable donor sets.
- (g) They can be linked to an appropriate support (e.g. silica) giving rise to modified catalysts or modified surfaces, bearing well defined molecular assemblies.
- (h) It is well known that other systems are excellent ligands for specific metal ions (i.e. crown ether, macrocyclic thioether, polyaza derivatives, etc.). Thus the fusion of different coordinating entities (i.e. a Schiff base and crown-ether moiety) into a unique ligand can give rise to very interesting systems capable of multiple selective and/or different metal ions recognition processes.

This work performs synthesis, crystal X-ray diffraction studies and physicochemical characterization of transition metal (Cr^{3+} , Cu^{2+} , and Ni^{2+}) complexes with aza or oxaaza 14-, 20-, and 22-membered macrocyclic

ligands. We prepare and isolate (1) Cr(III)-tetraaza 14-membered macrocyclic complexes; *cis*-[Cr([14]-decane)(*o*-OOC₆H₄OH)₂]ClO₄, *cis*-[Cr([14]-decane)(*p*-OC₆H₄NO₂)(OH)]ClO₄·H₂O { [14]-decane; 5,5,7,12,12,14-hexamethyl-1,4,8,11-tetraaza-cyclotetradecane}, (2) Cu(II)-dioxatetraaza 20-membered macrocyclic complexes; [Cu₂([20]-DCHDC)(O₂N)₂]·6H₂O {H₂[20]-DCHDC ; 14,29-dimethyl-3,10,18,25-tetraazapentacyclo-[25,3,1,0^{4,9},1^{12,16},0^{19,24}]ditriacontane -2,10,12,14,16(32),17,27(31),28,30-decane-31,32-diol}, and (3) Ni(II)-dioxatetraaza 22-membered macrocyclic complexes; [H₄[22]-HMTADO](NO₃)₂·H₂O, [Ni₂([22]-HMTADO)(μ-O₂N)(NO₂)-(OH₂)], and {[Ni₆(C₂₈H₃₄N₄O₂)₃(CN)₄][Ni(CN)₄]·5H₂O·8CH₃OH}_n {H₂[22]-HMTADO; 5,5,11,17,17,23-hexamethyl-3,7,15,19-tetraazatricyclo[19,3,1,1^{9,13}]hexacosa-1(25),2,7,9,11,13(26),14,19,21,23-decane-25,26-diol}.



II. Experimental section

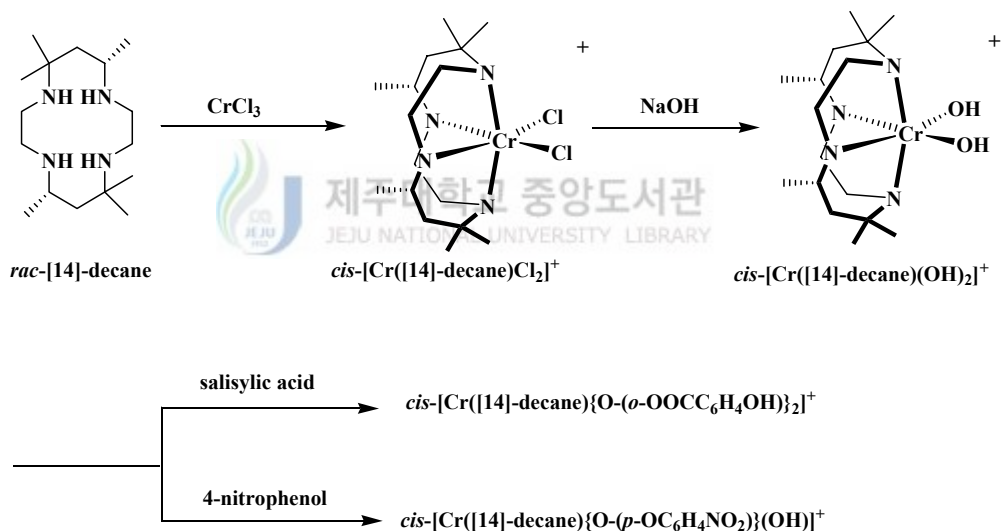
1. Chemicals and Physical Measurements

All chemicals were commercial analytical reagents and were used without further purification. For the spectroscopic and physical measurements, organic solvents were dried and purified according to the literature methods.⁵¹ Nanopure quality water was used throughout this work. Microanalyses of C, H, and N were carried out using LECO CHN-900 analyzer. Conductance measurements of the complexes were performed at $25\pm 1^\circ\text{C}$ using an ORION 162 conductivity temperature meter. IR spectra were recorded with a Bruker FSS66 FT-IR spectrometer in the range $4000\text{-}370\text{ cm}^{-1}$ using KBr pellets. Electronic absorption spectra were measured at 25°C on a UV-3150 UV-VIS-NIR Spectrophotometer (SHIMADZU). FAB-mass spectra were obtained on a JEOL JMS-700 Mass Spectrometer using argon (6 kV, 10 mA) as the FAB gas. The accelerating voltage was 10 kV and glycerol was used as the matrix. The mass spectrometer was operated in positive ion mode and mass spectrum was calibrated by Alkali-CsI positive.

2. Synthesis of Ligand and Complexes

1) Cr(III)-tetraaza 14-membered macrocyclic complexes

The *rac*-[14]-decane^{52,53}, *cis*-[Cr([14]-decane)(Cl)₂Cl], and *cis*-[Cr([14]-decane)(OH)₂]⁺ solution⁵⁴ were prepared according to the literature procedure.



Scheme 1. Synthesis of the Cr(III)-salicylato and -*p*-nitrophenolato tetraaza 14-membered macrocyclic complexes.

(1) Preparation of *cis*-[Cr([14]-decane)(*o*-OOCC₆H₄OH)₂]ClO₄

An aqueous solution of HClO₄ (70%, *ca.* 1 mL) was mixed with a freshly prepared 4×10^3 M *cis*-[Cr([14]-decane)(OH)₂]⁺ solution (10 mL). To this solution a salicylic acid (1.38 g) was added dropwise with constant stirring. After the addition the resulting mixture was stirred thoroughly for 2h at 10 °C. The resulting pink solution was left undisturbed at a room temperature to give pink product, and then the product was washed with ethanol, and dried *in vacuo*.

Yield 35%.

Anal. Calcd (Found) % for C₃₀H₄₆N₄O₁₀ClCr :

C, 50.74 (49.89) ; H, 6.53 (6.22) ; N, 7.89 (7.94).

λ_M (in DMF) : 69.2 ohm⁻¹cm²mol⁻¹.

(2) Preparation of the *cis*-[Cr([14]-decane)(*p*-OC₆H₄NO₂)(OH)]ClO₄·H₂O

To a freshly prepared 4×10^3 M *cis*-[Cr([14]-decane)(OH)₂]⁺ solution (10 ml), a solution of 4-nitrophenol (1.46 g) in methanol (30 ml) was slowly added in small portions. To this was added dropwise a saturated aqueous NaClO₄ solution (2ml) with stirring and solution was refluxed for 2h. The resulting solution was allowed to stand in a room temperature until dark green precipitate formed. The precipitates were filter, washed twice with methanol, and dried *in vacuo*.

Yield 77%.

Anal. Calcd (Found) % for $C_{22}H_{41}N_5O_8ClCr \cdot H_2O$:

C, 43.39 (43.20) ; H, 7.12 (7.38) ; N, 11.50 (11.55).

λ_M (in DMF) : $66.9 \text{ ohm}^{-1}\text{cm}^2\text{mol}^{-1}$.

2) Binuclear Cu(II)-dioxatetraaza 20-membered macrocyclic complexes

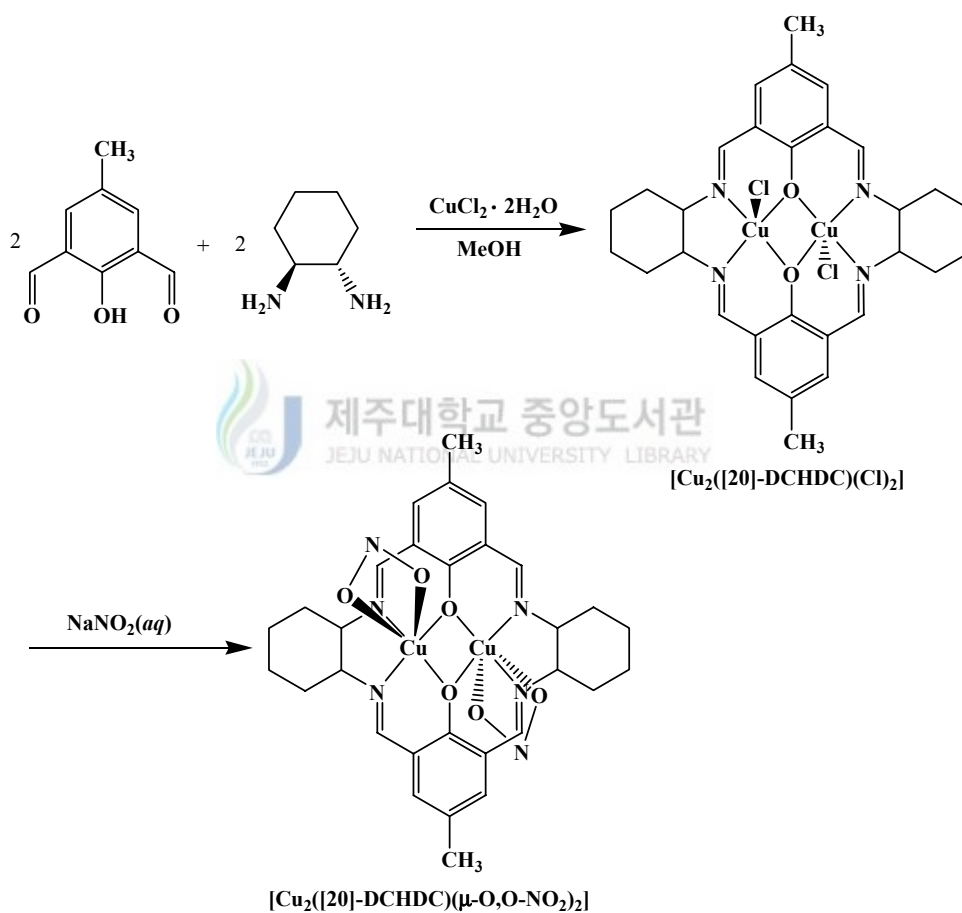
(1) Preparation of 2,6-diformyl-*p*-cresol.

The synthesis of 2,6-diformyl-*p*-cresol was prepared according to the methods previously reported.^{55,56} The dinuclear Cu(II) complexes with [2+2] symmetrical N_4O_2 compartmental macrocyclic ligand $\{([20]\text{-DCHDC})^{2-}\}$ containing bridging phenolic oxygen atoms was synthesized by the condensation reaction of Cu(II) ions, 2,6-diformyl-*p*-cresol and *trans*-1,2-diaminocyclohexane (Scheme 2).

(2) Preparation of $[Cu_2([20]\text{-DCHDC})Cl_2] \cdot H_2O$.

A solution of 2,6-diformyl-*p*-cresol (3.280 g) in the boiling methanol (50 mL) was added to the pale blue suspension formed by mixing *trans*-1,2-diaminocyclohexane (2.400 g) with a solution of cupric chloride dihydrate (3.410 g) in methanol (30 mL). The mixture was heated under reflux whereupon the initial pale green suspended solid first turned dark blue and then eventually dissolved. Methanol was removed by boiling at atmospheric pressure until precipitation had just commenced and the dark blue

mixture was poured into ten times its volume of tetrahydrofuran. The resulting pale green precipitate was filtered, thoroughly washed twice with water. Yielding crystal as dark blue platelets were dried over anhydrous calcium chloride at room temperature and atmospheric pressure. Prolonged heating in vacuum at 150°C was required for removal of the water.



Scheme 2. Synthesis of the Cu(II)-nitro tetraazadioxa 20-membered macrocyclic complexes.

Yield 64%.

Anal. Calc. (Found) % for $\text{Cu}_2(\text{C}_{30}\text{H}_{34}\text{N}_4\text{O}_2)(\text{Cl})_2(\text{H}_2\text{O})$:

C, 51.58 (51.62); H, 5.19 (5.01); N, 8.02 (8.15).

Solubility : water, methanol, hot ethanol, hot DMSO, hot DMF

Λ_M (methanol) : $64.9 \text{ ohm}^{-1}\text{cm}^2\text{mol}^{-1}$.

(3) $[\text{Cu}_2([\text{20}]\text{-DCHDC})(\text{O}_2\text{N})_2] \cdot 6\text{H}_2\text{O}$.

To a hot aqueous solution (150 mL) of $[\text{Cu}_2([\text{20}]\text{-DCHDC})\text{Cl}_2] \cdot \text{H}_2\text{O}$ (0.6986 g) a solution of NaNO_2 (0.3450 g) in water (20 mL) was added dropwise with stirring and refluxed for 2 h. The resulting green precipitates were filter, thoroughly washed twice with water, and dried *in vacuo*.

Yield 83 %.

Anal. Calc. (Found) for $\text{Cu}_2(\text{C}_{30}\text{H}_{34}\text{N}_4\text{O}_2)(\text{NO}_2)_2(\text{H}_2\text{O})_6$:

C, 44.50 (44.18); H, 5.73 (5.46); N, 10.38 (9.44).

Solubility : methanol, hot water, hot DMSO, hot chloroform

Λ_M (methanol) : $65.8 \text{ ohm}^{-1}\text{cm}^2\text{mol}^{-1}$.

The green crystal of $[\text{Cu}_2([\text{20}]\text{-DCHDC})(\text{O}_2\text{N})_2] \cdot 6\text{H}_2\text{O}$ suitable for structure determination was acquired from methanol and water (10 : 1 v/v) mixed solvent, by slow evaporation of solvent at room temperature.

3) Binuclear Ni(II)-tetraazadioxa 22-membered macrocyclic complexes

(1) Preparation of $[\text{H}_4[\text{22}]\text{-HMTADO}](\text{ClO}_4)_2$ macrocyclic ligand

To a solution of 2,2-dimethyl-1,3-propanediamine (0.206 g) in 20 mL of ethanol 0.17 mL of 70% HClO₄ was added. The mixture was added to a solution of 2,6-diformyl-*p*-cresol (0.328 g) in 20 mL of ethanol and the resulting red solution was refluxed for 1 h, after which time a yellow-red compound separated out. The solution was cooled to room temperature and the yellow-red product was filtered, thoroughly washed with ethanol, and dried *in vacuo*.

Yield 83%.

Anal. Calc. (Found) % for C₂₈H₃₈N₄O₂ · (ClO₄)₂ :

C, 50.84 (50.71) ; H, 5.79 (5.65); N, 8.47 (8.47).

Solubility : DMSO, DMF, acetonitrile.

UV-Vis (DMF) [λ_{max} (nm) (ϵ (M⁻¹cm⁻¹))]:

349 (10,490), 433 (13,990), 462 sh (8,220).

λ_{M} (DMF) : 245 ohm⁻¹cm²mol⁻¹.

FAB-mass (*m/z*, *M*⁺) : 461 (C₂₈H₃₆N₄O₂).

FT-IR (KBr, cm⁻¹) : 3437 ν (OH) ; 1662 ν (C=N) ; 1644, 1536 ν (C=C, aromatic) ; 1088, 624 ν (ClO₄⁻).

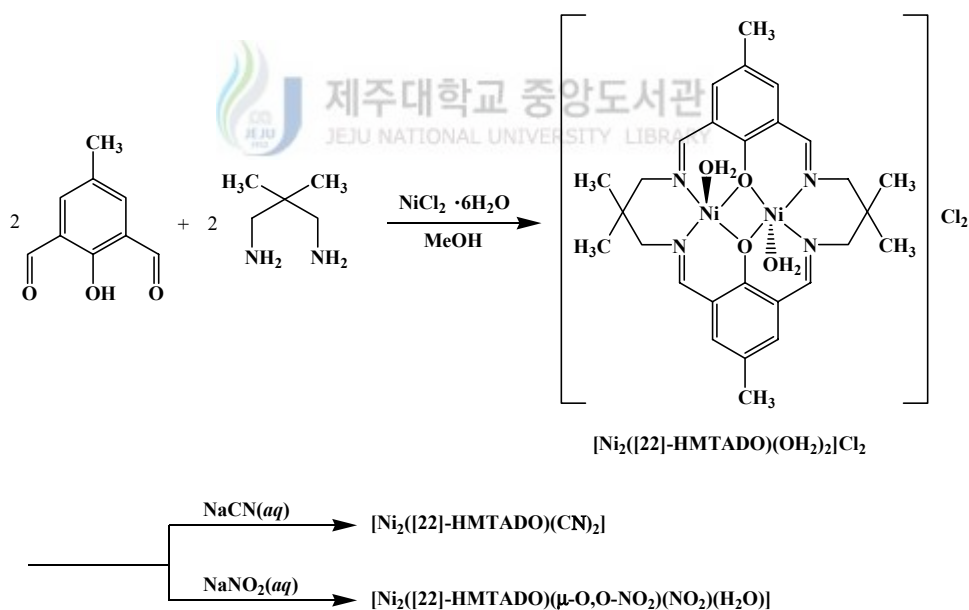
(2) Preparation of [H₄[22]-HMTADO](NO₃)₂ · H₂O crystals

To a 150 mL hot acetonitrile solution of [H₄[22]-HMTADO](ClO₄)₂ (0.330 g, 0.5 mmol), a 20 mL acetonitrile solution AgNO₃ (0.424 g, 2.5 mmol) was added dropwise with stirring. The resulting deep orange solution was

refluxed for 30 min. The solution on standing overnight afforded red single crystals of $[H_4[22]-HMTADO](NO_3)_2 \cdot H_2O$ macrocyclic ligand.

Anal. Calc. (Found) % for $(C_{28}H_{38}N_4O_2) \cdot (NO_3)_2(H_2O)$:
 C, 55.62 (54.62) ; H, 6.67 (6.68); N, 13.90 (13.81).

The dinuclear Ni(II) complexes with [2+2] symmetrical N_4O_2 compartmental macrocyclic ligand $\{([22]-HMTADO)^{2-}\}$ containing bridging phenolic oxygen atoms was synthesized by the condensation reaction of Ni(II) ions, of 2,6-diformyl-*p*-cresol and 2-dimethyl-1,3-propanediamine (Scheme 3).



Scheme 3. Synthesis of the Ni(II)-cyano and -nitro tetraazadioxa 22-membered macrocyclic complexes.

(3) Preparation of $[\text{Ni}_2([\text{22}]\text{-HMTADO})(\text{OH}_2)_2]\text{Cl}_2 \cdot \text{H}_2\text{O}$.

Nickel chloride hexahydrate (4.80 g), 2,6-diformyl-*p*-cresol (1.64 g), and 2-dimethyl-1,3-propanediamine (1.03 g) were heated under reflux in methanol (150 mL) for 4 h. The solution was cooled to room temperature and the pale green product was filtered, thoroughly washed with ice-cold methanol, and dried *in vacuo*.

Yield 42%.

Anal. Calc. (Found) % for $\text{Ni}_2(\text{C}_{28}\text{H}_{34}\text{N}_4\text{O}_2)(\text{Cl})(\text{H}_2\text{O})_3$:

C, 47.98 (47.99); H, 5.75 (5.02); N, 7.99 (7.66).

Solubility : water, DMSO, DMF, hot acetonitrile, hot acetone, chloroform.

Λ_{M} (water) : 205 $\text{ohm}^{-1}\text{cm}^2\text{mol}^{-1}$.

(4) Preparation of $[\text{Ni}_2([\text{22}]\text{-HMTADO})(\mu\text{-O}_2\text{N})(\text{NO}_2)(\text{OH}_2)]$.

A pale brown solution of $[\text{Ni}_2([\text{22}]\text{-HMTADO})(\text{OH}_2)_2]\text{Cl}_2 \cdot \text{H}_2\text{O}$ (0.701 g) in hot water (30 mL) was added dropwise to a solution of sodium nitrite (0.345 g) in water (30 mL) with stirring and the solution was refluxed for 2 h. The dark green precipitate was filtered, thoroughly washed with ice-cold water, and dried *in vacuo*.

Yield 60%.

Anal. Calc. (Found) % for $\text{Ni}_2(\text{C}_{28}\text{H}_{34}\text{N}_4\text{O}_2)(\text{NO}_2)_2(\text{H}_2\text{O})$:

C, 49.02 (48.93); H, 5.29 (5.08); N, 12.25 (12.07).

Solubility : methanol, DMSO, DMF, hot acetonitrile, chloroform.

Λ_M (methanol) : $60 \text{ ohm}^{-1}\text{cm}^2\text{mol}^{-1}$.

The green crystals of $[\text{Ni}_2([\text{22}]\text{-HMTADO})(\mu\text{-O}_2\text{N})(\text{NO}_2)(\text{OH}_2)]$ suitable for X-ray diffraction study which deposited on standing for *ca.* 1 month were recrystallized from methanol of this complex.

(5) Preparation of $[\text{Ni}_2([\text{22}]\text{-HMTADO})(\text{CN})_2] \cdot 0.5\text{H}_2\text{O}$.

A pale brown solution of $[\text{Ni}_2([\text{22}]\text{-HMTADO})(\text{OH}_2)_2]\text{Cl}_2 \cdot \text{H}_2\text{O}$ (0.701 g) in hot water (30 mL) was added dropwise to a solution of sodium cyanide (0.245 g) in water (30 mL) with stirring and the solution was refluxed for 2 h. The dark green precipitate was filtered, thoroughly washed twice with water, and dried *in vacuo*.

Yield 88%.

Anal. Calc. (Found) % for $\text{Ni}_2(\text{C}_{28}\text{H}_{34}\text{N}_4\text{O}_2)(\text{CN})_2(\text{H}_2\text{O})_{0.5}$:

C, 56.56 (56.33); H, 5.54 (5.52); N, 13.19 (13.14).

Solubility : methanol, DMSO, DMF, hot acetonitrile, chloroform.

Λ_M (methanol) : $9.5 \text{ ohm}^{-1}\text{cm}^2\text{mol}^{-1}$.

The green polymer crystals of $\{[\text{Ni}_6(\text{C}_{28}\text{H}_{34}\text{N}_4\text{O}_2)_3(\text{CN})_4][\text{Ni}(\text{CN})_4] \cdot 5\text{H}_2\text{O} \cdot 8\text{CH}_3\text{OH}\}_n$ suitable for X-ray diffraction study which deposited on standing for *ca.* 2 months were crystallized from methanol solution of this complex.

3. X-ray Diffraction Measurements

1) Cr(III)-tetraaza 14-membered macrocyclic complexes

(1) *cis*-[Cr([14]-decane)(*o*-OOCC₆H₄OH)₂]ClO₄

Suitable crystals of *cis*-[Cr([14]-decane)(*o*-OOCC₆H₄OH)₂]ClO₄ were obtained by slow evaporation of acetonitrile solution of the complex at atmospheric pressure. The pink crystal of *cis*-[Cr([14]-decane)(*o*-OOCC₆H₄OH)₂]ClO₄ was attached to glass fibers and mounted on a Bruker SMART diffractometer equipped with a graphite monochromated Mo K α ($= 0.71073 \text{ \AA}$) radiation, operating at 50 kV and 30 mA and a CCD detector ; 45 frames of two-dimensional diffraction images were collected and processed to obtain the cell parameters and orientation matrix. The crystallographic data, conditions for the collection of intensity data, and some features of the structure refinements are listed in Table 1, and atomic coordinates were given in Table 2. The intensity data were corrected for Lorentz and polarization effects. Absorption correction was not applied during processing. Of the 13,835 unique reflections measured, 7,718 reflections in the range $1.09^\circ \leq \theta \leq 27.53^\circ$ were considered to be observed ($I > 2\sigma(I)$) and were used in subsequent structure analysis. The program SAINTPLUS⁵⁷ was used for integration of the diffraction profiles. The structures were solved by direct methods using the SHELXS program of the SHELXTL package⁵⁸ and refined by full matrix least squares against F^2 for all data using SHELXL. All non-H atoms were

refined with anisotropic displacement parameters (Table 3). Hydrogen atoms were placed in idealized positions [$U_{\text{iso}} = 1.2U_{\text{eq}}$ (parent atom)]. Hydrogen coordinates and isotropic displacement parameters were given in Table 4.

Table 1. Crystal data and structure refinement for *cis*-[Cr([14]-decane)(*o*-OOC₆H₄OH)₂]ClO₄ complex

Empirical formula	C ₃₀ H ₄₆ ClCrN ₄ O ₁₀	
Formula weight	710.16	
Temperature	293(2) K	
Wavelength	0.71073 Å	
Crystal system	Monoclinic	
Space group	C ₂ /a	
Unit cell dimensions	$a = 15.9787(5)$ Å	$\alpha = 90^\circ$
	$b = 11.2818(4)$ Å	$\beta = 110.806(2)^\circ$
	$c = 19.9362(8)$ Å	$\gamma = 90^\circ$
Volume	3359.5(2) Å ³	
Z	4	
Density (calculated)	1.404 g/cm ³	
Absorption coefficient	0.480 mm ⁻¹	
<i>F</i> (000)	1500	
Theta range for data collection	1.09 to 27.53°.	
Index ranges	-20 ≤ <i>h</i> ≤ 20, -13 ≤ <i>k</i> ≤ 14, -25 ≤ <i>l</i> ≤ 25	
Reflections collected	13835	
Independent reflections	7718 [<i>R</i> (int) = 0.0719]	
Data / restraints / parameters	7718 / 0 / 415	
Goodness-of-fit on <i>F</i> ²	1.032	
Final R indices [<i>I</i> > 2σ(<i>I</i>)]	<i>R</i> ₁ = 0.0655, <i>wR</i> ₂ = 0.1633	
<i>R</i> indices (all data)	<i>R</i> ₁ = 0.1667, <i>wR</i> ₂ = 0.2419	

$$R = \frac{\sum ||F_o| - |F_c||}{\sum |F_o|}, \quad R_w = \left[\frac{\sum w(F_o^2 - F_c^2)^2}{\sum w(F_o^2)^2} \right]^{1/2}$$

$$w = 1/[\sigma^2(F_o^2) + (0.1292P)^2 + 0.0000P] \quad \text{where } P = (F_o^2 + 2F_c^2)/3.$$

Table 2. Atomic coordinates ($\text{\AA} \times 10^4$) and equivalent isotropic displacement parameters ($\text{\AA}^2 \times 10^3$) for *cis*-[Cr([14]-decane)(*o*-OOC₆H₄OH)₂]ClO₄ complex

atom	<i>x</i>	<i>y</i>	<i>z</i>	<i>U</i> (eq)
Cr(1)	2400(1)	1297(1)	2751(1)	33(1)
N(1)	2785(2)	2228(3)	3743(1)	40(1)
N(2)	1655(2)	239(3)	3206(2)	38(1)
N(3)	2095(2)	47(3)	1889(2)	37(1)
N(4)	3607(2)	332(4)	3157(2)	42(1)
C(1)	3997(4)	3598(5)	3779(3)	59(1)
C(2)	3741(3)	2589(5)	4172(2)	47(1)
C(3)	3820(4)	3078(6)	4919(3)	63(1)
C(4)	2369(3)	1598(5)	4202(3)	53(1)
C(5)	1491(3)	1036(5)	3745(3)	54(1)
C(6)	802(3)	-339(4)	2736(2)	41(1)
C(7)	394(3)	-1088(5)	3187(3)	58(1)
C(8)	950(3)	-1119(4)	2173(3)	46(1)
C(9)	506(3)	354(5)	1151(3)	55(1)
C(10)	1189(3)	-562(4)	1568(3)	42(1)
C(11)	1218(4)	-1537(5)	1038(3)	60(1)
C(12)	2841(3)	-812(5)	2072(3)	53(1)
C(13)	3710(3)	-228(5)	2517(3)	48(1)
C(14)	5247(4)	88(7)	3846(3)	81(2)
C(15)	4445(3)	954(5)	3607(3)	49(1)
C(16)	4343(3)	1526(5)	4269(3)	51(1)
C(17)	1226(3)	3429(5)	2372(3)	44(1)
C(18)	560(3)	4054(4)	1771(3)	44(1)
C(19)	22(4)	3463(6)	1146(4)	82(2)
C(20)	-602(5)	4024(7)	589(4)	99(3)

C(21)	-687(4)	5227(6)	625(4)	83(2)
C(22)	-189(4)	5854(5)	1229(4)	68(1)
C(23)	445(3)	5278(5)	1806(3)	50(1)
O(1)	1313(2)	2298(3)	2314(2)	45(1)
O(2)	1675(3)	3996(3)	2921(2)	65(1)
O(3)	912(3)	5947(3)	2367(2)	78(1)
C(24)	2839(3)	2631(4)	1624(2)	42(1)
C(25)	2960(3)	3875(4)	1435(2)	35(1)
C(26)	3075(3)	4794(4)	1923(3)	48(1)
C(27)	3146(4)	5949(5)	1741(3)	59(1)
C(28)	3099(4)	6204(5)	1051(3)	56(1)
C(29)	2990(3)	5319(5)	554(3)	52(1)
C(30)	2915(3)	4147(4)	737(2)	42(1)
O(4)	2989(2)	2399(3)	2289(2)	41(1)
O(5)	2602(3)	1864(3)	1142(2)	67(1)
O(6)	2788(3)	3331(4)	224(2)	70(1)
Cl(1)	3210(1)	-2643(1)	4034(1)	59(1)
O(7)	3601(7)	-2631(8)	3522(4)	210(5)
O(8)	3046(4)	-1462(5)	4200(3)	117(2)
O(9)	3741(3)	-3254(5)	4644(2)	96(1)
O(10)	2368(4)	-3181(8)	3790(5)	197(4)

U (eq) is defined as one third of the trace of the orthogonalized U_{ij} tensor.

Table 3. Anisotropic displacement parameters ($\text{\AA}^2 \times 10^3$) for *cis*-[Cr([14]-decane)(*o*-OOCC₆H₄OH)₂]ClO₄ complex

atom	U_{11}	U_{22}	U_{33}	U_{23}	U_{13}	U_{12}
Cr(1)	40.6(4)	28.7(4)	31.3(4)	1.6(3)	16.3(3)	1.7(3)
N(1)	45(2)	41(3)	34(2)	-1.1(18)	16.0(18)	3.4(18)
N(2)	42(2)	40(2)	37(2)	2.0(18)	20.3(17)	1.3(17)
N(3)	53(2)	26(2)	37(2)	2.7(17)	21.8(18)	0.2(17)
N(4)	47(2)	40(3)	42(2)	6.2(19)	20.7(18)	4.3(18)
C(1)	66(3)	61(4)	43(3)	-7(3)	13(3)	-17(3)
C(2)	50(3)	51(3)	36(3)	-2(2)	11(2)	-4(2)
C(3)	67(3)	77(5)	38(3)	-18(3)	9(3)	-11(3)
C(4)	61(3)	69(4)	38(3)	-8(3)	28(3)	-9(3)
C(5)	57(3)	67(4)	50(3)	-8(3)	35(3)	-3(3)
C(6)	39(2)	42(3)	46(3)	4(2)	18(2)	1(2)
C(7)	58(3)	57(4)	66(3)	-1(3)	33(3)	-14(3)
C(8)	50(3)	38(3)	49(3)	-1(2)	18(2)	-9(2)
C(9)	61(3)	52(4)	44(3)	-5(3)	8(3)	-8(3)
C(10)	51(3)	30(3)	45(3)	-6(2)	17(2)	-9(2)
C(11)	80(4)	49(4)	55(3)	-1.8(3)	30(3)	-17(3)
C(12)	67(3)	40(3)	62(3)	0(3)	34(3)	10(3)
C(13)	49(3)	47(3)	57(3)	-8(3)	27(2)	6(2)
C(14)	54(3)	109(6)	73(4)	6(4)	15(3)	22(3)
C(15)	40(3)	62(4)	44(3)	9(3)	14(2)	4(2)
C(16)	47(3)	64(4)	37(3)	7(3)	8(2)	-2(2)
C(17)	49(3)	32(3)	52(3)	2(2)	20(3)	7(2)
C(18)	49(3)	28(3)	53(3)	1(2)	18(2)	0(2)
C(19)	83(4)	45(4)	82(5)	-3(3)	-15(4)	16(3)
C(20)	101(5)	56(5)	95(5)	-5(4)	-23(4)	12(4)

C(21)	66(4)	69(5)	84(5)	27(4)	-10(4)	4(3)
C(22)	65(4)	37(3)	91(5)	23(3)	14(4)	4(3)
C(23)	45(3)	42(4)	62(3)	11(3)	18(3)	1(2)
O(1)	49.0(19)	34(2)	49(2)	-1.7(16)	13.5(16)	7.1(15)
O(2)	83(3)	45(2)	51(2)	-09(2)	4(2)	15(2)
O(3)	107(3)	32(2)	72(3)	-5(2)	3(3)	3(2)
C(24)	52(3)	39(3)	37(3)	-2(2)	19(2)	-3(2)
C(25)	43(2)	25(3)	35(2)	6(2)	12(2)	-3.2(19)
C(26)	66(3)	37(3)	35(3)	-1(2)	12(2)	-2(2)
C(27)	84(4)	31(3)	51(3)	-3(3)	9(3)	0(3)
C(28)	70(3)	33(3)	57(3)	11(3)	13(3)	0(3)
C(29)	66(3)	50(4)	42(3)	15(3)	22(3)	4(3)
C(30)	53(3)	32(3)	41(3)	2(2)	18(2)	-2(2)
O(4)	57.9(19)	37(2)	29.6(16)	1.0(14)	18.0(14)	-7.0(15)
O(5)	129(3)	37(2)	44(2)	-7.1(19)	43(2)	-22(2)
O(6)	134(4)	42(2)	45(2)	-3.5(19)	46(2)	-6(2)
C(11)	68.0(9)	60.4(10)	49.4(8)	134(7)	20.9(7)	13.3(7)
O(7)	356(12)	205(8)	158(6)	99(6)	202(8)	142(8)
O(8)	168(5)	75(4)	116(4)	12(3)	59(4)	44(3)
O(9)	96(3)	106(4)	72(3)	39(3)	14(3)	26(3)
O(10)	89(4)	200(8)	229(8)	-49(7)	-32(5)	-33(5)

The anisotropic displacement factor exponent takes the form: $-2\pi^2[h^2 a^{*2}U_{11} + \dots + 2hka^*b^*U_{12}]$.

Table 4. Hydrogen coordinates ($\text{\AA} \times 10^4$) and isotropic displacement parameters ($\text{\AA}^2 \times 10^3$) for *cis*-[Cr([14]-decane)(*o*-OOCC₆H₄OH)₂]ClO₄ complex

atom	<i>x</i>	<i>y</i>	<i>z</i>	<i>U</i> (eq)
H(1)	2481	2926	3632	47
H(2)	2025	-350	3455	46
H(3)	2148	471	1518	45
H(4)	3515	-265	3430	50
H(1A)	3588	4246	3724	88
H(1B)	3970	3331	3315	88
H(1C)	4594	3857	4051	88
H(3A)	3433	3752	4859	95
H(3B)	4427	3311	5177	95
H(3C)	3647	2474	5183	95
H(4A)	2265	2155	4535	64
H(4B)	2774	990	4479	64
H(5A)	1245	584	4046	64
H(5B)	1063	1646	3502	64
H(6)	374	284	2493	50
H(7A)	293	-597	3544	86
H(7B)	799	-1717	3418	86
H(7C)	-164	-1420	2881	86
H(8A)	409	-1581	1953	55
H(8B)	1423	-1674	2420	55
H(9A)	476	979	1469	83
H(9B)	-71	-14	947	83
H(9C)	680	676	775	83
H(11A)	1650	-2127	1287	90
H(11B)	1385	-1195	663	90

H(11C)	638	-1897	834	90
H(12A)	2891	-1125	1635	64
H(12B)	2718	-1469	2338	64
H(13A)	4185	-814	2667	58
H(13B)	3870	369	2234	58
H(14A)	5311	-274	3431	121
H(14B)	5145	-515	4148	121
H(14C)	5784	514	4107	121
H(15)	4572	1581	3317	59
H(16A)	4128	920	4513	62
H(16B)	4935	1754	4589	62
H(19)	96	2650	1113	99
H(20)	-964	3601	192	119
H(21)	-1087	5628	236	99
H(22)	-276	6666	1251	81
H(3D)	1265	5529	2676	117
H(26)	3104	4620	2387	57
H(27)	3225	6552	2076	71
H(28)	3142	6987	921	67
H(29)	2965	5506	93	62
H(6D)	2750	2674	387	105

(2) *cis*-[Cr([14]-decane)(*p*-OC₆H₄NO₂)(OH)]ClO₄·H₂O

Suitable crystals of *cis*-[Cr([14]-decane)(*p*-OC₆H₄NO₂)(OH)]ClO₄·H₂O were obtained by slow evaporation of acetonitrile solution of the complex at atmospheric pressure. The pink crystal of *cis*-[Cr([14]-decane)(*p*-OC₆H₄NO₂)(OH)]ClO₄·H₂O was attached to glass fibers and mounted on a Bruker SMART diffractometer equipped with a graphite monochromated Mo K α (λ = 0.71073 Å) radiation, operating at 50 kV and 30 mA and a CCD detector ; 45 frames of two-dimensional diffraction images were collected and processed to obtain the cell parameters and orientation matrix. The crystallographic data, conditions for the collection of intensity data, and some features of the structure refinements are listed in Table 5, and atomic coordinates were given in Table 6. The intensity data were corrected for Lorentz and polarization effects. Absorption correction was not applied during processing. Of the 8,333 unique reflections measured, 5,380 reflections in the range $1.81^\circ \leq \theta \leq 27.78^\circ$ were considered to be observed ($I > 2\sigma(I)$) and were used in subsequent structure analysis. The program SAINTPLUS⁵⁷ was used for integration of the diffraction profiles. The structures were solved by direct methods using the SHELXS program of the SHELXTL package⁵⁸ and refined by full matrix least squares against F^2 for all data using SHELXL. All non-H atoms were refined with anisotropic displacement parameters (Table 7). Hydrogen atoms were placed in idealized positions [$U_{\text{iso}} = 1.2U_{\text{eq}}$ (parent atom)]. Hydrogen coordinates and isotropic displacement parameters were given in Table 8.

Table 5. Crystal data and structure refinement for *cis*-[Cr([14]-decane)(*p*-OC₆H₄NO₂)(OH)]ClO₄·H₂O complex

Empirical formula	C ₂₂ H ₄₃ ClCrN ₅ O ₉	
Formula weight	609.06	
Temperature	293(2) K	
Wavelength	0.71073 Å	
Crystal system	Monoclinic	
Space group	C ₂ /n	
Unit cell dimensions	<i>a</i> = 10.735(5) Å	<i>α</i> = 90°
	<i>b</i> = 13.832(5) Å	<i>β</i> = 81.979(5)°.
	<i>c</i> = 19.382(5) Å	<i>γ</i> = 90°
Volume	2849.8(18) Å ³	
<i>Z</i>	4	
Density (calculated)	1.420 g/cm ³	
Absorption coefficient	0.551 mm ⁻¹	
<i>F</i> (000)	1292	
Theta range for data collection	1.81 to 27.78°.	
Index ranges	-13 ≤ <i>h</i> ≤ 130, -17 ≤ <i>k</i> ≤ 15, -25 ≤ <i>l</i> ≤ 25	
Reflections collected	8333	
Independent reflections	5380 [<i>R</i> (int) = 0.0525]	
Data / restraints / parameters	5380 / 0 / 343	
Goodness-of-fit on <i>F</i> ²	1.030	
Final <i>R</i> indices [<i>I</i> > 2σ(<i>I</i>)]	<i>R</i> ₁ = 0.0823, <i>wR</i> ₂ = 0.2286	
<i>R</i> indices (all data)	<i>R</i> ₁ = 0.1717, <i>wR</i> ₂ = 0.3046	

$$R = \frac{\sum ||F_o| - |F_c||}{\sum |F_o|}, \quad R_w = \left[\frac{\sum w(F_o^2 - F_c^2)^2}{\sum w(F_o^2)^2} \right]^{1/2}$$

$$w = 1/[\sigma^2(F_o^2) + (0.1843P)^2 + 0.0000P] \quad \text{where } P = (F_o^2 + 2F_c^2)/3.$$

Table 6. Atomic coordinates ($\text{\AA} \times 10^4$) and equivalent isotropic displacement parameters ($\text{\AA}^2 \times 10^3$) for *cis*-[Cr([14]-decane)(*p*-OC₆H₄NO₂)(OH)]ClO₄·H₂O complex

atom	<i>x</i>	<i>y</i>	<i>z</i>	<i>U</i> (eq)
Cr(1)	7144.5(8)	2059.4(8)	6483.1(5)	36.7(3)
N(1)	5683(4)	1697(4)	7314(3)	43.1(13)
N(2)	8345(4)	1757(4)	7236(2)	41.4(13)
N(3)	8786(4)	2132(4)	5708(3)	41.5(13)
N(4)	7071(4)	596(4)	6124(3)	42.8(13)
C(1)	3732(6)	1532(6)	6781(4)	59(2)
C(2)	4589(6)	1012(6)	7224(4)	51.1(2)
C(3)	3829(7)	762(7)	7930(4)	69(2)
C(4)	6328(6)	1392(6)	7917(3)	53.5(19)
C(5)	7516(6)	1910(6)	7913(3)	51.7(19)
C(6)	9525(6)	2350(6)	7188(3)	51.1(18)
C(7)	10278(7)	2093(7)	7793(4)	81(3)
C(8)	10412(6)	2187(5)	6498(3)	49.7(17)
C(9)	10001(6)	2598(5)	5829(3)	47.9(17)
C(10)	11089(6)	2398(6)	5233(4)	67(2)
C(11)	9809(6)	3690(6)	5878(4)	59(2)
C(12)	9014(6)	1117(6)	5434(4)	54.9(19)
C(13)	7783(6)	602(6)	5416(3)	51.8(18)
C(14)	5813(6)	131(6)	6128(4)	56.0(19)
C(15)	5890(8)	-873(7)	579(5)	83(3)
C(16)	5114(6)	72(5)	6862(4)	53.7(18)
O(1)	7112(3)	3364(3)	6810(2)	42.0(10)
C(17)	5406(5)	3030(5)	5557(3)	38.8(15)
C(18)	4668(6)	3624(5)	6033(3)	44.9(16)

atom	<i>x</i>	<i>y</i>	<i>z</i>	<i>U</i> (eq)
C(19)	3806(6)	4253(5)	5816(3)	47.7(17)
C(20)	3690(5)	4310(5)	5117(3)	42.5(15)
C(21)	4428(6)	3747(5)	4649(3)	50.2(18)
C(22)	5282(6)	3112(5)	4852(3)	45.0(17)
N(5)	2791(5)	4966(5)	4880(4)	61.4(18)
O(2)	6194(4)	2370(3)	5737(2)	46.7(12)
O(3)	2691(5)	4956(5)	4250(3)	77.8(18)
O(4)	2180(5)	5505(4)	5307(3)	74.8(17)
Cl(1)	8442.1(18)	1248.5(19)	34659(12)	75.9(7)
O(5)	8386(11)	1272(10)	2757(4)	214(6)
O(6)	9396(10)	1821(9)	3530(9)	249(8)
O(7)	8740(8)	333(6)	3696(4)	130(3)
O(8)	7317(6)	1539(8)	3795(4)	151(4)
O(1W)	6545(4)	4586(4)	7861(3)	66.4(15)

U(eq) is defined as one third of the trace of the orthogonalized U_{ij} tensor.

Table 7. Anisotropic displacement parameters ($\text{\AA}^2 \times 10^3$) for *cis*-[Cr([14]-decane)(*p*-OC₆H₄NO₂)(OH)]ClO₄·H₂O complex

atom	U_{11}	U_{22}	U_{33}	U_{23}	U_{13}	U_{12}
Cr(1)	37.6(6)	30.0(7)	43.5(6)	1.3(4)	-9.6(4)	2.2(4)
N(1)	47(3)	31(4)	52(3)	4(2)	-9(2)	2(2)
N(2)	41(3)	41(4)	44(3)	6(2)	-12(2)	0(2)
N(3)	44(3)	33(4)	48(3)	-1(2)	-9(2)	-4(2)
N(4)	44(3)	32(4)	54(3)	5(2)	-10(2)	0(2)
C(1)	45(4)	49(6)	83(5)	2(4)	-9(3)	-2(3)
C(2)	39(3)	44(5)	70(5)	1.3(3)	-4(3)	-7(3)
C(3)	54(4)	69(7)	81(6)	1.5(5)	7(4)	-4(4)
C(4)	56(4)	52(6)	52(4)	1.2(3)	-6(3)	9(3)
C(5)	50(4)	60(6)	48(4)	-2(3)	-19(3)	14(3)
C(6)	49(4)	46(6)	62(4)	-2(3)	-22(3)	-1(3)
C(7)	62(5)	112(9)	79(6)	-4(5)	-40(4)	14(5)
C(8)	45(4)	39(5)	66(4)	1(3)	-10(3)	2(3)
C(9)	45(4)	35(5)	63(4)	-1(3)	-5(3)	-3(3)
C(10)	50(4)	67(7)	78(5)	-2(4)	9(4)	-5(4)
C(11)	50(4)	48(6)	80(5)	11(4)	-10(3)	-11(3)
C(12)	49(4)	52(6)	61(4)	-1.2(4)	0(3)	0(3)
C(13)	53(4)	39(5)	61(4)	-1.1(3)	-3(3)	-6(3)
C(14)	50(4)	44(6)	75(5)	-3(4)	-14(3)	-4(3)
C(15)	74(5)	62(7)	113(7)	-29(5)	-9(5)	-23(5)
C(16)	47(4)	35(5)	79(5)	2(4)	-9(3)	-1(3)
O(1)	48(2)	26(3)	52(3)	1(2)	-9.9(18)	1.6(19)
C(17)	39(3)	28(5)	52(4)	1(3)	-19(3)	-3(3)
C(18)	51(4)	39(5)	47(4)	2(3)	-16(3)	6(3)
C(19)	49(4)	46(5)	48(4)	-1(3)	-3(3)	1(3)

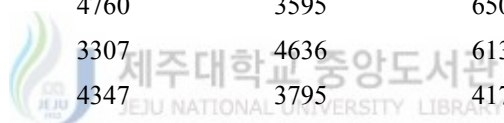
atom	U_{11}	U_{22}	U_{33}	U_{23}	U_{13}	U_{12}
C(20)	40(3)	30(5)	58(4)	6(3)	-9(3)	0(3)
C(21)	64(4)	42(5)	49(4)	9(3)	-25(3)	-7(3)
C(22)	55(4)	38(5)	45(4)	-4(3)	-15(3)	5(3)
N(5)	52(4)	50(5)	86(5)	21(4)	-24(3)	-3(3)
O(2)	51(3)	41(3)	53(3)	1(2)	-21.3(19)	4(2)
O(3)	88(4)	74(5)	77(4)	20(3)	-32(3)	18(3)
O(4)	67(3)	59(5)	97(4)	4(3)	-8(3)	23(3)
Cl(1)	59.7(12)	72(2)	90.7(16)	23.0(12)	5.9(10)	8.1(11)
O(5)	271(12)	281(16)	76(6)	53(7)	23(6)	102(11)
O(6)	158(9)	147(12)	460(2)	102(13)	-111(11)	-94(8)
O(7)	190(7)	71(6)	123(6)	18(5)	-4(5)	50(6)
O(8)	96(5)	209(10)	133(6)	33(6)	34(4)	87(6)
O(1W)	63(3)	48(4)	87(4)	-28(3)	-4(3)	-12(3)

The anisotropic displacement factor exponent takes the form: $-2\pi^2[h^2 a^{*2}U_{11} + \dots + 2hka^*b^*U_{12}]$.

Table 8. Hydrogen coordinates ($\text{\AA} \times 10^4$) and isotropic displacement parameters ($\text{\AA}^2 \times 10^3$) for *cis*-[Cr([14]-decane)(*p*-OC₆H₄NO₂)(OH)]ClO₄·H₂O complex

atom	<i>x</i>	<i>y</i>	<i>z</i>	<i>U</i> (eq)
H(1)	5309	2270	7447	52
H(2)	8564	1121	7202	50
H(3)	8534	2469	5348	50
H(4)	7511	227	6395	51
H(1A)	4201	1697	6339	88
H(1B)	3410	2110	7016	88
H(1C)	3045	1116	6711	88
H(3A)	4362	435	8214	104
H(3B)	3140	348	7860	104
H(3C)	3510	1345	8158	104
H(4A)	5783	1524	8350	64
H(4B)	6488	702	7891	64
H(5A)	7938	1680	8292	62
H(5B)	7350	2595	7982	62
H(6)	9293	3036	7224	61
H(7A)	9757	2195	8231	122
H(7B)	11010	2498	7766	122
H(7C)	10532	1427	7755	122
H(8A)	11224	2464	6549	60
H(8B)	10532	1496	6435	60
H(10A)	11227	1714	5189	100
H(10B)	11841	2707	5337	100
H(10C)	10872	2650	4804	100
H(11A)	9138	3834	6245	89
H(11B)	9600	3930	5444	89

atom	<i>x</i>	<i>y</i>	<i>z</i>	<i>U</i> (eq)
H(11C)	10570	3992	5977	89
H(12A)	9481	1139	4968	66
H(12B)	9513	765	5731	66
H(13A)	7302	930	5098	62
H(13B)	7938	-56	5253	62
H(14)	5320	544	5857	67
H(15A)	6330	-828	5325	125
H(15B)	5056	-1115	5776	125
H(15C)	6333	-1304	6059	125
H(16A)	5677	-220	7153	64
H(16B)	4415	-370	6854	64
H(1D)	7451	3717	6499	63
H(18)	4760	3595	6503	54
H(19)	3307	4636	6138	57
H(21)	4347	3795	4178	60
H(22)	5778	2736	4523	54



2) Binuclear Cu(II)-tetraazadioxa 20-membered macrocyclic complex

(1) $[\text{Cu}_2([\text{20}]\text{-DCHDC})(\text{O}_2\text{N})_2] \cdot 6\text{H}_2\text{O}$.

The green crystal of $[\text{Cu}_2([\text{20}]\text{-DCHDC})(\text{O}_2\text{N})_2] \cdot 6\text{H}_2\text{O}$ suitable for structure determination was acquired from methanol and water (10 : 1 v/v) mixed solvent, by slow evaporation of solvent at room temperature. The green crystal of $[\text{Cu}_2([\text{20}]\text{-DCHDC})(\text{O}_2\text{N})_2] \cdot 6\text{H}_2\text{O}$ was attached to glass fibers and mounted on a Bruker SMART diffractometer equipped with a graphite monochromated Mo $K\alpha$ ($= 0.71073 \text{ \AA}$) radiation, operating at 50 kV and 30 mA and a CCD detector ; 45 frames of two-dimensional diffraction images were collected and processed to obtain the cell parameters and orientation matrix. The crystallographic data, conditions for the collection of intensity data, and some features of the structure refinements are listed in Table 9, and atomic coordinates were given in Table 10. The intensity data were corrected for Lorentz and polarization effects. Absorption correction was not applied during processing. Of the 10,154 unique reflections measured, 2,078 reflections in the range $1.66^\circ \leq \theta \leq 28.28^\circ$ were considered to be observed ($I > 2\sigma(I)$) and were used in subsequent structure analysis. The program SAINTPLUS⁵⁷ was used for integration of the diffraction profiles. The structures were solved by direct methods using the SHELXS program of the SHELXTL package⁵⁸ and refined by full matrix least squares against F^2 for all data using SHELXL. All non-H atoms were refined with anisotropic displacement parameters (Table 11). Hydrogen atoms were placed in idealized positions [$U_{\text{iso}} = 1.2U_{\text{eq}}$ (parent atom)]. Hydrogen coordinates and isotropic

displacement parameters were given in Table 12.

Table 9. Crystal data and structure refinement for $[\text{Cu}_2([\text{20}]\text{-DCHDC})(\text{O}_2\text{N})_2] \cdot 6\text{H}_2\text{O}$ complex

Empirical formula	$\text{C}_{30}\text{H}_{46}\text{Cu}_2\text{N}_6\text{O}_{12}$	
Formula weight	809.81	
Temperature	173(2) K	
Wavelength	0.71073 Å	
Crystal system	Orthorhombic	
Space group	<i>Cmca</i>	
Unit cell dimensions	$a = 16.9119(12)$ Å	$\alpha = 90^\circ$
	$b = 8.0883(6)$ Å	$\beta = 90^\circ$
	$c = 24.5802(17)$ Å	$\gamma = 90^\circ$
Volume	3362.3(4) Å ³	
Z	4	
Density (calculated)	1.600 g/cm ³	
Absorption coefficient	1.337 mm ⁻¹	
$F(000)$	1688	
Crystal size	0.35 x 0.20 x 0.10 mm ³	
Theta range for data collection	1.66 to 28.28°	
Index ranges	-22 ≤ h ≤ 19, -10 ≤ k ≤ 10, -32 ≤ l ≤ 24	
Reflections collected	10154	
Independent reflections	2078 [$R(\text{int}) = 0.0614$]	
Completeness to theta = 28.28°	95.80%	
Absorption correction	None	
Refinement method	Full-matrix least-squares on F^2	
Data / restraints / parameters	2078 / 0 / 141	
Goodness-of-fit on F^2	1.071	
Final R indices [$I > 2\sigma(I)$]	$R_1 = 0.0457$, $wR_2 = 0.1291$	
R indices (all data)	$R_1 = 0.0557$, $wR_2 = 0.1413$	

$$R = \frac{\sum ||F_o| - |F_c||}{\sum |F_o|}, \quad R_w = \left[\frac{\sum w(F_o^2 - F_c^2)^2}{\sum w(F_o^2)^2} \right]^{1/2}$$

$$w = 1/[s^2(F_o^2) + (0.0791P)^2 + 5.7782P] \quad \text{where } P = (F_o^2 + 2F_c^2)/3.$$

Table 10. Atomic coordinates ($\text{\AA} \times 10^4$) and equivalent isotropic displacement parameters ($\text{\AA}^2 \times 10^3$) for $[\text{Cu}_2([\text{20}]\text{-DCHDC})(\text{O}_2\text{N})_2] \cdot 6\text{H}_2\text{O}$ complex

atom	<i>x</i>	<i>y</i>	<i>z</i>	<i>U</i> (eq)
Cu(1)	0	528(1)	4425(1)	39(1)
O(1)	718(2)	0	5000	44(1)
N(1)	787(2)	1669(3)	4018(1)	41(1)
C(1)	1495(3)	0	5000	37(1)
C(2)	1916(2)	754(3)	4567(1)	37(1)
C(3)	2744(2)	743(3)	4582(1)	40(1)
C(4)	3167(3)	0	5000	40(1)
C(5)	4056(3)	0	5000	47(1)
C(6)	1535(2)	1625(3)	4112(1)	41(1)
C(7)	373(3)	2218(7)	3496(2)	34(1)
C(7')	436(4)	2931(7)	3654(2)	35(1)
C(8)	880(2)	3408(3)	3160(1)	43(1)
C(9)	463(5)	4565(9)	2797(3)	44(2)
C(9')	371(5)	3961(10)	2668(3)	43(2)
O(1W)	2511(16)	450(5)	2433(6)	59(2)
O(2W)	1918(2)	2078(3)	6782(1)	67(1)
N(2)	0	-2304(4)	3795(1)	33(1)
O(2)	-578(3)	-2001(6)	3895(2)	132(2)

U(eq) is defined as one third of the trace of the orthogonalized U_{ij} tensor.

Table 11. Anisotropic displacement parameters ($\text{\AA}^2 \times 10^3$) for $[\text{Cu}_2([\text{20}]\text{-DCHDC})\text{-}(\text{O}_2\text{N})_2] \cdot 6\text{H}_2\text{O}$ complex

atom	U_{11}	U_{22}	U_{33}	U_{23}	U_{13}	U_{12}
Cu(1)	61(1)	39(1)	18(1)	10(1)	0	0
O(1)	53(2)	58(2)	21(1)	16(1)	0	0
N(1)	63(2)	38(1)	21(1)	10(1)	6(1)	8(1)
C(1)	63(2)	31(2)	18(1)	1(1)	0	0
C(2)	61(2)	30(1)	21(1)	0(1)	2(1)	0(1)
C(3)	61(2)	31(1)	26(1)	0(1)	4(1)	-2(1)
C(4)	59(2)	32(2)	29(2)	-3(1)	0	0
C(5)	58(3)	49(2)	36(2)	-1(2)	0	0
C(6)	65(2)	34(1)	25(1)	8(1)	9(1)	5(1)
C(7)	65(3)	22(2)	13(2)	1(2)	-1(2)	2(2)
C(7')	64(3)	23(2)	17(2)	2(2)	0(2)	2(2)
C(8)	71(2)	34(1)	23(1)	6(1)	3(1)	-3(1)
C(9)	73(5)	28(4)	32(4)	8(3)	4(3)	-3(3)
C(9')	72(4)	36(4)	20(3)	11(3)	4(3)	-2(3)
O(1W)	107(3)	43(2)	26(7)	-7(2)	13(5)	-13(4)
O(2W)	91(2)	55(1)	57(2)	3(1)	16(1)	0(1)
N(2)	32(1)	30(2)	38(2)	16(1)	0	0
O(2)	204(5)	124(4)	69(2)	27(2)	1(3)	34(4)

The anisotropic displacement factor exponent takes the form: $-2\pi^2[h^2 a^{*2}U_{11} + \dots + 2hka^*b^*U_{12}]$.

Table 12. Hydrogen coordinates ($\text{\AA} \times 10^4$) and isotropic displacement parameters ($\text{\AA}^2 \times 10^3$) for $[\text{Cu}_2([\text{20}]\text{-DCHDC})(\text{O}_2\text{N})_2] \cdot 6\text{H}_2\text{O}$ complex

atom	<i>x</i>	<i>y</i>	<i>z</i>	<i>U</i> (eq)
H(3A)	3026	1262	4295	47
H(5A)	4249	-578	5324	57
H(5B)	4249	1142	5002	57
H(5C)	4249	-565	4673	57
H(6)	1869	2202	3866	50
H(7)	460	1194	3276	40
H(7'A)	532	3940	3880	42
H(8A)	1207	4065	3415	51
H(8B)	1246	2740	2935	51
H(8C)	1206	2452	3046	51
H(8D)	1246	4319	3254	51
H(9A)	641	4339	2421	53
H(9B)	641	5696	2890	53
H(9'A)	536	5105	2581	51
H(9'B)	536	3266	2357	51
H(1W)	2392	204	2758	70
H(2WA)	2038	2904	6978	81
H(2WB)	1435	2030	6696	81

3) Binuclear Ni(II)-tetraazadioxa 22-membered macrocyclic complexes

(1) [H₄[22]-HMTADO](NO₃)₂ · H₂O

Suitable crystals of [H₄[22]-HMTADO](NO₃)₂ · H₂O were obtained by slow evaporation of acetonitrile solution of the compound at atmospheric pressure. The red crystal of [H₄[22]-HMTADO](NO₃)₂ · H₂O was attached to glass fibers and mounted on a Bruker SMART diffractometer equipped with a graphite monochromated Mo K α (= 0.71073 Å) radiation, operating at 50 kV and 30 mA and a CCD detector ; 45 frames of two-dimensional diffraction images were collected and processed to obtain the cell parameters and orientation matrix. The crystallographic data, conditions for the collection of intensity data, and some features of the structure refinements are listed in Table 13, and atomic coordinates were given in Table 14. The intensity data were corrected for Lorentz and polarization effects. Absorption correction was not applied during processing. Of the 18,606 unique reflections measured, 6,839 reflections in the range $2.03^\circ \leq \theta \leq 28.27^\circ$ were considered to be observed ($I > 2\sigma(I)$) and were used in subsequent structure analysis. The program SAINTPLUS⁵⁷ was used for integration of the diffraction profiles. The structures were solved by direct methods using the SHELXS program of the SHELXTL package⁵⁸ and refined by full matrix least squares against F^2 for all data using SHELXL. All non-H atoms were refined with anisotropic displacement parameters (Table 15). Hydrogen atoms were placed in idealized positions [$U_{\text{iso}} = 1.2U_{\text{eq}}$ (parent atom)]. Hydrogen coordinates and isotropic displacement parameters were given in Table 16.

Table 13. Crystal data and structure refinement for [H₄[22]-HMTADO](NO₃)₂ · H₂O

Empirical formula	C ₂₈ H ₄₀ N ₆ O ₉	
Formula weight	604.66	
Temperature	173(2) K	
Wavelength	0.71073 Å	
Crystal system	Monoclinic	
Space group	<i>P</i> 2 ₁ / <i>c</i>	
Unit cell dimensions	<i>a</i> = 9.0298(5) Å	<i>α</i> = 90°
	<i>b</i> = 30.6184(16) Å	<i>β</i> = 107.6870(10)°
	<i>c</i> = 11.1720(6) Å	<i>γ</i> = 90°
Volume	2942.8(3) Å ³	
<i>Z</i>	4	
Density (calculated)	1.365 g/cm ³	
Absorption coefficient	0.103 mm ⁻¹	
<i>F</i> (000)	1288	
Crystal size	0.45 x 0.35 x 0.20 mm ³	
Theta range for data collection	2.03 to 28.27°	
Index ranges	-11 ≤ <i>h</i> ≤ 11, -39 ≤ <i>k</i> ≤ 25, -14 ≤ <i>l</i> ≤ 14	
Reflections collected	18606	
Independent reflections	6839 [<i>R</i> (int) = 0.0453]	
Completeness to theta = 28.27°	94.00%	
Absorption correction	None	
Refinement method	Full-matrix least-squares on <i>F</i> ²	
Data / restraints / parameters	6839 / 0 / 388	
Goodness-of-fit on <i>F</i> ²	1.021	
Final <i>R</i> indices [<i>I</i> > 2σ(<i>I</i>)]	<i>R</i> ₁ = 0.0561, <i>wR</i> ₂ = 0.1324	
<i>R</i> indices (all data)	<i>R</i> ₁ = 0.0947, <i>wR</i> ₂ = 0.1528	

$$R = \frac{\sum ||F_o| - |F_c||}{\sum |F_o|}, \quad R_w = \left[\frac{\sum w(F_o^2 - F_c^2)^2}{\sum w(F_o^2)^2} \right]^{1/2}$$

$$w = 1/[σ^2(F_o^2) + (0.0666P)^2 + 1.7755P] \quad \text{where } P = (F_o^2 + 2F_c^2)/3.$$

Table 14. Atomic coordinates ($\text{\AA} \times 10^4$) and equivalent isotropic displacement parameters ($\text{\AA}^2 \times 10^3$) for $[\text{H}_4[22]\text{-HMTADO}](\text{NO}_3)_2 \cdot \text{H}_2\text{O}$

atom	<i>x</i>	<i>y</i>	<i>z</i>	<i>U</i> (eq)
O(1)	6077(2)	1681(1)	601(1)	25(1)
O(2)	6374(2)	721(1)	-600(1)	24(1)
N(1)	6835(2)	1285(1)	2825(2)	22(1)
N(2)	7082(2)	400(1)	1674(2)	23(1)
N(3)	5439(2)	1200(1)	-2672(2)	22(1)
N(4)	5076(2)	2064(1)	-1577(2)	21(1)
C(1)	4736(2)	1753(1)	731(2)	20(1)
C(2)	3514(2)	1976(1)	-212(2)	20(1)
C(3)	2089(2)	2066(1)	-13(2)	23(1)
C(4)	1760(2)	1950(1)	1079(2)	23(1)
C(5)	2900(2)	1721(1)	1978(2)	23(1)
C(6)	4353(2)	1620(1)	1836(2)	20(1)
C(7)	5435(2)	1380(1)	2813(2)	22(1)
C(8)	7953(2)	1055(1)	3874(2)	23(1)
C(9)	9072(2)	746(1)	3495(2)	20(1)
C(10)	8282(3)	320(1)	2879(2)	25(1)
C(11)	5606(2)	368(1)	1501(2)	23(1)
C(12)	4473(2)	511(1)	375(2)	22(1)
C(13)	2906(3)	495(1)	316(2)	26(1)
C(14)	1726(3)	665(1)	-679(2)	28(1)
C(15)	2160(2)	863(1)	-1642(2)	26(1)
C(16)	3711(2)	887(1)	-1649(2)	22(1)
C(17)	4952(2)	704(1)	-626(2)	19(1)
C(18)	4049(3)	1130(1)	-2623(2)	24(1)
C(19)	5781(3)	1475(1)	-3628(2)	25(1)

atom	<i>x</i>	<i>y</i>	<i>z</i>	<i>U</i> (eq)
C(20)	6513(2)	1918(1)	-3147(2)	22(1)
C(21)	5413(3)	2216(1)	-2714(2)	25(1)
C(22)	3763(2)	2115(1)	-1354(2)	22(1)
C(23)	225(3)	2068(1)	1286(2)	32(1)
C(24)	10294(3)	610(1)	4730(2)	27(1)
C(25)	9866(3)	978(1)	2640(2)	25(1)
C(26)	53(3)	657(1)	-683(3)	44(1)
C(27)	8058(3)	1865(1)	-2107(2)	34(1)
C(28)	6787(3)	2145(1)	-4290(2)	31(1)
N(5)	6928(3)	227(1)	6652(2)	33(1)
O(3)	7537(2)	560(1)	6367(2)	52(1)
O(4)	5487(2)	214(1)	6477(2)	40(1)
O(5)	7759(2)	-95(1)	7130(2)	43(1)
N(6)	1021(2)	1888(1)	5089(2)	31(1)
O(6)	-203(2)	2014(1)	4300(2)	36(1)
O(7)	1004(3)	1759(1)	6137(2)	59(1)
O(8)	2263(2)	1892(1)	4806(2)	54(1)
O(1W)	4051(2)	782(1)	4409(2)	45(1)

U(eq) is defined as one third of the trace of the orthogonalized U_{ij} tensor.

Table 15. Anisotropic displacement parameters ($\text{\AA}^2 \times 10^3$) for $[\text{H}_4[22]\text{-HMTADO}]\text{-}(\text{NO}_3)_2 \cdot \text{H}_2\text{O}$

atom	U_{11}	U_{22}	U_{33}	U_{23}	U_{13}	U_{12}
O(1)	25(1)	31(1)	22(1)	5(1)	10(1)	8(1)
O(2)	21(1)	29(1)	24(1)	5(1)	7(1)	1(1)
N(1)	23(1)	22(1)	20(1)	5(1)	8(1)	4(1)
N(2)	27(1)	21(1)	19(1)	3(1)	3(1)	0(1)
N(3)	29(1)	20(1)	18(1)	1(1)	7(1)	1(1)
N(4)	27(1)	23(1)	14(1)	1(1)	6(1)	4(1)
C(1)	22(1)	17(1)	20(1)	-3(1)	7(1)	1(1)
C(2)	24(1)	18(1)	18(1)	-2(1)	6(1)	0(1)
C(3)	20(1)	24(1)	22(1)	0(1)	3(1)	2(1)
C(4)	20(1)	25(1)	25(1)	0(1)	9(1)	0(1)
C(5)	26(1)	24(1)	22(1)	0(1)	9(1)	-1(1)
C(6)	22(1)	19(1)	19(1)	0(1)	6(1)	0(1)
C(7)	24(1)	24(1)	19(1)	0(1)	9(1)	-1(1)
C(8)	23(1)	28(1)	17(1)	4(1)	4(1)	5(1)
C(9)	19(1)	23(1)	18(1)	3(1)	2(1)	1(1)
C(10)	28(1)	22(1)	21(1)	6(1)	0(1)	2(1)
C(11)	29(1)	19(1)	20(1)	1(1)	6(1)	-4(1)
C(12)	26(1)	19(1)	18(1)	-3(1)	4(1)	-3(1)
C(13)	29(1)	27(1)	21(1)	-2(1)	10(1)	-6(1)
C(14)	21(1)	32(1)	30(1)	-6(1)	7(1)	-4(1)
C(15)	22(1)	29(1)	23(1)	-4(1)	1(1)	0(1)
C(16)	24(1)	19(1)	20(1)	-3(1)	4(1)	0(1)
C(17)	24(1)	15(1)	19(1)	-3(1)	5(1)	0(1)
C(18)	28(1)	21(1)	19(1)	-3(1)	2(1)	1(1)
C(19)	34(1)	25(1)	18(1)	1(1)	11(1)	0(1)

atom	U_{11}	U_{22}	U_{33}	U_{23}	U_{13}	U_{12}
C(20)	24(1)	25(1)	18(1)	3(1)	9(1)	2(1)
C(21)	34(1)	25(1)	20(1)	6(1)	12(1)	5(1)
C(22)	25(1)	20(1)	18(1)	-1(1)	4(1)	3(1)
C(23)	25(1)	39(1)	34(1)	10(1)	13(1)	9(1)
C(24)	25(1)	32(1)	21(1)	5(1)	0(1)	3(1)
C(25)	25(1)	28(1)	23(1)	4(1)	8(1)	2(1)
C(26)	24(1)	65(2)	43(2)	-1(1)	11(1)	-3(1)
C(27)	24(1)	45(2)	32(1)	4(1)	5(1)	2(1)
C(28)	34(1)	33(1)	29(1)	7(1)	17(1)	1(1)
N(5)	48(1)	31(1)	24(1)	5(1)	15(1)	8(1)
O(3)	55(1)	45(1)	61(1)	24(1)	26(1)	4(1)
O(4)	43(1)	40(1)	41(1)	7(1)	16(1)	5(1)
O(5)	57(1)	31(1)	38(1)	6(1)	9(1)	14(1)
N(6)	32(1)	26(1)	32(1)	-5(1)	5(1)	3(1)
O(6)	33(1)	41(1)	31(1)	0(1)	5(1)	3(1)
O(7)	78(2)	64(2)	33(1)	15(1)	15(1)	25(1)
O(8)	30(1)	62(1)	70(1)	-8(1)	14(1)	3(1)
O(1W)	48(1)	34(1)	44(1)	6(1)	2(1)	-9(1)

The anisotropic displacement factor exponent takes the form: $-2\pi^2[h^2 a^{*2}U_{11} + \dots + 2hka^*b^*U_{12}]$.

Table 16. Hydrogen coordinates ($\text{\AA}\times 10^4$) and isotropic displacement parameters ($\text{\AA}^2\times 10^3$) for $[\text{H}_4[22]\text{-HMTADO}](\text{NO}_3)_2 \cdot \text{H}_2\text{O}$

atom	<i>x</i>	<i>y</i>	<i>z</i>	<i>U</i> (eq)
H(1N)	7154	1404	2194	26
H(2N)	7357	509	1010	28
H(3N)	6211	1082	-2042	27
H(4N)	5832	1938	-982	26
H(3)	1312	2213	-654	27
H(5)	2686	1629	2721	28
H(7)	5105	1283	3499	26
H(8A)	7363	884	4329	27
H(8B)	8574	1275	4466	27
H(10A)	9081	122	2740	30
H(10B)	7803	172	3458	30
H(11)	5260	245	2149	27
H(13)	2636	360	987	31
H(15)	1373	986	-2326	31
H(18)	3202	1246	-3273	28
H(19A)	4803	1526	-4314	30
H(19B)	6495	1313	-3990	30
H(21A)	5879	2511	-2554	30
H(21B)	4422	2242	-3403	30
H(22)	2931	2251	-1976	26
H(23A)	211	1959	2107	38
H(23B)	-630	1935	624	38
H(23C)	102	2386	1260	38
H(24A)	10835	870	5158	33
H(24B)	11046	411	4545	33

atom	<i>x</i>	<i>y</i>	<i>z</i>	<i>U</i> (eq)
H(24C)	9778	462	5273	33
H(25A)	10362	1246	3048	30
H(25B)	9088	1051	1839	30
H(25C)	10654	785	2485	30
H(26A)	-20	505	69	53
H(26B)	-580	504	-1434	53
H(26C)	-327	957	-687	53
H(27A)	7876	1721	-1380	41
H(27B)	8523	2153	-1859	41
H(27C)	8765	1686	-2416	41
H(28A)	7254	2432	-4039	37
H(28B)	5792	2180	-4950	37
H(28C)	7488	1967	-4607	37
H(1W)	3602	560	3810	54
H(2W)	4728	624	5114	54

(2) [Ni₂([22]-HMTADO)(μ-O₂N)(NO₂)(OH₂)].

The green crystals of [Ni₂([22]-HMTADO)(μ-O₂N)(NO₂)(OH₂)] suitable for X-ray diffraction study which deposited on standing for *ca.* 1 month were recrystallized from methanol of this complex. The green crystal of [Ni₂([22]-HMTADO)(μ-O₂N)(NO₂)(OH₂)] was attached to glass fibers and mounted on a Bruker SMART diffractometer equipped with a graphite monochromated Mo Kα (= 0.71073 Å) radiation, operating at 50 kV and 30 mA and a CCD detector ; 45 frames of two-dimensional diffraction images were collected and processed to obtain the cell parameters and orientation matrix. The crystallographic data, conditions for the collection of intensity data, and some features of the structure refinements are listed in Table 17, and atomic coordinates were given in Table 18. The intensity data were corrected for Lorentz and polarization effects. Absorption correction was applied during processing. Of the 18,407 unique reflections measured, 6,821 reflections in the range $1.67^\circ \leq \theta \leq 28.26^\circ$ were considered to be observed ($I > 2\sigma(I)$) and were used in subsequent structure analysis. The program SAINTPLUS⁵⁷ was used for integration of the diffraction profiles. The structures were solved by direct methods using the SHELXS program of the SHELXTL package⁵⁸ and refined by full matrix least squares against F^2 for all data using SHELXL. All non-H atoms were refined with anisotropic displacement parameters (Table 19). Hydrogen atoms were placed in idealized positions [$U_{\text{iso}} = 1.2U_{\text{eq}}$ (parent atom)]. Hydrogen coordinates and isotropic displacement parameters were given in Table 20.

Table 17. Crystal data and structure refinement for [Ni₂([22]-HMTADO)(μ-O₂N)(NO₂)(OH₂)]

Empirical formula	C ₂₈ H ₃₆ N ₆ Ni ₂ O ₇	
Formula weight	686.05	
Temperature	173(2) K	
Wavelength	0.71073 Å	
Crystal system	Monoclinic	
Space group	P2 ₁ /c	
Unit cell dimensions	<i>a</i> = 12.5260(10) Å	<i>α</i> = 90°
	<i>b</i> = 12.8514(10) Å	<i>β</i> = 103.616(2)°
	<i>c</i> = 18.9480(15) Å	<i>γ</i> = 90°
Volume	2964.5(4) Å ³	
Z	4	
Density (calculated)	1.537 g/cm ³	
Absorption coefficient	1.326 mm ⁻¹	
<i>F</i> (000)	1432	
Crystal size	0.25 x 0.20 x 0.08 mm ³	
Theta range for data collection	1.67 to 28.26°	
Index ranges	-14 ≤ <i>h</i> ≤ 15, -16 ≤ <i>k</i> ≤ 16, -23 ≤ <i>l</i> ≤ 24	
Reflections collected	18407	
Independent reflections	6821 [<i>R</i> (int) = 0.0593]	
Completeness to theta = 28.26°	92.90%	
Absorption correction	Empirical(SADABS Bruker)	
Refinement method	Full-matrix least-squares on <i>F</i> ²	
Data / restraints / parameters	6821 / 4 / 394	
Goodness-of-fit on <i>F</i> ²	1.172	
Final <i>R</i> indices [<i>I</i> > 2σ(<i>I</i>)]	<i>R</i> ₁ = 0.0745, <i>wR</i> ₂ = 0.1405	
<i>R</i> indices (all data)	<i>R</i> ₁ = 0.1079, <i>wR</i> ₂ = 0.1522	

$$R = \frac{\sum ||F_o| - |F_c||}{\sum |F_o|}, \quad R_w = \left[\frac{\sum w(F_o^2 - F_c^2)^2}{\sum w(F_o^2)^2} \right]^{1/2}$$

$$w = 1/[σ^2(F_o^2) + (0.0528P)^2 + 5.1211P] \quad \text{where } P = (F_o^2 + 2F_c^2)/3.$$

Table 18. Atomic coordinates ($\text{\AA} \times 10^4$) and equivalent isotropic displacement parameters ($\text{\AA}^2 \times 10^3$) for $[\text{Ni}_2([\text{22}]\text{-HMTADO})(\mu\text{-O}_2\text{N})(\text{NO}_2)(\text{OH}_2)]$

atom	<i>x</i>	<i>y</i>	<i>z</i>	<i>U</i> (eq)
Ni(1)	2088(1)	1572(1)	1589(1)	14(1)
Ni(2)	2126(1)	3684(1)	2286(1)	13(1)
O(1)	2515(3)	2191(2)	2610(2)	16(1)
O(1W)	487(3)	1205(3)	1677(2)	25(1)
O(2)	1470(3)	3011(2)	1303(2)	15(1)
O(3)	3605(3)	2141(3)	1437(2)	22(1)
O(4)	3642(3)	3668(3)	1926(2)	23(1)
O(5)	18(3)	2791(3)	2517(2)	34(1)
O(6)	414(3)	4208(3)	3092(2)	27(1)
N(1)	2741(3)	184(3)	1998(2)	18(1)
N(2)	2919(3)	4242(3)	3279(2)	17(1)
N(3)	1726(3)	5112(3)	1847(2)	15(1)
N(4)	1644(3)	1079(3)	545(2)	20(1)
N(5)	4094(4)	3005(3)	1593(2)	27(1)
N(6)	654(3)	3552(3)	2669(2)	17(1)
C(1)	2415(5)	-739(4)	793(3)	24(1)
C(2)	2413(5)	-794(4)	1603(3)	25(1)
C(3)	3473(4)	117(4)	2585(3)	21(1)
C(4)	3868(4)	917(4)	3125(3)	16(1)
C(5)	4737(4)	621(4)	3708(3)	24(1)
C(6)	5160(4)	1256(4)	4296(3)	24(1)
C(7)	4700(4)	2241(4)	4280(3)	22(1)
C(8)	3854(4)	2592(4)	3705(3)	20(1)
C(9)	3381(4)	1924(4)	3117(3)	17(1)
C(10)	3545(4)	3675(4)	3760(3)	20(1)

atom	<i>x</i>	<i>y</i>	<i>z</i>	<i>U</i> (eq)
C(11)	2764(5)	5324(4)	3513(3)	22(1)
C(12)	2734(4)	6155(4)	2929(3)	20(1)
C(13)	1706(4)	6032(4)	2310(3)	20(1)
C(14)	1485(4)	5276(4)	1165(2)	16(1)
C(15)	1422(4)	4546(4)	577(2)	15(1)
C(16)	1341(4)	4976(4)	-115(2)	17(1)
C(17)	1323(4)	4406(4)	-728(2)	18(1)
C(18)	1354(4)	3333(4)	-650(3)	20(1)
C(19)	1427(4)	2838(4)	27(2)	16(1)
C(20)	1456(4)	3438(3)	666(2)	14(1)
C(21)	1427(4)	1711(4)	6(3)	22(1)
C(22)	1492(5)	-30(4)	374(3)	25(1)
C(23)	2158(6)	-1838(4)	486(3)	36(2)
C(24)	3543(5)	-374(4)	705(3)	31(1)
C(25)	6065(4)	911(5)	4931(3)	34(1)
C(26)	3786(4)	6131(4)	2643(3)	28(1)
C(27)	2651(5)	7204(4)	3301(3)	26(1)
C(28)	1279(5)	4916(4)	-1452(3)	27(1)

U(eq) is defined as one third of the trace of the orthogonalized U_{ij} tensor.

Table 19. Anisotropic displacement parameters ($\text{\AA}^2 \times 10^3$) for $[\text{Ni}_2([\text{22}]-\text{HMTADO})(\mu\text{-O}_2\text{N})(\text{NO}_2)(\text{OH}_2)]$

atom	U_{11}	U_{22}	U_{33}	U_{23}	U_{13}	U_{12}
Ni(1)	21(1)	9(1)	14(1)	1(1)	5(1)	2(1)
Ni(2)	17(1)	9(1)	13(1)	1(1)	3(1)	2(1)
O(1)	18(2)	14(2)	15(2)	2(1)	3(1)	5(1)
O(1W)	31(2)	16(2)	28(2)	-1(2)	10(2)	-3(2)
O(2)	19(2)	13(2)	13(2)	4(1)	5(1)	3(1)
O(3)	23(2)	20(2)	25(2)	-3(2)	8(2)	3(2)
O(4)	27(2)	13(2)	30(2)	-3(2)	10(2)	-2(1)
O(5)	33(2)	23(2)	51(3)	-9(2)	20(2)	-7(2)
O(6)	39(2)	20(2)	27(2)	-2(2)	17(2)	6(2)
N(1)	28(2)	13(2)	15(2)	3(2)	8(2)	3(2)
N(2)	18(2)	14(2)	20(2)	0(2)	5(2)	0(2)
N(3)	15(2)	16(2)	17(2)	-4(2)	8(2)	-1(2)
N(4)	25(2)	12(2)	24(2)	0(2)	7(2)	0(2)
N(5)	27(3)	23(2)	32(3)	-2(2)	9(2)	3(2)
N(6)	23(2)	11(2)	17(2)	4(2)	5(2)	4(2)
C(1)	39(3)	15(2)	20(3)	-3(2)	7(2)	7(2)
C(2)	40(3)	15(3)	23(3)	3(2)	13(2)	4(2)
C(3)	29(3)	13(2)	26(3)	4(2)	16(2)	3(2)
C(4)	18(2)	15(2)	19(2)	8(2)	9(2)	5(2)
C(5)	23(3)	22(3)	30(3)	9(2)	10(2)	4(2)
C(6)	18(3)	27(3)	26(3)	14(2)	2(2)	-2(2)
C(7)	23(3)	21(3)	19(3)	2(2)	-3(2)	-5(2)
C(8)	19(3)	22(3)	17(3)	7(2)	0(2)	3(2)
C(9)	21(3)	17(2)	16(2)	7(2)	11(2)	0(2)
C(10)	21(3)	22(3)	15(2)	-1(2)	2(2)	-3(2)

atom	U_{11}	U_{22}	U_{33}	U_{23}	U_{13}	U_{12}
C(11)	35(3)	19(3)	12(2)	1(2)	2(2)	5(2)
C(12)	25(3)	12(2)	24(3)	-3(2)	8(2)	-2(2)
C(13)	26(3)	13(2)	22(3)	1(2)	7(2)	2(2)
C(14)	21(3)	14(2)	16(2)	4(2)	8(2)	1(2)
C(15)	16(2)	17(2)	10(2)	3(2)	1(2)	1(2)
C(16)	17(2)	20(2)	15(2)	8(2)	3(2)	4(2)
C(17)	21(3)	23(3)	11(2)	5(2)	3(2)	2(2)
C(18)	21(3)	23(3)	16(2)	-1(2)	2(2)	2(2)
C(19)	19(3)	16(2)	11(2)	0(2)	0(2)	-2(2)
C(20)	13(2)	14(2)	15(2)	0(2)	3(2)	2(2)
C(21)	34(3)	18(3)	14(2)	-5(2)	4(2)	1(2)
C(22)	35(3)	20(3)	19(3)	0(2)	4(2)	-1(2)
C(23)	62(4)	20(3)	26(3)	-5(2)	9(3)	9(3)
C(24)	41(4)	30(3)	26(3)	0(2)	16(3)	12(3)
C(25)	22(3)	32(3)	42(4)	19(3)	-3(3)	3(2)
C(26)	28(3)	20(3)	36(3)	-2(2)	8(2)	-6(2)
C(27)	40(3)	15(3)	23(3)	-5(2)	7(2)	1(2)
C(28)	34(3)	30(3)	16(3)	9(2)	5(2)	0(2)

The anisotropic displacement factor exponent takes the form: $-2\pi^2[h^2 a^{*2}U_{11} + \dots + 2hka^*b^*U_{12}]$.

Table 20. Hydrogen coordinates ($\text{\AA}\times 10^4$) and isotropic displacement parameters ($\text{\AA}^2\times 10^3$) for $[\text{Ni}_2([\text{22}]\text{-HMTADO})(\mu\text{-O}_2\text{N})(\text{NO}_2)(\text{OH}_2)]$

atom	x	y	z	U(eq)
H(1WA)	360(50)	610(20)	1830(30)	29
H(1WB)	360(50)	1700(30)	1940(30)	29
H(2A)	1666	-983	1649	30
H(2B)	2920	-1353	1834	30
H(3)	3810	-546	2686	25
H(5)	5048	-51	3697	29
H(7)	4969	2698	4676	27
H(10)	3848	4005	4211	24
H(11A)	3368	5492	3938	27
H(11B)	2068	5357	3674	27
H(13A)	1055	5985	2520	24
H(13B)	1621	6664	2002	24
H(14)	1322	5979	1023	20
H(16)	1295	5712	-161	21
H(18)	1325	2914	-1067	24
H(21)	1244	1403	-463	27
H(22A)	1431	-125	-153	30
H(22B)	789	-258	477	30
H(23A)	1433	-2053	546	43
H(23B)	2717	-2323	747	43
H(23C)	2158	-1841	-31	43
H(24A)	4114	-837	979	37
H(24B)	3679	338	890	37
H(24C)	3555	-390	190	37
H(25A)	6286	198	4848	41

atom	x	y	z	U(eq)
H(25B)	5797	934	5377	41
H(25C)	6697	1377	4980	41
H(26A)	4429	6209	3051	33
H(26B)	3769	6703	2299	33
H(26C)	3832	5467	2399	33
H(27A)	3301	7304	3699	31
H(27B)	1991	7211	3493	31
H(27C)	2607	7768	2946	31
H(28A)	1260	5673	-1398	32
H(28B)	617	4686	-1805	32
H(28C)	1931	4719	-1623	32



(3) $\{[\text{Ni}_6([\text{22}]\text{-HMTADO})_3(\text{CN})_4][\text{Ni}(\text{CN})_4]\cdot 5\text{H}_2\text{O}\cdot 8\text{CH}_3\text{OH}\}_n$

The green polymer crystals of $\{[\text{Ni}_6([\text{22}]\text{-HMTADO})_3(\text{CN})_4][\text{Ni}(\text{CN})_4]\cdot 5\text{H}_2\text{O}\cdot 8\text{CH}_3\text{OH}\}_n$ suitable for X-ray diffraction study which deposited on standing for *ca.* 2 month were recrystallized from methanol solution of $[\text{Ni}([\text{22}]\text{-HMTADO})(\text{CN})_2]\cdot \text{H}_2\text{O}$ complex. The green polymer crystal of $\{[\text{Ni}_6([\text{22}]\text{-HMTADO})_3(\text{CN})_4][\text{Ni}(\text{CN})_4]\cdot 5\text{H}_2\text{O}\cdot 8\text{CH}_3\text{OH}\}_n$ was attached to glass fibers and mounted on a Bruker SMART diffractometer equipped with a graphite monochromated Mo $\text{K}\alpha$ ($= 0.71073 \text{ \AA}$) radiation, operating at 50 kV and 30 mA and a CCD detector ; 45 frames of two-dimensional diffraction images were collected and processed to obtain the cell parameters and orientation matrix. The crystallographic data, conditions for the collection of intensity data, and some features of the structure refinements are listed in Table 21, and atomic coordinates were given in Table 22. The intensity data were corrected for Lorentz and polarization effects. Absorption correction was applied during processing. Of the 16,667 unique reflections measured, 11,329 reflections in the range $1.81^\circ \leq \theta \leq 26.37^\circ$ were considered to be observed ($I > 2\sigma(I)$) and were used in subsequent structure analysis. The program SAINTPLUS⁵⁷ was used for integration of the diffraction profiles. The structures were solved by direct methods using the SHELXS program of the SHELXTL package⁵⁸ and refined by full matrix least squares against F^2 for all data using SHELXL. All non-H atoms were refined with anisotropic displacement parameters (Table 23). Hydrogen atoms were placed in idealized positions [$U_{\text{iso}} = 1.2U_{\text{eq}}$ (parent atom)]. Hydrogen coordinates and isotropic displacement parameters were given in Table 24.

Table 21. Crystal data and structure refinement for $\{[\text{Ni}_6([\text{22}]\text{-HMTADO})_3\text{-(CN)}_4][\text{Ni}(\text{CN})_4]\cdot 5\text{H}_2\text{O}\cdot 8\text{CH}_3\text{OH}\}_n$

Empirical formula	$\text{C}_{100}\text{H}_{144}\text{N}_{20}\text{Ni}_7\text{O}_{19}$	
Formula weight	2341.32	
Temperature	173(2) K	
Wavelength	0.71073 Å	
Crystal system	Triclinic	
Space group	$P\bar{1}$	
Unit cell dimensions	$a = 11.8665(13)$ Å	$\alpha = 114.381(2)^\circ$
	$b = 15.4683(17)$ Å	$\beta = 102.613(2)^\circ$
	$c = 17.7916(19)$ Å	$\gamma = 96.351(2)^\circ$
Volume	2827.7(5) Å ³	
Z	1	
Density (calculated)	1.375 g/cm ³	
Absorption coefficient	1.211 mm ⁻¹	
$F(000)$	1232	
Crystal size	0.35 x 0.30 x 0.20 mm ³	
Theta range for data collection	1.81 to 26.37°	
Index ranges	-14 ≤ h ≤ 13, -18 ≤ k ≤ 19, -19 ≤ l ≤ 22	
Reflections collected	16667	
Independent reflections	11329 [$R(\text{int}) = 0.0389$]	
Completeness to theta = 26.37°	98.00%	
Absorption correction	Empirical(SADABS)	
Refinement method	Full-matrix least-squares on F^2	
Data / restraints / parameters	11329 / 7 / 666	
Goodness-of-fit on F^2	1.04	
Final R indices [$I > 2\sigma(I)$]	$R_1 = 0.0639$, $wR_2 = 0.1548$	
R indices (all data)	$R_1 = 0.1089$, $wR_2 = 0.1787$	

$$R = \frac{\sum \|F_o\| - |F_c|}{\sum |F_o|}, \quad R_w = \left[\frac{\sum w(F_o^2 - F_c^2)^2}{\sum w(F_o^2)^2} \right]^{1/2}$$

$$w = 1/[\sigma^2(F_o^2) + (0.0852P)^2 + 3.1894P] \quad \text{where } P = (F_o^2 + 2F_c^2)/3.$$

Table 22. Atomic coordinates ($\text{\AA} \times 10^4$) and equivalent isotropic displacement parameters ($\text{\AA}^2 \times 10^3$) for $\{[\text{Ni}_6([\text{22}]\text{-HMTADO})_3(\text{CN})_4][\text{Ni}(\text{CN})_4] \cdot 5\text{H}_2\text{O} \cdot 8\text{CH}_3\text{OH}\}_n$

atom	<i>x</i>	<i>y</i>	<i>z</i>	<i>U</i> (eq)
Ni(1)	8637(1)	8273(1)	3614(1)	18(1)
Ni(2)	8488(1)	8401(1)	5372(1)	18(1)
Ni(3)	5161(1)	5257(1)	4235(1)	20(1)
Ni(4)	0	5000	0	44(1)
O(1)	7563(3)	8625(2)	4388(2)	22(1)
O(2)	9387(3)	7840(2)	4501(2)	19(1)
O(3)	5466(3)	4297(2)	4723(2)	22(1)
N(1)	7313(4)	8253(3)	2663(3)	23(1)
N(2)	9392(4)	7370(3)	2792(3)	23(1)
N(3)	9497(4)	8050(3)	6211(3)	21(1)
N(4)	7420(4)	8979(3)	6094(3)	24(1)
N(5)	5313(4)	4302(3)	3107(3)	27(1)
N(6)	4071(4)	5914(3)	3714(3)	24(1)
N(7)	7305(4)	6995(3)	4799(3)	24(1)
N(8)	-124(7)	4510(6)	828(5)	84(2)
N(9)	1268(7)	6043(6)	848(5)	80(2)
N(10)	9634(4)	9758(3)	5895(3)	23(1)
C(1)	6439(4)	8616(3)	4219(3)	20(1)
C(2)	5831(4)	8818(4)	4868(3)	23(1)
C(3)	4640(5)	8853(4)	4662(4)	27(1)
C(4)	3958(5)	8645(4)	3838(4)	28(1)
C(5)	4542(4)	8444(4)	3219(4)	29(1)
C(6)	5757(5)	8442(4)	3388(3)	25(1)

atom	x	y	z	U(eq)
C(7)	6255(5)	8305(4)	2678(3)	26(1)
C(8)	7595(5)	8205(4)	1887(4)	34(1)
C(9)	8140(5)	7353(4)	1446(3)	33(1)
C(10)	9393(5)	7474(4)	2006(3)	32(1)
C(11)	9893(5)	6730(4)	2898(3)	26(1)
C(12)	10109(4)	6519(4)	3635(3)	23(1)
C(13)	10631(5)	5731(4)	3557(4)	30(1)
C(14)	10930(4)	5467(4)	4217(4)	26(1)
C(15)	10718(5)	6048(4)	4984(4)	27(1)
C(16)	10191(4)	6842(4)	5103(3)	22(1)
C(17)	9865(4)	7089(3)	4414(3)	21(1)
C(18)	10097(4)	7394(4)	5969(3)	24(1)
C(19)	9628(5)	8569(4)	7133(3)	30(1)
C(20)	8447(5)	8691(4)	7352(3)	32(1)
C(21)	7853(5)	9359(4)	7028(3)	29(1)
C(22)	6396(5)	9055(4)	5762(4)	26(1)
C(23)	2641(5)	8625(5)	3639(4)	40(2)
C(24)	7329(6)	6381(5)	1215(4)	47(2)
C(25)	8297(6)	7382(5)	619(4)	48(2)
C(26)	11510(5)	4620(4)	4105(4)	34(1)
C(27)	7604(6)	7718(4)	7011(4)	39(2)
C(28)	8763(6)	9214(5)	8337(4)	48(2)
C(29)	5915(4)	3530(4)	4413(3)	23(1)
C(30)	6423(4)	3115(4)	4953(3)	23(1)
C(31)	6915(5)	2316(4)	4621(4)	28(1)
C(32)	6883(5)	1845(4)	3771(4)	30(1)
C(33)	6391(5)	2252(4)	3245(4)	32(1)

atom	<i>x</i>	<i>y</i>	<i>z</i>	<i>U</i> (eq)
C(34)	5943(5)	3087(4)	3555(3)	27(1)
C(35)	5582(5)	3477(4)	2955(4)	33(1)
C(36)	5159(5)	4567(4)	2392(3)	33(1)
C(37)	4008(5)	4872(4)	2166(3)	32(1)
C(38)	4025(6)	5860(4)	2856(4)	35(1)
C(39)	3542(5)	6531(4)	4146(4)	26(1)
C(40)	7355(6)	935(4)	3430(5)	44(2)
C(41)	2950(6)	4104(5)	2014(4)	49(2)
C(42)	3940(7)	4968(5)	1332(4)	49(2)
C(43)	6588(5)	6320(4)	4598(3)	24(1)
C(44)	-216(8)	4227(6)	1303(5)	58(2)
C(45)	2001(6)	6692(5)	1367(5)	54(2)
C(46)	9722(4)	9517(4)	3910(3)	19(1)
O(50)	-911(10)	3129(7)	2067(6)	152(4)
C(50)	-1801(11)	3654(17)	2376(12)	182(10)
O(51)	6148(9)	3548(8)	79(8)	179(4)
C(51)	5378(11)	2666(8)	-139(9)	141(6)
O(52)	2273(18)	-1650(8)	1195(7)	283(10)
C(52)	1486(16)	-1805(11)	331(12)	165(6)
O(53)	4880(30)	30(19)	1463(14)	570(30)
C(53)	4420(20)	-1040(20)	1254(12)	256(13)
O(1W)	4982(13)	1816(8)	809(6)	227(7)
O(2W)	7350(20)	9774(13)	10412(13)	360(12)
O(3W)	7150(20)	1430(18)	1250(11)	199(11)

U(eq) is defined as one third of the trace of the orthogonalized U_{ij} tensor.

Table 23. Anisotropic displacement parameters ($\text{\AA}^2 \times 10^3$) for $\{[\text{Ni}_6([\text{22}]\text{-HMTADO})_3(\text{CN})_4][\text{Ni}(\text{CN})_4] \cdot 5\text{H}_2\text{O} \cdot 8\text{CH}_3\text{OH}\}_n$

atom	U_{11}	U_{22}	U_{33}	U_{23}	U_{13}	U_{12}
Ni(1)	16(1)	15(1)	22(1)	8(1)	6(1)	1(1)
Ni(2)	17(1)	14(1)	23(1)	9(1)	7(1)	3(1)
Ni(3)	21(1)	15(1)	23(1)	9(1)	7(1)	2(1)
Ni(4)	43(1)	49(1)	33(1)	9(1)	15(1)	17(1)
O(1)	14(2)	21(2)	30(2)	12(2)	6(2)	5(1)
O(2)	21(2)	14(2)	26(2)	10(2)	10(2)	5(1)
O(3)	28(2)	18(2)	26(2)	12(2)	13(2)	9(2)
N(1)	22(2)	19(2)	23(2)	8(2)	4(2)	0(2)
N(2)	23(2)	21(2)	22(2)	7(2)	7(2)	2(2)
N(3)	22(2)	19(2)	21(2)	10(2)	6(2)	1(2)
N(4)	28(2)	18(2)	26(2)	10(2)	12(2)	4(2)
N(5)	34(3)	23(2)	25(2)	9(2)	11(2)	7(2)
N(6)	26(2)	20(2)	29(2)	14(2)	7(2)	3(2)
N(7)	24(2)	19(2)	26(2)	8(2)	6(2)	1(2)
N(8)	65(5)	66(5)	80(6)	-7(4)	19(4)	20(4)
N(9)	98(6)	100(6)	79(5)	50(5)	56(5)	64(5)
N(10)	22(2)	21(2)	25(2)	9(2)	7(2)	4(2)
C(1)	18(3)	10(2)	30(3)	8(2)	6(2)	0(2)
C(2)	21(3)	15(3)	33(3)	10(2)	10(2)	3(2)
C(3)	24(3)	18(3)	41(3)	13(3)	16(2)	5(2)
C(4)	16(3)	21(3)	46(4)	16(3)	5(2)	3(2)
C(5)	17(3)	20(3)	43(3)	13(3)	0(2)	1(2)
C(6)	21(3)	17(3)	34(3)	10(2)	6(2)	6(2)
C(7)	26(3)	22(3)	25(3)	9(2)	-1(2)	2(2)
C(8)	39(3)	42(4)	25(3)	19(3)	6(3)	11(3)

atom	U_{11}	U_{22}	U_{33}	U_{23}	U_{13}	U_{12}
C(9)	40(3)	29(3)	22(3)	7(3)	8(3)	3(3)
C(10)	36(3)	34(3)	27(3)	12(3)	15(3)	12(3)
C(11)	22(3)	21(3)	27(3)	3(2)	10(2)	4(2)
C(12)	19(3)	17(3)	31(3)	9(2)	6(2)	4(2)
C(13)	29(3)	20(3)	35(3)	8(3)	11(2)	5(2)
C(14)	17(3)	20(3)	43(3)	17(3)	8(2)	6(2)
C(15)	24(3)	21(3)	38(3)	17(3)	9(2)	1(2)
C(16)	16(3)	15(2)	36(3)	11(2)	9(2)	2(2)
C(17)	15(2)	13(2)	29(3)	5(2)	6(2)	-2(2)
C(18)	20(3)	21(3)	30(3)	13(2)	5(2)	-2(2)
C(19)	36(3)	32(3)	24(3)	13(3)	10(2)	9(3)
C(20)	41(3)	36(3)	24(3)	17(3)	13(3)	13(3)
C(21)	35(3)	27(3)	30(3)	12(3)	15(3)	11(2)
C(22)	26(3)	23(3)	37(3)	14(3)	17(2)	9(2)
C(23)	23(3)	38(4)	65(4)	32(3)	10(3)	6(3)
C(24)	48(4)	35(4)	32(3)	-1(3)	2(3)	-6(3)
C(25)	58(4)	57(5)	26(3)	16(3)	11(3)	15(4)
C(26)	24(3)	28(3)	57(4)	22(3)	19(3)	10(2)
C(27)	50(4)	35(3)	46(4)	26(3)	25(3)	9(3)
C(28)	61(5)	59(5)	32(4)	23(3)	21(3)	23(4)
C(29)	22(3)	15(3)	32(3)	9(2)	9(2)	3(2)
C(30)	20(3)	20(3)	31(3)	14(2)	8(2)	2(2)
C(31)	23(3)	24(3)	44(4)	20(3)	11(2)	4(2)
C(32)	28(3)	22(3)	44(4)	14(3)	18(3)	7(2)
C(33)	33(3)	22(3)	38(3)	9(3)	17(3)	5(2)
C(34)	30(3)	19(3)	28(3)	7(2)	9(2)	1(2)
C(35)	40(3)	23(3)	28(3)	4(3)	13(3)	9(3)

atom	U_{11}	U_{22}	U_{33}	U_{23}	U_{13}	U_{12}
C(36)	49(4)	30(3)	21(3)	13(3)	14(3)	7(3)
C(37)	43(4)	34(3)	18(3)	14(3)	7(2)	3(3)
C(38)	44(4)	37(3)	31(3)	22(3)	11(3)	9(3)
C(39)	24(3)	21(3)	38(3)	18(3)	8(2)	6(2)
C(40)	45(4)	25(3)	65(5)	16(3)	28(3)	16(3)
C(41)	50(4)	44(4)	38(4)	13(3)	1(3)	-4(3)
C(42)	67(5)	56(4)	28(3)	21(3)	13(3)	20(4)
C(43)	25(3)	19(3)	26(3)	9(2)	7(2)	4(2)
C(44)	74(6)	72(6)	32(4)	30(4)	16(4)	7(4)
C(45)	40(4)	44(4)	40(4)	-7(3)	-4(3)	-4(3)
C(46)	20(3)	16(3)	17(2)	4(2)	7(2)	3(2)
O(50)	186(10)	136(8)	128(7)	100(6)	-13(7)	-31(7)
C(50)	55(7)	350(30)	217(18)	220(20)	17(9)	-9(11)
O(51)	147(9)	228(13)	231(12)	150(11)	82(9)	61(9)
C(51)	99(9)	67(7)	193(14)	50(8)	-45(9)	-22(7)
O(52)	480(30)	118(9)	134(9)	30(8)	31(13)	-132(12)
C(52)	183(16)	115(12)	182(16)	43(12)	67(14)	42(11)
O(53)	580(40)	390(30)	290(20)	-150(20)	-210(20)	330(30)
C(53)	290(30)	280(30)	122(15)	55(17)	-53(16)	140(30)
O(1W)	342(18)	153(9)	101(7)	-7(6)	90(9)	-55(10)
O(2W)	550(30)	253(19)	380(20)	195(18)	210(20)	80(20)
O(3W)	220(20)	220(20)	89(13)	28(14)	57(14)	-50(20)

The anisotropic displacement factor exponent takes the form: $-2\pi^2[h^2 a^{*2}U_{11} + \dots + 2hka^*b^*U_{12}]$.

Table 24. Hydrogen coordinates ($\text{\AA}\times 10^4$) and isotropic displacement parameters ($\text{\AA}^2\times 10^3$) for $\{[\text{Ni}_6([\text{22}]\text{-HMTADO})_3(\text{CN})_4][\text{Ni}(\text{CN})_4]\cdot 5\text{H}_2\text{O}\cdot 8\text{CH}_3\text{OH}\}_n$

atom	<i>x</i>	<i>y</i>	<i>z</i>	<i>U</i> (eq)
H(3)	4271	9029	5110	32
H(5)	4106	8301	2650	34
H(7)	5728	8247	2166	32
H(8A)	8152	8819	2045	41
H(8B)	6859	8159	1469	41
H(10A)	9776	6981	1659	38
H(10B)	9873	8126	2173	38
H(11)	10163	6335	2433	31
H(13)	10787	5360	3028	35
H(15)	10943	5900	5456	32
H(18)	10528	7252	6405	29
H(19A)	10151	9222	7369	36
H(19B)	10023	8212	7424	36
H(21A)	7177	9496	7267	35
H(21B)	8430	9987	7263	35
H(22)	5940	9300	6149	32
H(23A)	2318	8464	3029	47
H(23B)	2522	9267	3999	47
H(23C)	2234	8133	3761	47
H(24A)	6540	6326	860	57
H(24B)	7264	6354	1745	57
H(24C)	7663	5842	892	57
H(25A)	7522	7311	239	58

atom	<i>x</i>	<i>y</i>	<i>z</i>	<i>U</i> (eq)
H(25B)	8657	6848	321	58
H(25C)	8813	8006	771	58
H(26A)	11578	4311	3518	41
H(26B)	11028	4144	4205	41
H(26C)	12302	4854	4521	41
H(27A)	6863	7821	7156	46
H(27B)	7966	7332	7274	46
H(27C)	7437	7370	6384	46
H(28A)	8039	9309	8510	57
H(28B)	9302	9848	8556	57
H(28C)	9151	8818	8577	57
H(31)	7295	2082	5004	34
H(33)	6359	1949	2653	38
H(35)	5536	3071	2373	39
H(36A)	5200	4002	1873	39
H(36B)	5830	5108	2543	39
H(38A)	4721	6332	2924	42
H(38B)	3307	6068	2654	42
H(39)	3058	6795	3835	31
H(40A)	7655	768	3899	53
H(40B)	7999	1050	3195	53
H(40C)	6716	397	2973	53
H(41A)	3001	4039	2545	59
H(41B)	2954	3477	1552	59
H(41C)	2215	4300	1848	59
H(42A)	3207	5164	1160	59
H(42B)	3946	4340	872	59
H(42C)	4624	5461	1431	59

III. Results and Discussion

1. Description of structure and physicochemical properties of Cr(III)-tetraaza 14-membered macrocyclic complexes

1) Properties of *cis*-[Cr([14]-decane)(OH)₂]⁺ solution.

The reaction of anhydrous chromium(III) chloride with [14]-decane gives a good yield of a bluish-green complex *cis*-[Cr([14]-decane)Cl₂]Cl.⁵⁴ Base hydrolysis of *cis*-[Cr([14]-decane)Cl₂]⁺ has been studied.⁵⁹ The two moles of OH⁻ ion are consumed per mole of *cis*-[Cr([14]-decane)Cl₂]⁺ complex in the pH range 7.8-9.4, and the final visible absorption spectrum is identical to that obtained from *cis*-[Cr([14]-decane)(OH)₂]⁺ solution. A DMF solution of this complex displayed a molar conductance of 71.4 ohm⁻¹cm²mol⁻¹, which is in the range of 1 : 1 electrolyte. From the acid dissociation constants⁵⁴ it is seen that the *cis*-[Cr([14]-decane)(OH)₂]³⁺ cation is a significantly stronger acid than a number of other *cis*-tetraaminediaquachromium(III) cations. This result is due to differences in cation-solvent interactions by the restriction of ligand cyclization, steric effects, and hydrophobic bonding effect. This complex ion can be used to prepare a large variety of other complexes containing auxiliary ligands. It shows that the absorption bands to shorter wavelength shift on addition of HClO₄ solution to the aqueous Cr(III) complex solution. The absorption spectrum of this species is compared with several related compounds in Table 25. The first ligand field(LF) band (⁴A_{2g}

$\rightarrow {}^4T_{2g}$ (O_h symmetry) is observed at 612 nm, while the second LF band (${}^4A_{2g} \rightarrow {}^4T_{1g}$) is centered at 379 nm.^{60,61} The molar absorptivities of the two *d-d* bands are substantially greater than those of the *trans* analogues, consistent with the given geometric assignment. However, the first *d-d* bands for *cis*-[Cr(cyclam)(NH₃)₂]³⁺, *cis*-[Cr([14]-decane)(OH)₂]⁺, and *cis*-[Cr([14]-decane)-(H₂O)₂]³⁺ complex ions characterized by an increased intensity and a lower energy than that for *cis*-[Cr(en)₂(NH₃)₂]³⁺. This result indicates that, for these *cis* systems, cyclam and [14]-decane are slightly lower in the spectrochemical series than ethylenediamine (en). These effects may qualitatively be accounted for with reference to geometric structure of complex which shows a pronounced octahedral distortion of the CrN₄O₂-plane apparently induced by two methyl groups above and below the CrN₂O₂ plane.



Table 25. Electronic transition spectral data of *cis*-[Cr([14]-decane){O-(*o*-OCC₆H₄OH)}₂]⁺, *cis*-[Cr([14]-decane){O-(*p*-OC₆H₄NO₂)}(OH)]⁺, and related Cr(III) complexes

Complexes	λ , nm (ϵ , M ⁻¹ cm ⁻¹)	ref.
<i>trans</i> -[Cr(en) ₂ Cl ₂] ⁺	578 (24.5), 453 (23), 396 (34)	59
<i>trans</i> -[Cr(cyclam)Cl ₂] ⁺	572 (19.9), 407 (35), 365 (41)	59
<i>trans</i> -[Cr(<i>meso</i> -[14]-decane)Cl ₂] ⁺	574 (25), 440 (27), 387 (47)	59
<i>cis</i> -[Cr(en) ₂ Cl ₂] ⁺	528 (71), 402 (69)	59
<i>cis</i> -[Cr(en) ₂ (H ₂ O) ₂] ³⁺	484 (67), 366 (43)	59
<i>cis</i> -[Cr(en) ₂ (NH ₃) ₂] ³⁺	460 (66), 351 (54)	61, 62
<i>cis</i> -[Cr(cyclam)Cl ₂] ⁺	529 (111), 404 (106)	63
<i>cis</i> -[Cr(cyclam)(H ₂ O) ₂] ³⁺	483 (126), 370 (38)	61, 63
<i>cis</i> -[Cr(cyclam)(H ₂ O)(NH ₃)] ³⁺	476 (110), 362 (87)	61
<i>cis</i> -[Cr(cyclam)(NH ₃) ₂] ³⁺	468 (115), 355 (80)	61
<i>cis</i> -[Cr([14]-decane)(OH) ₂] ⁺	609 (111), 380 (73)	54
<i>cis</i> -[Cr([14]-decane)(OH)(H ₂ O)] ²⁺	572 (130), 407 (53)	54
<i>cis</i> -[Cr([14]-decane)(H ₂ O) ₂] ³⁺	529 (169), 388 (82)	54
<i>cis</i> -[Cr([14]-decane)(bz) ₂] ⁺ *	548 (223), 394 (131)	64
<i>cis</i> -[Cr([14]-decane)(cbz) ₂] ⁺ *	547 (221), 394 (127)	64
<i>cis</i> -[Cr([14]-decane)(μ -cit) ₂] ²⁺ *	532 (186), 385 (97)	65
<i>cis</i> -[Cr([14]-decane)(NCS) ₂] ⁺	541 (135), 406 (78)	66
<i>cis</i> -[Cr([14]-decane)(N ₃) ₂] ⁺	572 (213), 426 (127)	66
<i>cis</i> -[Cr([14]-decane)(caa) ₂] ⁺ *	537 (201), 390 (108)	66
<i>cis</i> -[Cr([14]-decane)(acac)] ²⁺ *	536 (190), 388 (269)	67
<i>cis</i> -[Cr([14]-decane)(ox)] ⁺ *	533 (157), 386 (82)	67
<i>cis</i> -[Cr([14]-decane)(mal)] ⁺ *	551 (164), 387 (71)	67
<i>cis</i> -[Cr([14]-decane){O-(<i>o</i> -OCC ₆ H ₄ OH)} ₂] ⁺	541 (223), 391 (134)	this
<i>cis</i> -[Cr([14]-decane){O-(<i>p</i> -OC ₆ H ₄ NO ₂)}(OH)] ⁺	578 (172), 473sh (326)	this

* Abbreviations, bz, cbz, cit, caa, acac, ox, and mal are benzoate, chlorobenzoate, citrate, acetylacetoate, oxalate, and malonate, respectively.

2) Structure and physicochemical properties of *cis*-[Cr([14]-decane)(*o*-OCC₆H₄OH)₂]ClO₄ (**I**)

The crystal structure of (**I**) complex consists of monomeric cation of the indicated formula and non-coordinated perchlorate anion. An ORTEP drawing of (**I**) with the atomic labeling scheme is depicted in Figure 1. The bond distances and angles are listed in Table 26 and 27. The monomeric cation, [Cr([14]-decane)(*o*-OCC₆H₄OH)₂]⁺ shows a distorted octahedral environment, where the chromium(III) ion is coordinated by four secondary amines of the macrocycle and by the two carboxylate oxygen atoms of the monodentate salicylate ligands in *cis* positions. The *rac*-form, [14]-decane readily folds to give *cis*-chromium(III) complexes with the (*RRRR,SSSS*) *sec*-NH configuration and two equatorial and one axial methyl substituents on each six-membered chelate ring. Therefore, two salicylates are bonded to the chromium(III) by monodentate ligand rather than single salicylate bonding by bidentate, so as to form a sterically stable six-coordinate complex. If the salicylate acts bidentate ligand, a four membered ring causing much more strain in the complex structure is formed. Therefore, two salicylates functioned as monodentate ligand result more preferable structure.

The oxygen atoms from the salicylate ligands and two nitrogen donors (positions of *C-methyl* group) of the [14]-decane define the equatorial coordination plane (CrN₂O₂ *xy*-plane). Hexa-coordination is accomplished via the remaining two nitrogens of macrocyclic ligand (positions of *C-dimethyl* group) (**1**(page 70)). The tetra-aza ligand is folded along the N(1)-Cr-N(3) axis (axial position).

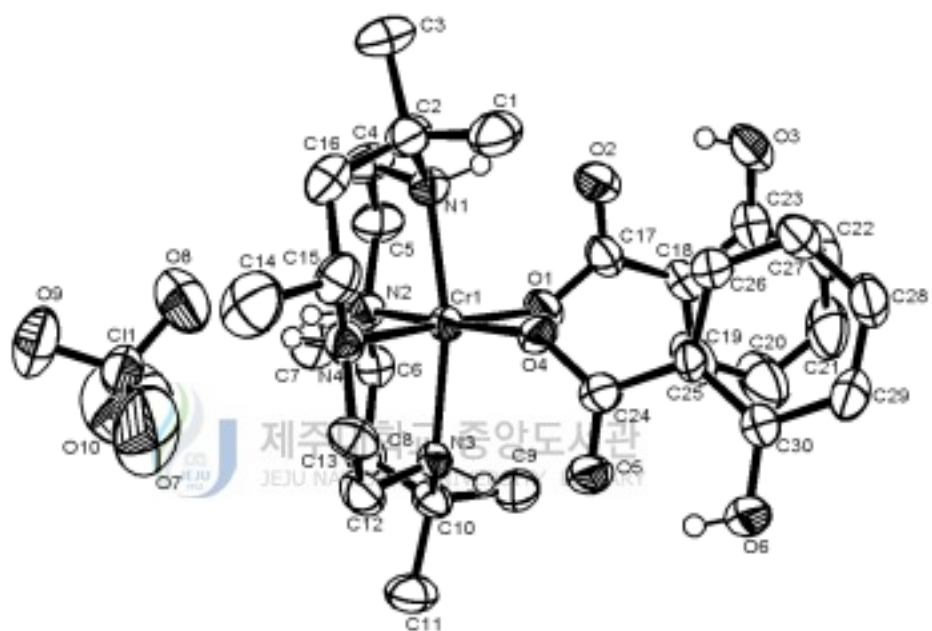
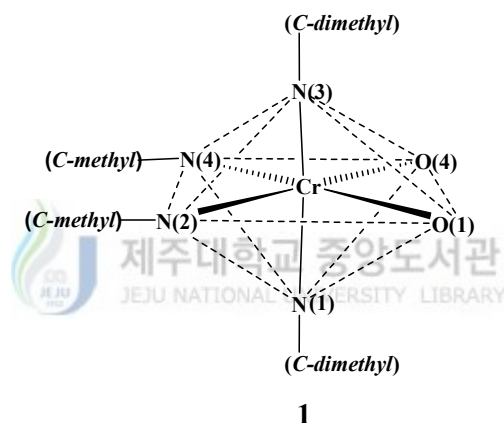


Figure 1. An ORTEP view of core structure (top view) for the *cis*-[Cr([14]-decane)(*o*-OOCC₆H₄OH)₂]ClO₄ (**I**) complex showing 40% probability thermal ellipsoids and labels for non-H atoms.

This configuration is often referred to as the Bosnich type-V stereochemistry.⁶⁸ A similar type of configuration was reported for *cis*-[Cr(cyclam)Cl(dmsu)]²⁺, *cis*-[Cr([14]-decane)(cbz)₂]⁺, *cis*-[Cr([14]-decane)(μ-cit)₂]²⁺, *cis*-[Cr([14]-decane)(NCS)₂]⁺, and *cis*-[Cr([14]-decane)(acac)]²⁺.^{64-67,69} The Cr-N (secondary amines) bond distances are in the range of 2.105(3) ~ 2.141(4) Å, and Cr-O (salicylate) distances are 1.974(3) and 1.993(4) Å (Table 26).

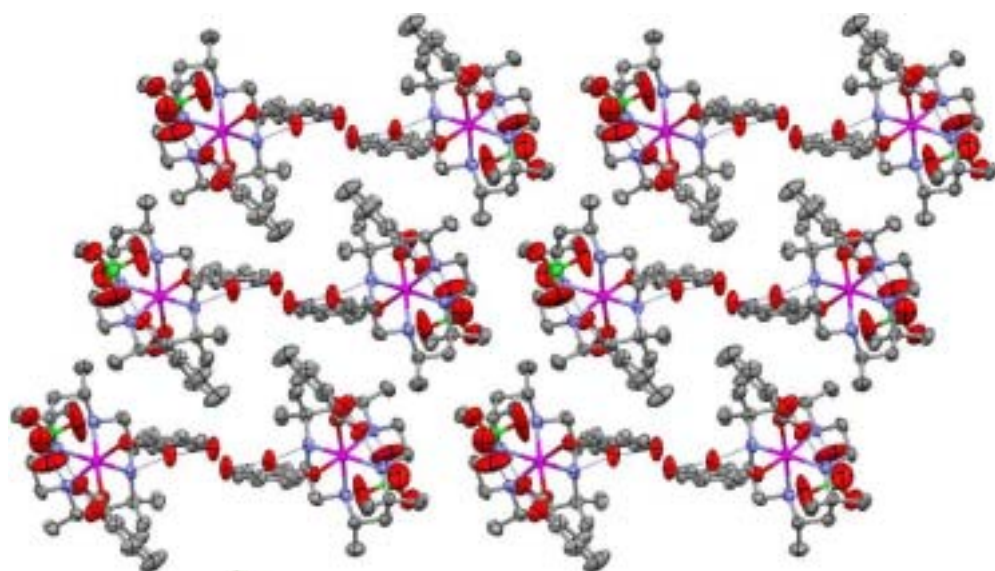


The bond angles are N(2)-Cr-N(4), N(1)-Cr-N(3) and O(4)-Cr-O(1) 96.97(15)°, 168.27(15)° and 85.70(13)°, respectively (Table 27). These values are well within the general trend with those found in the *cis*-forms of other tetraaza macrocyclic complexes of Cr(III).⁷⁰ It is known that in *cis* octahedral complexes of macrocycles of medium size (12~14 membered rings) the pattern of metal-ligand distance and the angle between the axial donors and the metal center are particularly affected by the cavity size.⁷¹

In this complex Cr-N(2)(2.105(3)Å) and Cr-N(4)(2.111(4)Å) distances are

shorter than Cr-N(1) axial(2.128(4)Å) and Cr-N(3) axial(2.141(4)Å) and the angle N(1)-Cr-N(3) (168.27(15)°) is smaller than the ideal value of 180°, indicating that the donor atoms are not able to achieve the axial positions of a perfect octahedron. By contrast, in *cis*-[Cr(cyclam)X₂] octahedral complexes, the angle N_{axial}-Cr-N_{axial} is closer to 180° than that of the title complex and the axial and equatorial distances have similar values.⁷⁰

There have been reports that the hydrogen bond systems in the related tetraaza metallo-macrocycles play an important role in reinforcing the coordination of the axial ligands as well as in determining the whole structures of the molecules and the coordination geometries about the central metals.⁷²⁻⁷⁴ As shown in Figure 2 and Table 28, there are three types of hydrogen bonds. The uncoordinated carboxylic oxygen atoms of salicylate ligand form of the type N-H···O with the secondary amine hydrogen of the macrocycle {N(1)···O(2) 2.783 Å, N(1)-H(1)···O(2) 150.09°, N(3)···O(5) 2.816 Å, and N(3)-H(3)···O(5) 151.03°}. Under this situation, the self-organization seems to make the structure more stable by the hydrogen bonding interaction, in which the carboxylate oxygen O(1) of salicylate anion is coordinated to the central Cr(III) and O(2) is H-bonded with H(1) to form six-membered ring.^{75,76} The counter ion ClO₄⁻ forms of the type N-H···O with the secondary amine hydrogen of the macrocycle {N(2)···O(8) 3.069 Å, N(2)-H(2)···O(8) 168.13°. The uncoordinated carboxylic oxygen atom and hydroxy of salicylate ligand form internal hydrogen bond {O(2)···O(3) 2.568 Å, O(2)···H(3d)-O(3) 144.98°, O(5)···O(6) 2.816 Å, and O(5)···H(6d)-O(6) 144.95°}.



제주대학교 중앙도서관
JEJU NATIONAL UNIVERSITY LIBRARY

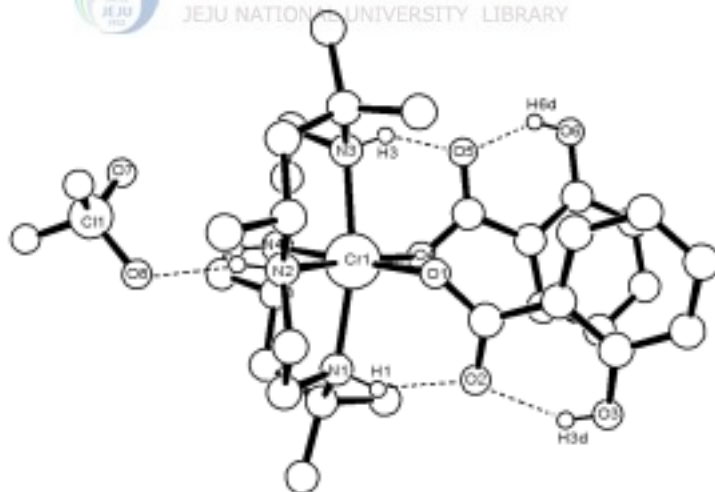


Figure 2. The molecular packing diagram and hydrogen-bonding scheme of the *cis*-[Cr([14]-decane)(*o*-OOCC₆H₄OH)₂]ClO₄ (**I**) complex.

Table 26. Bond lengths (Å) for *cis*-[Cr([14]-decane)(*o*-OOCC₆H₄OH)₂]ClO₄ (**I**) complex

Cr(1)-O(4)	1.974(3)	C(15)-C(16)	1.528(7)
Cr(1)-O(1)	1.993(3)	C(17)-O(2)	1.251(6)
Cr(1)-N(2)	2.105(3)	C(17)-O(1)	1.293(6)
Cr(1)-N(4)	2.111(4)	C(17)-C(18)	1.469(7)
Cr(1)-N(1)	2.128(4)	C(18)-C(23)	1.397(7)
Cr(1)-N(3)	2.141(4)	C(18)-C(19)	1.406(8)
N(1)-C(4)	1.488(6)	C(19)-C(20)	1.357(9)
N(1)-C(2)	1.518(6)	C(20)-C(21)	1.368(9)
N(2)-C(5)	1.494(6)	C(21)-C(22)	1.380(9)
N(2)-C(6)	1.502(6)	C(22)-C(23)	1.395(7)
N(3)-C(12)	1.478(6)	C(23)-O(3)	1.336(6)
N(3)-C(10)	1.522(6)	C(24)-O(5)	1.248(6)
N(4)-C(13)	1.484(6)	C(24)-O(4)	1.286(5)
N(4)-C(15)	1.495(6)	C(24)-C(25)	1.484(6)
C(1)-C(2)	1.518(7)	C(25)-C(26)	1.390(6)
C(2)-C(16)	1.506(7)	C(25)-C(30)	1.401(6)
C(2)-C(3)	1.551(7)	C(26)-C(27)	1.368(7)
C(4)-C(5)	1.515(7)	C(27)-C(28)	1.380(7)
C(6)-C(8)	1.511(7)	C(28)-C(29)	1.373(7)
C(6)-C(7)	1.537(6)	C(29)-C(30)	1.388(7)
C(8)-C(10)	1.523(6)	C(30)-O(6)	1.336(6)
C(9)-C(10)	1.518(7)	C(11)-O(7)	1.373(5)
C(10)-C(11)	1.537(7)	C(11)-O(9)	1.393(4)
C(12)-C(13)	1.509(7)	C(11)-O(10)	1.396(6)
C(14)-C(15)	1.547(7)	C(11)-O(8)	1.420(5)

Table 27. Angles (°) for *cis*-[Cr([14]-decane)(*o*-OOC₆H₄OH)₂]ClO₄ (I) complex

O(4)-Cr(1)-O(1)	85.70(13)	N(3)-C(10)-C(11)	110.8(4)
O(4)-Cr(1)-N(2)	174.08(14)	C(8)-C(10)-C(11)	109.0(4)
O(1)-Cr(1)-N(2)	88.41(14)	N(3)-C(12)-C(13)	110.6(4)
O(4)-Cr(1)-N(4)	88.92(14)	N(4)-C(13)-C(12)	109.4(4)
O(1)-Cr(1)-N(4)	174.58(14)	N(4)-C(15)-C(16)	111.7(4)
N(2)-Cr(1)-N(4)	96.97(15)	N(4)-C(15)-C(14)	110.8(5)
O(4)-Cr(1)-N(1)	95.43(13)	C(16)-C(15)-C(14)	109.4(4)
O(1)-Cr(1)-N(1)	92.64(14)	C(2)-C(16)-C(15)	119.0(4)
N(2)-Cr(1)-N(1)	84.26(14)	O(2)-C(17)-O(1)	122.5(5)
N(4)-Cr(1)-N(1)	88.55(15)	O(2)-C(17)-C(18)	119.5(5)
O(4)-Cr(1)-N(3)	92.92(13)	O(1)-C(17)-C(18)	118.1(5)
O(1)-Cr(1)-N(3)	96.19(13)	C(23)-C(18)-C(19)	117.6(5)
N(2)-Cr(1)-N(3)	88.28(14)	C(23)-C(18)-C(17)	120.2(5)
N(4)-Cr(1)-N(3)	83.37(14)	C(19)-C(18)-C(17)	122.2(5)
N(1)-Cr(1)-N(3)	168.27(15)	C(20)-C(19)-C(18)	122.9(6)
C(4)-N(1)-C(2)	111.2(4)	C(19)-C(20)-C(21)	118.6(7)
C(4)-N(1)-Cr(1)	106.9(3)	C(20)-C(21)-C(22)	121.2(6)
C(2)-N(1)-Cr(1)	123.8(3)	C(21)-C(22)-C(23)	120.3(6)
C(5)-N(2)-C(6)	110.9(3)	O(3)-C(23)-C(22)	116.9(5)
C(5)-N(2)-Cr(1)	103.9(3)	O(3)-C(23)-C(18)	123.8(5)
C(6)-N(2)-Cr(1)	120.3(3)	C(22)-C(23)-C(18)	119.3(5)
C(12)-N(3)-C(10)	111.8(4)	C(17)-O(1)-Cr(1)	128.6(3)
C(12)-N(3)-Cr(1)	107.5(3)	O(5)-C(24)-O(4)	123.1(5)
C(10)-N(3)-Cr(1)	123.1(3)	O(5)-C(24)-C(25)	119.4(4)
C(13)-N(4)-C(15)	111.5(3)	O(4)-C(24)-C(25)	117.5(4)
C(13)-N(4)-Cr(1)	104.8(3)	C(26)-C(25)-C(30)	118.7(4)
C(15)-N(4)-Cr(1)	119.3(3)	C(26)-C(25)-C(24)	121.6(4)
C(16)-C(2)-C(1)	112.8(4)	C(30)-C(25)-C(24)	119.7(4)

C(16)-C(2)-N(1)	109.1(4)	C(27)-C(26)-C(25)	121.8(5)
C(1)-C(2)-N(1)	108.2(4)	C(26)-C(27)-C(28)	118.9(5)
C(16)-C(2)-C(3)	109.3(4)	C(29)-C(28)-C(27)	121.0(5)
C(1)-C(2)-C(3)	106.5(4)	C(28)-C(29)-C(30)	120.2(5)
N(1)-C(2)-C(3)	111.0(4)	O(6)-C(30)-C(29)	117.3(4)
N(1)-C(4)-C(5)	110.6(4)	O(6)-C(30)-C(25)	123.3(4)
N(2)-C(5)-C(4)	108.8(4)	C(29)-C(30)-C(25)	119.4(4)
N(2)-C(6)-C(8)	111.7(4)	C(24)-O(4)-Cr(1)	131.5(3)
N(2)-C(6)-C(7)	110.7(4)	O(7)-C(11)-O(9)	110.9(4)
C(8)-C(6)-C(7)	109.0(4)	O(7)-C(11)-O(10)	112.5(7)
C(6)-C(8)-C(10)	119.8(4)	O(9)-C(11)-O(10)	107.6(5)
C(9)-C(10)-N(3)	108.3(4)	O(7)-C(11)-O(8)	109.6(4)
C(9)-C(10)-C(8)	112.4(4)	O(9)-C(11)-O(8)	111.5(3)
N(3)-C(10)-C(8)	108.8(4)	O(10)-C(11)-O(8)	104.7(5)
C(9)-C(10)-C(11)	107.6(4)		

Table 28. Selected bond lengths (Å) and angles(°) for hydrogen bond of *cis*-[Cr([14]-decane)(*o*-OOCC₆H₄OH)₂]ClO₄ (**I**) complex

D-H...A	d(D-H)	d(H...A)	<DHA	d(D...A)
macrocycle (NH) - carboxylate (salicylate ligand)				
N(1)-H(1)···O(2)	0.910	1.957	150.09	2.783
N(3)-H(3)···O(5)	0.910	1.986	151.03	2.816
internal salicylate ligand (hydroxy - carboxylate)				
O(3)-H(3d)···O(2)	0.820	1.852	144.98	2.568
O(6)-H(6d)···O(5)	0.820	1.847	144.95	2.561
macrocycle (NH) - ClO ₄ ⁻				
N(2)-H(2)···O(8)	0.910	2.173	168.13	3.069

The value of molar conductance for *cis*-[Cr([14]-decane)(*o*-OOC₆H₄OH)₂]-ClO₄ was measured in DMF or DMSO correspond to a 1 : 1 electrolyte ($\Lambda_M = 69.2 \text{ ohm}^{-1}\text{cm}^2\text{mol}^{-1}$), indicating that the auxiliary salicylate ligands in the Cr(III) complexes are not dissociated from the complex in these polar solvents.⁷⁷

The absorption spectra of *cis*-[Cr([14]-decane){O-(*o*-OOC₆H₄OH)}₂]⁺ complex ion in DMF solution at room temperature is represented in Figure 3. This is overlapping absorption parts in the spectrum of the title complex including the two distinct bands. In *O_h* symmetry, three ligand field bands are expected for a *d*³ ion ${}^4A_{2g} \rightarrow {}^4T_{2g}$, ${}^4A_{2g} \rightarrow {}^4T_{1g}(\text{F})$ and the two electron transition ${}^4A_{2g} \rightarrow {}^4T_{1g}(\text{P})$.⁶¹

The two *d-d* bands of title complex observed at 18484, 25575 cm⁻¹ can be related to the spin-allowed transitions, ${}^4A_{2g} \rightarrow {}^4T_{2g}$ and ${}^4A_{2g} \rightarrow {}^4T_{1g}$, respectively. The assignment of geometric configuration is confirmed by the *d-d* absorption spectra. The less symmetrical *cis*-isomers have much higher extinction coefficients than those of more symmetrical *trans*-isomers.⁵⁹

A chromium complexes in tetragonal symmetry are expected to have four absorption bands in *d-d* region, but each spectrum apparently has two major components. Thus, we fitted the spectra roughly with two Gaussian functions first and then added a minor component to reproduce the more suitable shape of the spectra in the region of interest. Finally, we performed least-squares fitting procedures, and the dotted lines in Figure 3 are Gaussian bands representing the approximate deconvolution of the spectra yielded by the calculations. The four peak positions calculated at 18038, 18553, 24915 and 25726 cm⁻¹ can be assigned to the 4E (${}^4T_{2g}$ in *O_h* symmetry), 4B_2 (${}^4T_{2g}$), 4E

(${}^4T_{1g}$) and 4A_2 (${}^4T_{1g}$), respectively.^{78,79}

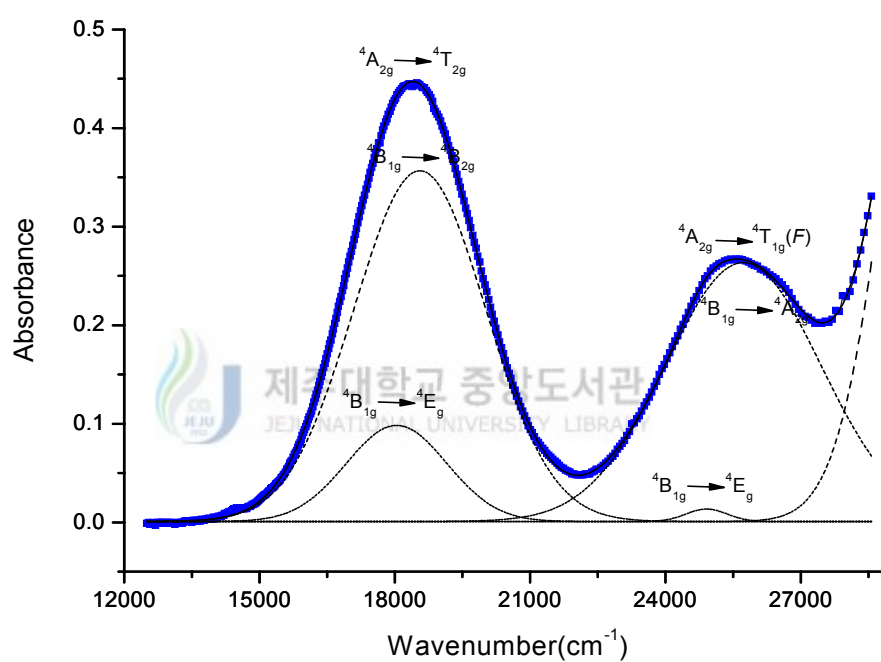


Figure 3. The electronic absorption spectrum of 2.0×10^{-3} M *cis*-[Cr([14]-decane)(*o*-OOCC₆H₄OH)₂]⁺ in DMF solution at 298 K.

The infrared spectrum of *cis*-[Cr([14]-decane)(*o*-OOCC₆H₄OH)₂]ClO₄ recorded at room temperature is presented in Figure 4. The infrared spectrum of this complex, taken from KBr pellet, is in accord with the structure determined by X-ray diffraction. The IR spectrum displayed N-H stretches at 3194 and 3083 cm⁻¹, C-H stretches at 2976 and 2887 cm⁻¹, and a strong ionic ClO₄⁻ band at near 1120 cm⁻¹ and 623 cm⁻¹. The band occurring in the IR spectrum of the complex in the ~3447 cm⁻¹ region may probably be due to the ν (OH) vibration of hydroxy of salicylate ligand. A weak bands at near 444 cm⁻¹ region associated with the Cr-N(macrocycle) vibration.^{80,81}

The spectrum of title complex exhibit characteristic absorption bands for the carbonyls of the salicylate carboxylate ligands in the symmetric and asymmetric vibration regions. Specifically, symmetric stretching vibrations, $\nu_s(\text{COO}^-)$ appear at 1387 cm⁻¹ and asymmetric stretching vibrations, $\nu_{as}(\text{COO}^-)$ are observed at 1620 cm⁻¹. The title complex gives a typical band of non-bonded and undissociated carboxylic acid group at 1730 cm⁻¹. All of the carbonyl absorption bands are shifted to lower frequencies compared to those of free salicylic acid, denoting the changes in the vibrational status of that ligand upon complexation to chromium. The differences between the symmetric and antisymmetric stretches, $\Delta\nu \{= \nu_{as}(\text{COO}^-) - \nu_s(\text{COO}^-)\}$ are on the order of 213 cm⁻¹, indicating that carboxylate groups are either free or coordinated to the metal ion in a monodentate fashion.⁸²

This observation is consistent with the observed X-ray crystal structure of the title complex.

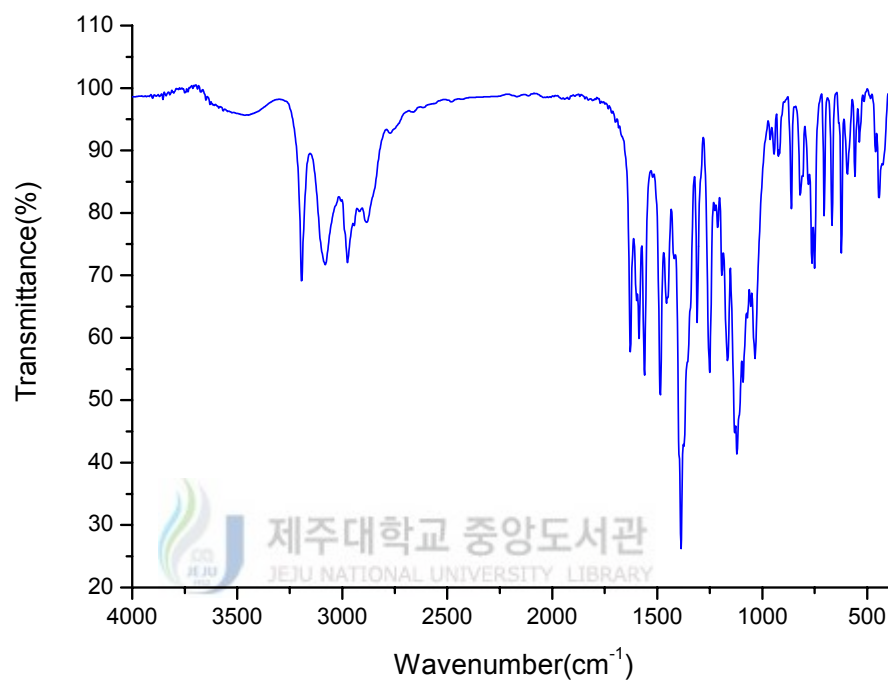


Figure 4. IR spectrum of *cis*-[Cr([14]-decane)(*o*-OOCC₆H₄OH)₂]ClO₄ complex.

In the FAB mass spectrum of *cis*-[Cr([14]-decane)(*o*-OOC₆H₄OH)₂]ClO₄, this is a peak at *m/z* 610.3 corresponding to the molecular ion *cis*-[Cr([14]-decane)(*o*-OOC₆H₄OH)₂]⁺ (Figure 5). The molecular ion of the *cis*-[Cr([14]-decane)(*o*-OOC₆H₄OH)₂]⁺ undergoes fragmentation to give species such as *cis*-[Cr([14]-decane)(*o*-OOC₆H₄OH)]⁺, and [Cr([14]-decane)-3H]⁺ at *m/z* 472.3 and 333.3, respectively.

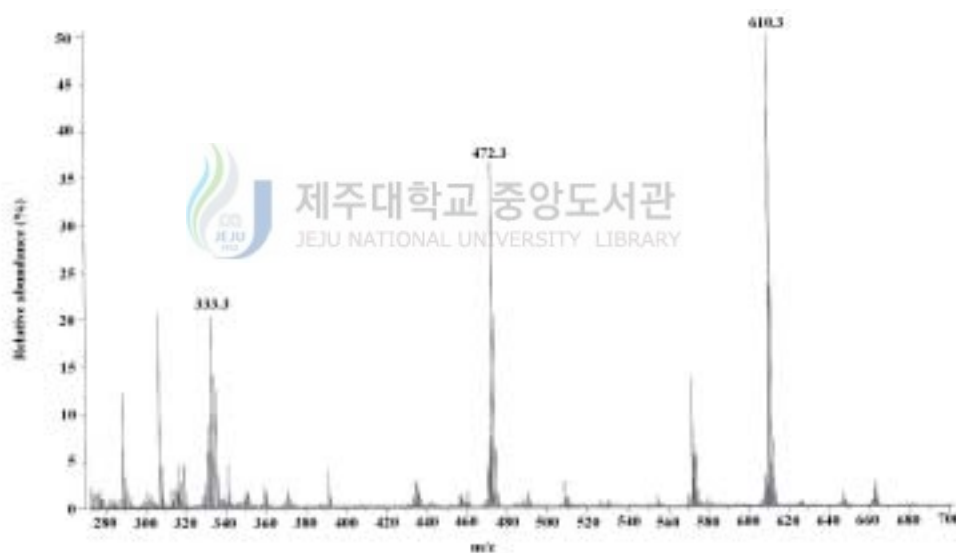


Figure 5. The FAB mass spectrum of the *cis*-[Cr([14]-decane)(*o*-OOC₆H₄OH)₂]ClO₄.

3) Structure and physicochemical properties of *cis*-[Cr([14]-decane)(*p*-OC₆H₄NO₂)(OH)]ClO₄·H₂O (**II**)

The crystal structure of (**II**) complex consists of monomeric cation of the indicated formula, and uncoordinating perchlorate anion and one water molecule. An ORTEP drawing of (**II**) with the atomic labeling scheme is depicted in Figure 6. The bond distances and angles are listed in Table 29 and 30, respectively. The monomeric cation, [Cr([14]-decane)(*p*-OC₆H₄NO₂)(OH)]⁺ shows a distorted octahedral environment, where the chromium(III) ion is coordinated by four secondary amines of the macrocycle, one phenolic oxygen atom of the monodentate *p*-nitrophenolate ligand and one hydroxo oxygen atom in *cis* positions. The *rac*-form, [14]-decane readily folds to give *cis*-chromium(III) complexes with the (*RRRR,SSSS*) *sec*-NH configuration and two equatorial and one axial methyl substituent on each six-membered chelate ring.

The oxygen atoms from the *p*-nitrophenolate and hydroxo ligands and two nitrogen donors (positions of *C-methyl* group) of the [14]-decane define the equatorial coordination plane (CrN₂O₂ *xy*-plane). Hexa-coordination is accomplished via the remaining two nitrogens of macrocyclic ligand (positions of *C-dimethyl* group) **2**. The tetra-aza ligand is folded along the N(1)-Cr-N(3) axis (axial position).

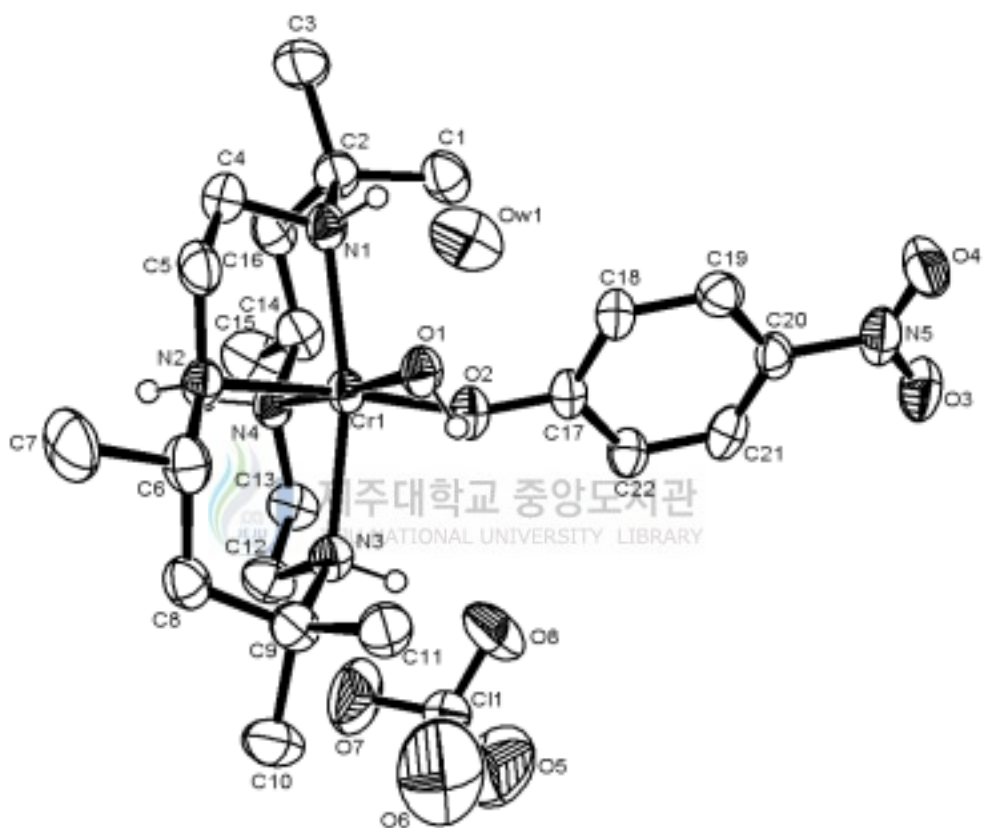
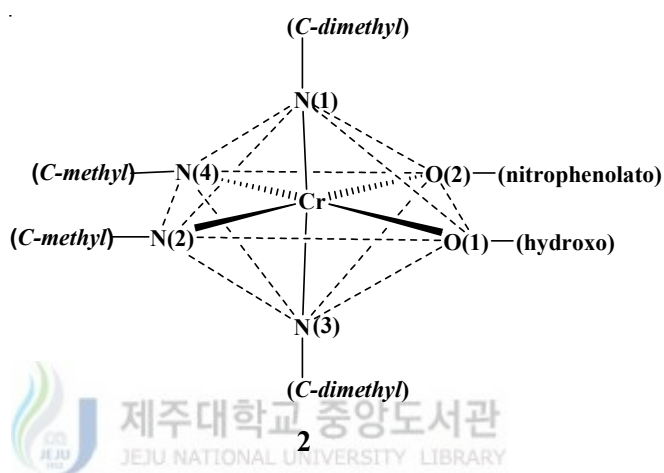


Figure 6. An ORTEP view of core structure (top view) for the *cis*-[Cr([14]-decane)(*p*-OC₆H₄NO₂)(OH)]ClO₄·H₂O (**II**) complex showing 40% probability thermal ellipsoids and labels for non-H atoms.

This configuration is often referred to as the Bosnich type-V stereochemistry.⁶⁸ The Cr-N (secondary amines) bond distances are in the range of 2.119(4) ~ 2.153(5) Å, and Cr-O (salicylate) distances are 1.912(5) and 1.931(4) Å (Table 29).

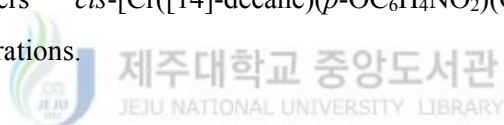


The bond angles of N(2)-Cr-N(4), N(1)-Cr-N(3) and O(1)-Cr-O(2) are 95.2(2)°, 167.6(2)° and 92.89(19)°, respectively (Table 30). These values are well within the general trend with those found in the *cis*-forms of other tetraaza macrocyclic complexes of Cr(III).⁷⁰ It is known that in *cis* octahedral complexes of macrocycles of medium size (12~14 membered rings) the pattern of metal-ligand distance and the angle between the axial donors and the metal center are particularly affected by the cavity size.⁷¹

In this complex, Cr-N(2) distances of 2.119(4) Å are shorter than Cr-N(3) of 2.153(5) Å and the angle N(1)-Cr-N(3) of 167.6(2)° is smaller than the ideal value of 180°, indicating that the donor atoms are not able to achieve the axial positions of a perfect octahedron. By contrast, in *cis*-[Cr(cyclam)X₂]

octahedral complexes, the angle $N_{\text{axial}}\text{-Cr-}N_{\text{axial}}$ is closer to 180° than that of the title complex and the axial and equatorial distances have similar values.⁷⁰

In general, hydrogen bonding plays a principal role in the packing of the title compound. There are two types of H-bonds, including N-H \cdots Ow and O-H \cdots Ow (Table 31). The secondary amine hydrogens of the macrocycle as well as hydroxo ligand give rise to hydrogen bonds with uncoordinated lattice waters {N(2) \cdots Ow(1) (1.5-x, -1/2+y, 1.5-z) 3.010 Å, N(2)-H(2) \cdots Ow(1) (1.5-x, -1/2+y, 1.5-z) 162.00°; N(4) \cdots Ow(1) (1.5-x, -1/2+y, 1.5-z) 2.974 Å, N(4)-H(2) \cdots Ow(1) (1.5-x, -1/2+y, 1.5-z) 169.79°; O(1) \cdots Ow(1) 2.652 Å, O(1)-H(1d) \cdots Ow(1) 61.73°}. These interactions lead to the a formation of polymeric chains (Figure 7). This chain forms a related layer structure, but within the layers *cis*-[Cr([14]-decane)(*p*-OC₆H₄NO₂)(OH)]⁺ ions arrange of zig-zag configurations.



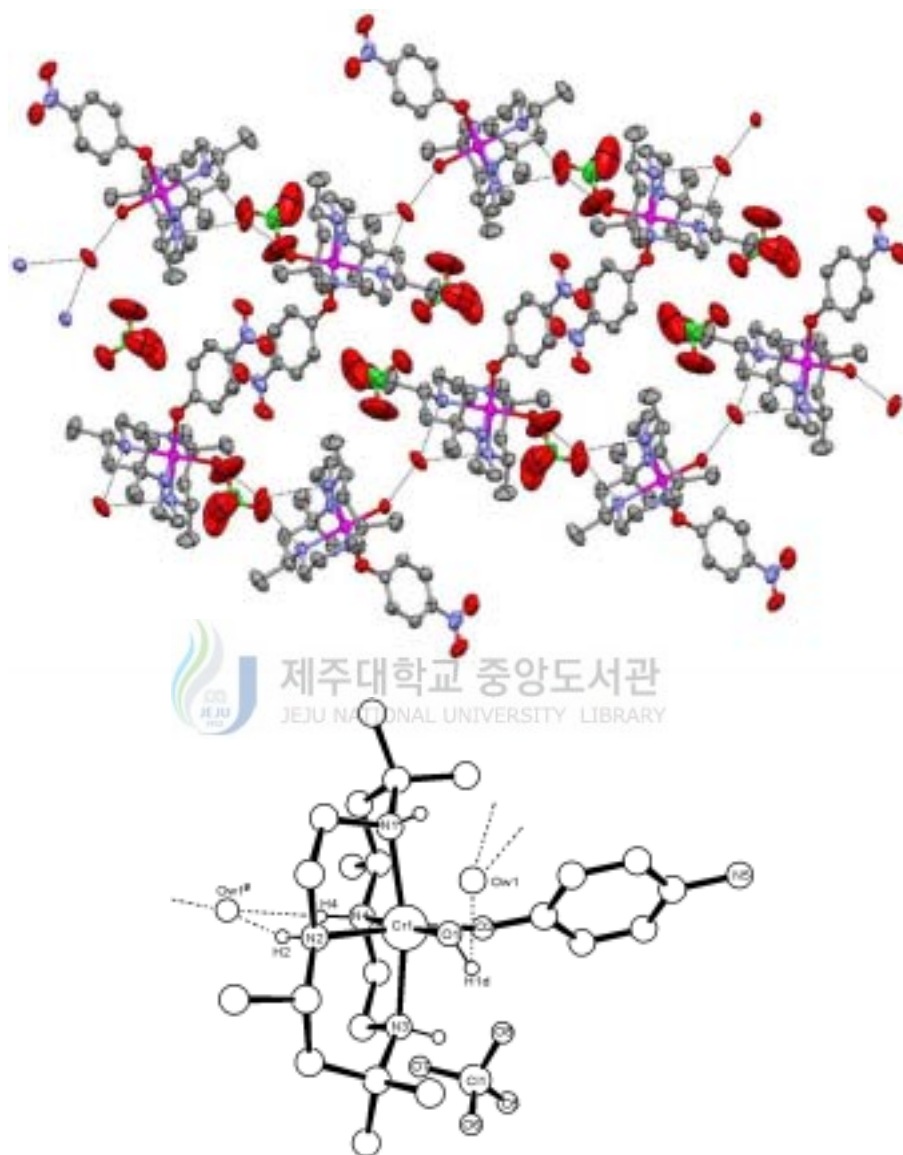


Figure 7. The molecular packing diagram and hydrogen-bonding scheme of the *cis*-[Cr([14]-decane)(*p*-OC₆H₄NO₂)(OH)]ClO₄·H₂O (**II**) complex.

Table 29. Bond lengths (Å) for *cis*-[Cr([14]-decane)(*p*-OC₆H₄NO₂)(OH)]-ClO₄·H₂O (**II**) complex

Cr(1)-O(1)	1.912(5)	C(8)-C(9)	1.537(9)
Cr(1)-O(2)	1.931(4)	C(9)-C(11)	1.526(10)
Cr(1)-N(2)	2.119(4)	C(9)-C(10)	1.548(9)
Cr(1)-N(1)	2.145(5)	C(12)-C(13)	1.505(9)
Cr(1)-N(4)	2.146(6)	C(14)-C(16)	1.515(10)
Cr(1)-N(3)	2.153(5)	C(14)-C(15)	1.531(11)
N(1)-C(4)	1.500(7)	C(17)-O(2)	1.323(7)
N(1)-C(2)	1.537(8)	C(17)-C(22)	1.396(8)
N(2)-C(5)	1.495(8)	C(17)-C(18)	1.396(9)
N(2)-C(6)	1.501(8)	C(18)-C(19)	1.378(8)
N(3)-C(9)	1.502(8)	C(19)-C(20)	1.380(8)
N(3)-C(12)	1.509(9)	C(20)-C(21)	1.364(9)
N(4)-C(13)	1.474(8)	C(20)-N(5)	1.445(8)
N(4)-C(14)	1.495(8)	C(21)-C(22)	1.368(9)
C(1)-C(2)	1.523(9)	N(5)-O(4)	1.233(8)
C(2)-C(3)	1.532(9)	N(5)-O(3)	1.241(7)
C(2)-C(16)	1.547(10)	Cl(1)-O(6)	1.314(9)
C(4)-C(5)	1.462(9)	Cl(1)-O(8)	1.346(6)
C(6)-C(8)	1.547(9)	Cl(1)-O(5)	1.385(9)
C(6)-C(7)	1.556(9)	Cl(1)-O(7)	1.394(7)

Table 30. Angles (°) for *cis*-[Cr([14]-decane)(*p*-OC₆H₄NO₂)(OH)]ClO₄·H₂O (**II**) complex

O(1)-Cr(1)-O(2)	92.89(19)	C(9)-N(3)-C(12)	110.6(5)
O(1)-Cr(1)-N(2)	86.8(2)	C(9)-N(3)-Cr(1)	123.7(4)
O(2)-Cr(1)-N(2)	174.47(18)	C(12)-N(3)-Cr(1)	106.2(4)
O(1)-Cr(1)-N(1)	89.7(2)	C(13)-N(4)-C(14)	111.0(5)
O(2)-Cr(1)-N(1)	101.93(18)	C(13)-N(4)-Cr(1)	105.0(4)
N(2)-Cr(1)-N(1)	83.59(18)	C(14)-N(4)-Cr(1)	118.6(4)
O(1)-Cr(1)-N(4)	176.87(17)	C(1)-C(2)-C(3)	108.7(6)
O(2)-Cr(1)-N(4)	85.4(2)	C(1)-C(2)-N(1)	107.7(6)
N(2)-Cr(1)-N(4)	95.2(2)	C(3)-C(2)-N(1)	110.9(6)
N(1)-Cr(1)-N(4)	88.1(2)	C(1)-C(2)-C(16)	110.6(6)
O(1)-Cr(1)-N(3)	99.3(2)	C(3)-C(2)-C(16)	109.3(6)
O(2)-Cr(1)-N(3)	86.18(19)	N(1)-C(2)-C(16)	109.5(5)
N(2)-Cr(1)-N(3)	88.44(19)	C(5)-C(4)-N(1)	110.8(6)
N(1)-Cr(1)-N(3)	167.6(2)	C(4)-C(5)-N(2)	110.4(5)
N(4)-Cr(1)-N(3)	83.2(2)	N(2)-C(6)-C(8)	112.7(5)
C(4)-N(1)-C(2)	111.0(5)	N(2)-C(6)-C(7)	110.6(6)
C(4)-N(1)-Cr(1)	106.4(4)	C(8)-C(6)-C(7)	107.2(6)
C(2)-N(1)-Cr(1)	123.3(4)	C(9)-C(8)-C(6)	117.5(6)
C(5)-N(2)-C(6)	111.7(5)	N(3)-C(9)-C(11)	108.8(5)
C(5)-N(2)-Cr(1)	103.4(3)	N(3)-C(9)-C(8)	109.3(5)
C(6)-N(2)-Cr(1)	116.0(4)	C(11)-C(9)-C(8)	111.4(6)
N(3)-C(9)-C(10)	112.8(6)	C(21)-C(20)-N(5)	119.9(6)
C(11)-C(9)-C(10)	107.7(6)	C(19)-C(20)-N(5)	120.3(6)
C(8)-C(9)-C(10)	106.7(6)	C(20)-C(21)-C(22)	121.7(6)
C(13)-C(12)-N(3)	110.4(5)	C(21)-C(22)-C(17)	119.6(6)
N(4)-C(13)-C(12)	108.9(5)	O(4)-N(5)-O(3)	123.8(6)

N(4)-C(14)-C(16)	110.9(5)	O(4)-N(5)-C(20)	118.9(6)
N(4)-C(14)-C(15)	113.1(6)	O(3)-N(5)-C(20)	117.3(7)
C(16)-C(14)-C(15)	110.0(7)	C(17)-O(2)-Cr(1)	140.8(4)
C(14)-C(16)-C(2)	118.8(6)	O(6)-Cl(1)-O(8)	115.8(9)
O(2)-C(17)-C(22)	117.7(6)	O(6)-Cl(1)-O(5)	102.8(8)
O(2)-C(17)-C(18)	123.8(5)	O(8)-Cl(1)-O(5)	107.6(5)
C(22)-C(17)-C(18)	118.4(6)	O(6)-Cl(1)-O(7)	107.5(7)
C(19)-C(18)-C(17)	120.9(6)	O(8)-Cl(1)-O(7)	110.5(6)
C(18)-C(19)-C(20)	119.5(6)	O(5)-Cl(1)-O(7)	112.5(7)
C(21)-C(20)-C(19)	119.8(6)		

Table 31. Selected bond lengths (Å) and angles(°) for hydrogen bond of *cis*-[Cr([14]-decane)(*p*-OC₆H₄NO₂)(OH)]ClO₄·H₂O (**II**) complex

D-H···A	d(D-H)	d(H···A)	<DHA	d(D···A)
macrocycle (NH) - water				
N(2)-H(2)···O _w (1) ^{#1}	0.911	2.131	162.00	3.010
N(4)-H(4)···O _w (1) ^{#1}	0.910	3.074	169.79	2.974
hydroxo ligand - water				
O(1)-H(1d)···O _w (1)	0.820	2.940	61.73	2.652

Symmetry transformations used to generate equivalent atoms : #1 ; 1.5-x, -1/2+y, 1.5-z.

The value of molar conductance for *cis*-[Cr([14]-decane){O-(*p*-OC₆H₄NO₂)}-(OH)]ClO₄·H₂O measured in DMF or DMSO correspond to a 1 : 1 electrolyte ($\Lambda_M = 66.9 \text{ ohm}^{-1}\text{cm}^2\text{mol}^{-1}$), indicating that the auxiliary *p*-nitrophenolate ligand and hydroxo ligand in the Cr(III) complexes are not dissociated from the complex in these polar solvents.⁷⁷

The absorption spectra of *cis*-[Cr([14]-decane)(*p*-OC₆H₄NO₂)(OH)]⁺ complex ion in DMF solution at room temperature is represented in Figure 8. This is overlapping absorption parts in the spectrum of the title complex including the two distinct bands. In *O_h* symmetry, three ligand field bands are expected for a *d*³ ion ${}^4A_{2g} \rightarrow {}^4T_{2g}$, ${}^4A_{2g} \rightarrow {}^4T_{1g}(F)$ and the two electron transition ${}^4A_{2g} \rightarrow {}^4T_{1g}(P)$.⁶¹

The two *d-d* bands of title complex was observed at 17301, 21114 cm⁻¹ (sh) can be related to the spin-allowed transitions, ${}^4A_{2g} \rightarrow {}^4T_{2g}$ and ${}^4A_{2g} \rightarrow {}^4T_{1g}$, respectively. The assignment of geometric configuration is confirmed by the *d-d* absorption spectra. The less symmetrical *cis*-isomers have much higher extinction coefficients than those of more symmetrical *trans*-isomers.⁵⁹

A chromium complexes in tetragonal symmetry are expected to have four absorption bands in *d-d* region, but each spectrum apparently has two major components. Thus, we fitted the spectra roughly with two Gaussian functions first and then added a minor component to reproduce the more suitable shape of the spectra in the region of interest. Finally, we performed least-squares fitting procedures, and the dotted lines in Figure 8 are Gaussian bands representing the approximate deconvolution of the spectra yielded by the calculations. The four peak positions calculated at 16578, 18368, 20741 and 21793 cm⁻¹ can be assigned to the 4E (${}^4T_{2g}$ in *O_h* symmetry), 4B_2 (${}^4T_{2g}$), 4E

(${}^4T_{1g}$) and 4A_2 (${}^4T_{1g}$), respectively.^{78,79}

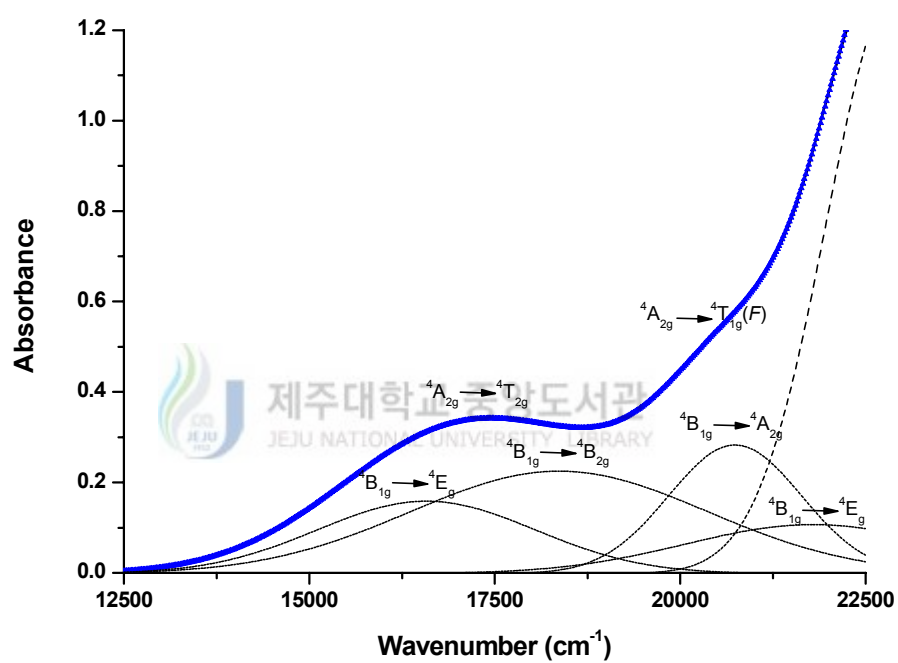


Figure 8. The electronic absorption spectrum of 2.0×10^{-3} M *cis*-[Cr([14]-decane)(*p*-OC₆H₄NO₂)(OH)]⁺ in DMF solution at 298 K.

The infrared spectrum of *cis*-[Cr([14]-decane)(*p*-OC₆H₄NO₂)(OH)] ·ClO₄·H₂O (**II**) recorded at room temperature is presented in Figure 9. The infrared spectrum of this complex, taken from KBr pellet, is in accord with the structure determined by X-ray diffraction. The IR spectrum displayed N-H stretches at 3243 and 3172 cm⁻¹, C-H stretches at 2978 and 2897 cm⁻¹, and a strong ionic ClO₄⁻ band at near 1111 cm⁻¹ and 625 cm⁻¹. The band occurring in the IR spectrum of the complex in the 3560 and 3512 cm⁻¹ region may probably be due to the ν(OH) vibration of hydroxo ligand and lattice water, respectively. A weak bands at near 418 cm⁻¹ region associated with the Cr-N(macrocycle) vibration.^{80,81}

In the literature, experimental results of nitro compound show that wave numbers of the NO₂ antisymmetric ν_{as}(NO₂) and symmetric ν_s(NO₂) stretching vibrations of aromatic nitro compounds appear in the 1500~1560 cm⁻¹ region and in the 1330~1380 cm⁻¹ region, respectively.⁸³⁻⁸⁸ The symmetric vibration band is stronger than the antisymmetric vibration band in the Raman spectra; the contrary holds in the infrared. Hence, the very strong infrared bands observed at 1494 and 1302 cm⁻¹ can be attributed to ν_{as}(NO₂) and ν_s(NO₂), respectively, in good agreement with the values given in the literature.⁸³⁻⁸⁸ In the *p*-nitrophenol case, the intense infrared absorption bands located at 1286, 1327 and 1344 cm⁻¹ are allotted to the vibration modes ν₃, ν₁₁ and to the ν_s(NO₂), respectively.^{85,87,89,90} In the infrared absorption spectra, the three bands of *cis*-[Cr([14]-decane)(*p*-OC₆H₄NO₂)(OH)]ClO₄·H₂O are formed a broad band centred at 1302 cm⁻¹.

This observation is consistent with the observed X-ray crystal structure of the title complex.

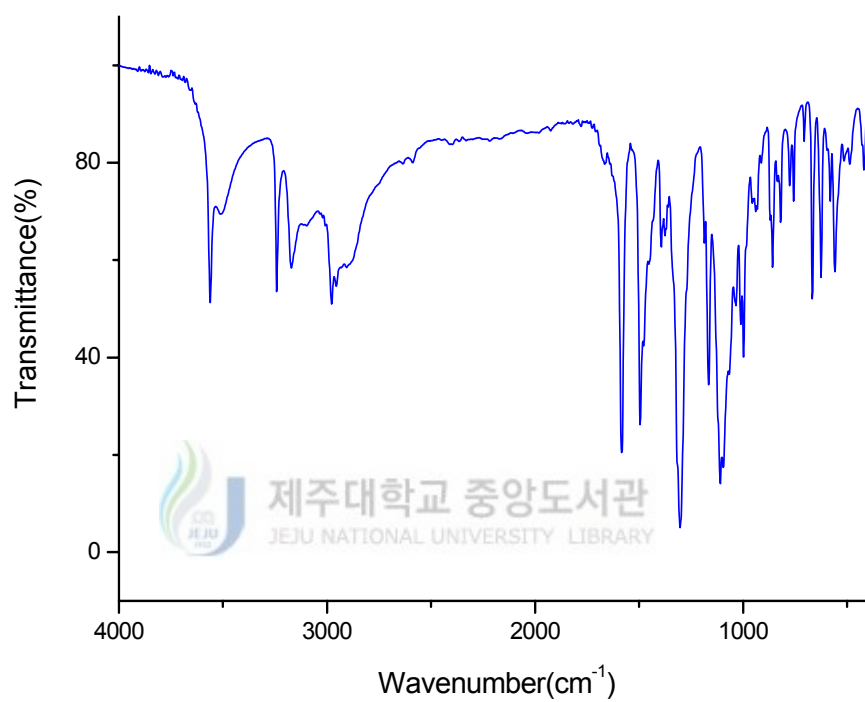


Figure 9. IR spectrum of *cis*-[Cr([14]-decane)(*p*-OC₆H₄NO₂)(OH)]ClO₄ · H₂O (**II**) complex.

In the FAB mass spectrum of *cis*-[Cr([14]-decane)(*p*-OC₆H₄NO₂)(OH)]ClO₄·H₂O, this is a peak at *m/z* 491.3 corresponding to the molecular ion *cis*-[Cr([14]-decane)(*p*-OC₆H₄NO₂)(OH)]⁺ (Figure 10). The molecular ion of the *cis*-[Cr([14]-decane)(*p*-OC₆H₄NO₂)(OH)]⁺ undergoes fragmentation to give species such as *cis*-[Cr([14]-decane)(*p*-OC₆H₄NO₂)]⁺, [Cr([14]-decane)]⁺ at *m/z* 473.3 and 336, respectively.

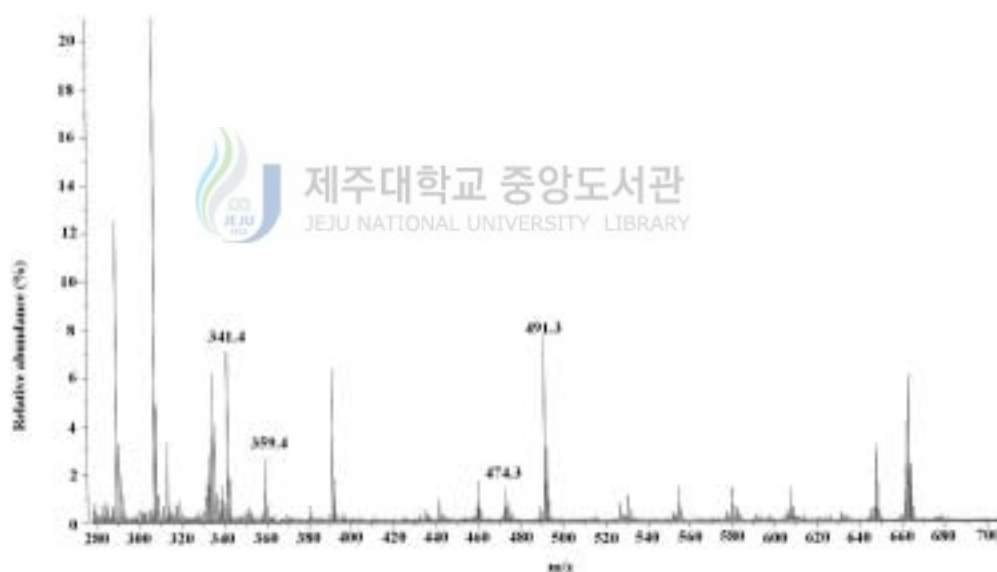


Figure 10. The FAB mass spectrum of the *cis*-[Cr([14]-decane)(*p*-OC₆H₄NO₂)-(OH)]ClO₄·H₂O.

2. Description of structure and physicochemical properties of Cu(II)-dioxatetraaza 20-membered macrocyclic complex

1) Structure and physicochemical properties of $[\text{Cu}_2([\text{20}]\text{-DCHDC})(\text{O}_2\text{N})_2] \cdot 6\text{H}_2\text{O}$ (III)

The green crystal of $[\text{Cu}_2([\text{20}]\text{-DCHDC})(\text{O}_2\text{N})_2] \cdot 6\text{H}_2\text{O}$ (III) suitable for structure determination was acquired from methanol and water (10 : 1 v/v) mixed solvent, by slow evaporation of solvent at room temperature. In the crystal structure, dinuclear complex III is sitting on two two-folded axes perpendicular to each other. Therefore, the asymmetric unit consist of a quarter of complex III and one water molecule. The unit cell is packed by four formular unit. An ORTEP drawing of asymmetric unit and core structure (top view) for the complex are given in Figure 11 and 12, respectively.

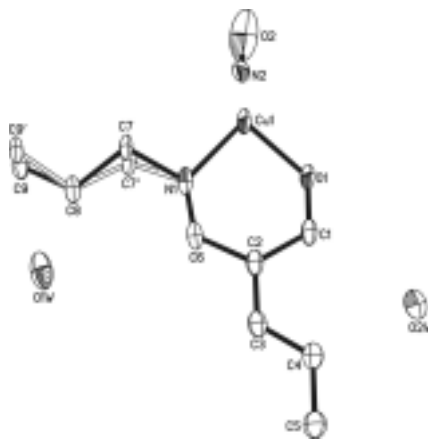


Figure 11. Structural representation of asymmetric unit of $[\text{Cu}_2([\text{20}]\text{-DCHDC})(\text{O}_2\text{N})_2] \cdot 6\text{H}_2\text{O}$ complex.

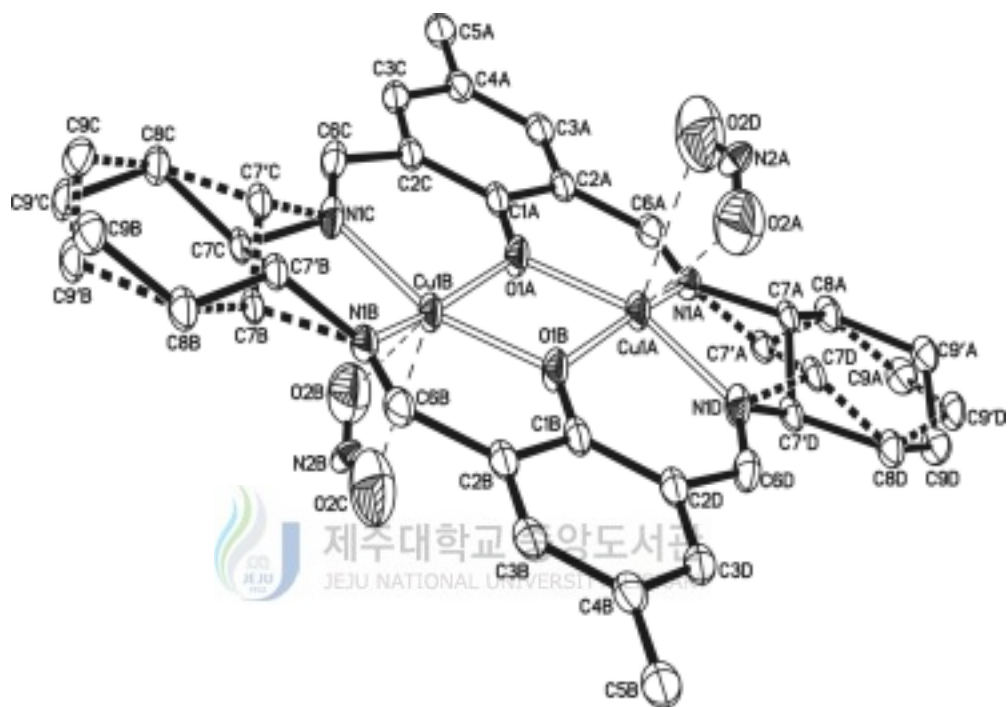
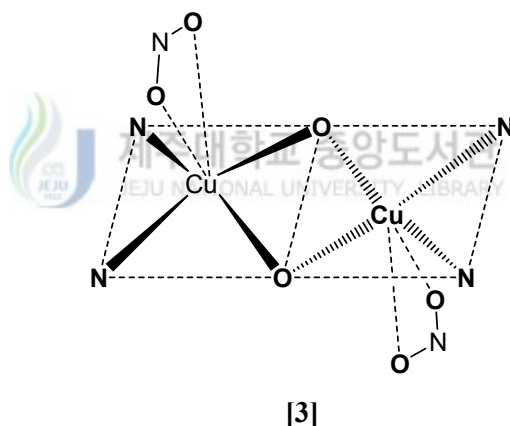


Figure 12. An ORTEP view of core structure (top view) for the $[\text{Cu}_2([\text{20}]\text{-DCHDC})(\text{O}_2\text{N})_2] \cdot 6\text{H}_2\text{O}$ complex showing 50% probability thermal ellipsoids and labels for non-H atoms.

The relevant bond distances and angles are given in Table 32 and 33. The binuclear core structures are centrosymmetry, with each copper(II) ion is six-coordinate defined by capped square-pyramidal geometry of interactions with two nitrogen and two oxygen atoms of the binucleating ligand [20]-DCHDC and two oxygen atoms each from the bidentated nitrite ligands at an apical site (**[3]**). The copper ions are displaced by 0.3288 Å from the basal least-squares plane toward nitrite ions. Two nitrite ions attached to two central metal Cu are situated *trans* to each other with respect to the mean molecular plane (**[3]**).

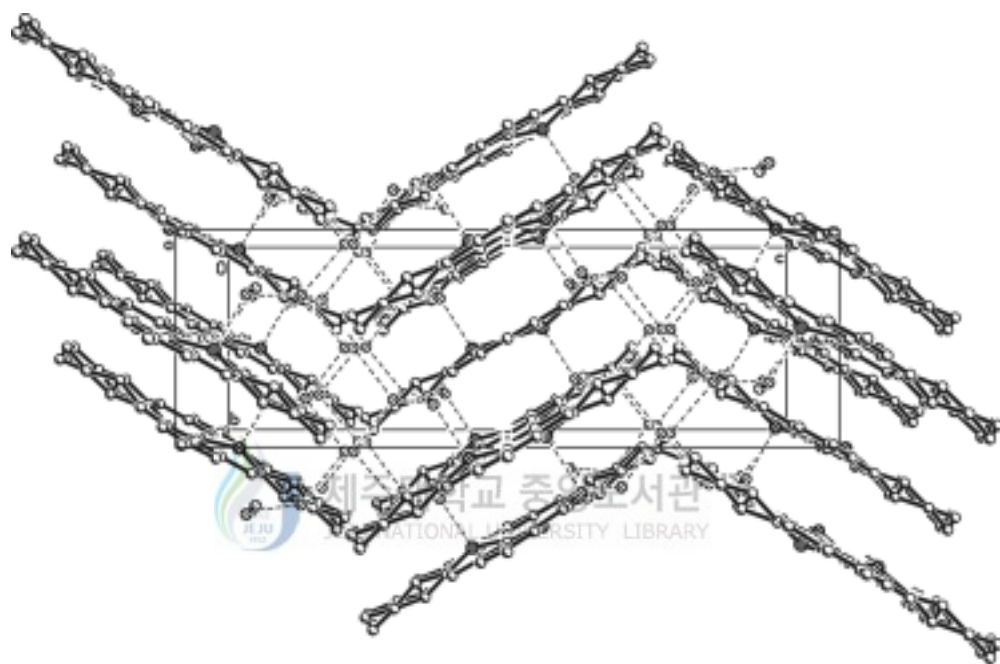


The interatomic Cu...Cu separation is 2.9542(8) Å. In the basal plane Cu-to-donor distances range from 1.903(2) Å to 1.912(2) Å. The axial Cu-O(2; nitrite) bond distance is 2.614(5) Å.

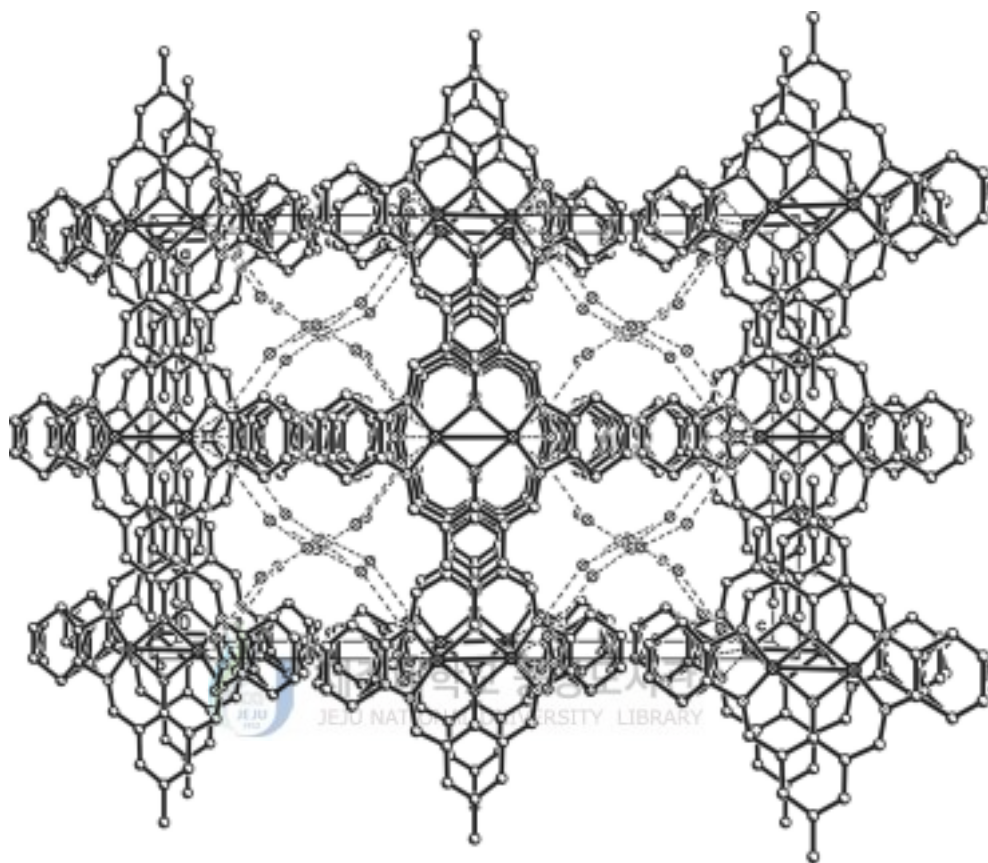
The macrocyclic complex adopts a non-flat structure with two square-pyramidal copper centers bridged by the two phenoxide oxygen atoms; the dihedral angle between the plane defined by N(1A), O(1A), and O(1B)

and the plane defined by Cu(1B), O(1A), and O(1B) is 167.57°. The angle of C(1)-O(1A)-O(1B) is exactly 180.00°, indicating that the two phenol mean planes are able to flat. The dihedral angle between the plane defined by nitrite {N(2A), O(2A), and O(2D)} and the plane defined by O(1A), C(2A), and C(2D) is 96.72°.

As shown in Figure 13 and Table 34, there are two types of intermolecular hydrogen bonds. The coordinated nitrite molecule form hydrogen bonds of the type Ow-H...O (nitrite) with lattice water {Ow(2)...O(2); 2.812 Å and Ow(2)-Hw(2B)...O(2); 149.37°}. The structure of the compound is further consolidated by another hydrogen bond of the type Ow-H...Ow between the lattice water molecules {Ow(1)...Ow(2) (x, -y, -z+1); 2.985 Å, Ow(1)-Hw(1)...Ow(2) (x, -y, -z+1); 137.10°, Ow(2)...Ow(1) (x, -y+1/2, z+1/2); 2.751 Å, Ow(2)-Hw(2A)...Ow(1)(x, -y+1/2, z+1/2); 168.40°, Ow(2)...Ow(1) (-x+1/2, -y+1/2, -z+1); 2.942 Å, and Ow(2)-Hw(2A)...Ow(1) (-x+1/2, -y+1/2, -z+1); 166.72°}. These interactions result in a formation of polymeric chains in the packing of the title compound (Figure 13).



(a) A view along the a -axis



(b) A view along the *b*-axis

Figure 13. The molecular packing diagram and hydrogen bonding scheme of $[\text{Cu}_2([\text{20}]\text{-DCHDC})(\text{O}_2\text{N})_2] \cdot 6\text{H}_2\text{O}$.

Table 32. Bond lengths (Å) for [Cu₂([20]-DCHDC)(O₂N)₂] · 6H₂O

Cu(1)-N(1)	1.903(2)	C(2)-C(6)	1.472(4)
Cu(1)-N(1)#1	1.903(2)	C(3)-C(4)	1.390(4)
Cu(1)-O(1)#2	1.912(2)	C(4)-C(3)#3	1.390(4)
Cu(1)-O(1)	1.912(2)	C(4)-C(5)	1.503(7)
Cu(1)-O(2)	2.614(5)	C(7)-C(7)#1	1.262(12)
Cu(1)-Cu(1)#2	2.9542(8)	C(7)-C(8)	1.531(6)
O(1)-C(1)	1.314(5)	C(7')-C(7')#1	1.476(12)
O(1)-Cu(1)#2	1.912(2)	C(7')-C(8)	1.479(6)
N(1)-C(6)	1.287(4)	C(8)-C(9)	1.472(9)
N(1)-C(7')	1.482(5)	C(8)-C(9')	1.551(8)
N(1)-C(7)	1.528(5)	C(9)-C(9)#1	1.567(19)
C(1)-C(2)#3	1.418(3)	C(9')-C(9')#1	1.254(18)
C(1)-C(2)	1.418(3)	N(2)-O(2)#1	1.038(6)
C(2)-C(3)	1.400(4)	N(2)-O(2)	1.038(6)

Symmetry transformations used to generate equivalent atoms:

#1 -x, y, z #2 -x, -y, -z+1 #3 x, -y, -z+1

Table 33. Angles [°] for [Cu₂([20]-DCHDC)(O₂N)₂] · 6H₂O

N(1)-Cu(1)-N(1)#1	88.75(14)	C(6)-N(1)-Cu(1)	125.54(18)
N(1)-Cu(1)-O(1)#2	160.15(8)	C(7')-N(1)-Cu(1)	111.8(3)
N(1)#1-Cu(1)-O(1)#2	93.01(10)	C(7)-N(1)-Cu(1)	105.2(3)
N(1)-Cu(1)-O(1)	93.01(10)	O(1)-C(1)-C(2)#3	120.2(2)
N(1)#1-Cu(1)-O(1)	160.15(8)	O(1)-C(1)-C(2)	120.2(2)
O(1)#2-Cu(1)-O(1)	78.82(14)	C(2)#3-C(1)-C(2)	119.7(4)
N(1)-Cu(1)-O(2)	112.32(12)	C(3)-C(2)-C(1)	118.7(3)
N(1)#1-Cu(1)-O(2)	81.76(13)	C(3)-C(2)-C(6)	117.4(2)
O(1)#2-Cu(1)-O(2)	87.49(11)	C(1)-C(2)-C(6)	123.8(3)
O(1)-Cu(1)-O(2)	115.54(10)	C(4)-C(3)-C(2)	122.5(3)
N(1)-Cu(1)-Cu(1)#2	129.99(7)	C(3)#3-C(4)-C(3)	118.0(4)
N(1)#1-Cu(1)-Cu(1)#2	129.99(7)	C(3)#3-C(4)-C(5)	121.0(2)
O(1)#2-Cu(1)-Cu(1)#2	39.41(7)	C(3)-C(4)-C(5)	121.0(2)
O(1)-Cu(1)-Cu(1)#2	39.41(7)	N(1)-C(6)-C(2)	125.4(2)
O(2)-Cu(1)-Cu(1)#2	104.51(8)	C(7)#1-C(7)-N(1)	117.3(2)
C(1)-O(1)-Cu(1)#2	129.41(7)	C(7)#1-C(7)-C(8)	124.1(2)
C(1)-O(1)-Cu(1)	129.41(7)	N(1)-C(7)-C(8)	112.3(4)
Cu(1)#2-O(1)-Cu(1)	101.18(14)	C(7')#1-C(7')-C(8)	120.5(3)
C(6)-N(1)-C(7')	121.3(3)	C(7')#1-C(7')-N(1)	113.6(3)
C(6)-N(1)-C(7)	127.4(3)	C(8)-C(7')-N(1)	118.2(4)
C(7')-N(1)-C(7)	27.0(2)	C(9)-C(8)-C(7')	114.8(5)
C(9)-C(8)-C(7)	117.3(5)	C(8)-C(9)-C(9)#1	118.6(4)
C(7')-C(8)-C(7)	27.0(2)	C(9')#1-C(9')-C(8)	123.7(3)
C(9)-C(8)-C(9')	22.8(3)	O(2)#1-N(2)-O(2)	140.9(7)
C(7')-C(8)-C(9')	115.7(4)	N(2)-O(2)-Cu(1)	87.2(4)
C(7)-C(8)-C(9')	106.9(4)		

Symmetry transformations used to generate equivalent atoms:

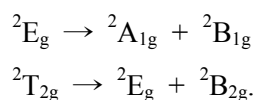
#1 -x, y, z #2 -x, -y, -z+1 #3 x, -y, -z+1

Table 34. Selected bond lengths (Å) and angles(°) for hydrogen bond of [Cu₂([20]-DCHDC)(O₂N)₂] · 6H₂O complex

D-H···A	d(D-H)	d(H···A)	<DHA	d(D···A)
lattice water - lattice water				
Ow(1)-Hw(1)···Ow(2) ^{#1}	0.846	2.309	137.10	2.985
Ow(2)-Hw(2A)···Ow(1) ^{#2}	0.849	1.913	168.40	2.751
Ow(2)-Hw(2A)···Ow(1) ^{#3}	0.849	2.109	166.72	2.942
lattice water - nitrite ligand				
Ow(2)-Hw(2B)···O(2)	0.844	2.053	149.37	2.812

Symmetry transformations used to generate equivalent atoms: #1 ; x, -y, -z+1, #2 ; x, -y+1/2, z+1/2, #3 ; -x+1/2, -y+1/2, -z+1.

The electronic absorption spectrum of [Cu₂([20]-DCHDC)(O₂N)₂] · 6H₂O complex at room temperature was represented in Figure 14. As shown this spectrum exhibited one band at 530 nm due to the ²E_g → ²T_{2g} (O_h) transitions. The symmetry of the octahedron, elongated or squashed along one axis, is D_{4h}, exactly that of the square plane. For tetragonal Cu²⁺ (d⁹) complexes the octahedral doublet ²E_g and ²T_{2g} are seen to split as



The relative energies of the tetragonal components depend upon whether the octahedron is elongated or squashed, for ground state of elongated form

is ${}^2B_{1g}$.⁹¹ Instead of the single ${}^2E_g \rightarrow {}^2T_{2g}$ transition which occurs for the regular octahedron, the tetragonally distorted molecule will exhibit two transitions ${}^2B_{1g} \rightarrow {}^2B_{2g}$ and ${}^2B_{1g} \rightarrow {}^2E_g$ at about the octahedral frequency. A further band at much lower energy is expected from ${}^2B_{1g} \rightarrow {}^2A_{1g}$ transition.⁹¹

The one *d-d* band of title complex observed at $18,868\text{ cm}^{-1}$ can be related to the spin-allowed transition, ${}^2E_g \rightarrow {}^2T_{2g}$. Copper complexes in tetragonal symmetry are expected to have three absorption bands in *d-d* region, but title spectra apparently have one major component. Thus, we fitted the spectrum roughly with Gaussian functions first and then added a minor component to reproduce the more suitable shape of the spectrum in the region of interest. Finally, we performed least-squares fitting procedures, and the dotted lines in Figure 14 are Gaussian bands representing the approximate deconvolution of the spectrum yielded by the calculations. The two peak positions calculated at $18,878$ and $22,038\text{ cm}^{-1}$ can be assigned to the ${}^2B_{1g} \rightarrow {}^2B_{2g}$ and ${}^2B_{1g} \rightarrow {}^2E_g$, respectively. The ${}^2B_{1g} \rightarrow {}^2A_{1g}$ transition bands have expected at much lower energy. The $23,576\text{ cm}^{-1}$ band are clearly associated with ligand to metal charge transfer transitions.

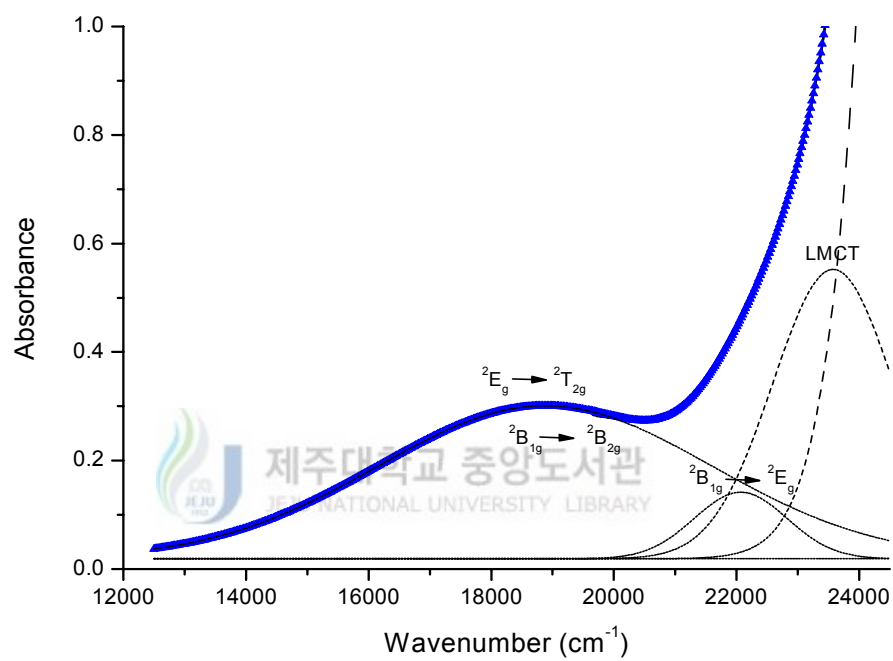


Figure 14. Electronic absorption spectrum of $[\text{Cu}_2([\text{20}]\text{-DCHDC})(\text{O}_2\text{N})_2] \cdot 6\text{H}_2\text{O}$ in methanol ($2.5 \times 10^{-3}\text{M}$).

IR spectra of the $[\text{Cu}_2([\text{20}]\text{-DCHDC})(\text{O}_2\text{N})_2] \cdot 6\text{H}_2\text{O}$ complex was presented in Figure 15. The strong and sharp absorption band occurring at 1627 cm^{-1} is attributed to $\nu(\text{C}=\text{N})$ of the coordinated $[\text{20}]\text{-DCHDC}$ ligand, and the absence of any carbonyl bands associated with the diformylphenol starting materials or nonmacrocyclic intermediates.^{92,93} The IR spectra displayed three C-H stretching vibrations from 3000 to 2800 cm^{-1} . A strong band at 15480 cm^{-1} region associated with the aromatic ring C=C vibrations. The sharp absorption band occurring at 1238 cm^{-1} region is attributed to phenolic C-O stretching vibration. The present complex exhibited four C-H deformation bands at 1450 , 1380 , 1350 and 1320 cm^{-1} regions and three out-of-plan vibration bands at 860 , 820 and 770 cm^{-1} regions. The bands occurring in the IR spectra of the complex in the 3398 cm^{-1} region may probably be due to the $\nu(\text{OH})$ vibration of the lattice water. A weak band at near 503 cm^{-1} region associated with the Cu-N(macrocycle) vibration.

Linkage isomerism is possible in the case of metal complexes containing the NO_2 unit. Coordination to the metal atom may occur through the nitrogen atom, resulting in a nitro-complex, or through an oxygen atom, resulting in a nitrito-complex. Nitro-complexes exhibit bands due to asymmetric and symmetric $-\text{NO}_2$ stretching vibration and, in addition, one due to a NO_2 deformation vibration. The nitrito-complexes exhibit bands due to asymmetric and symmetric $-\text{ONO}$ stretching vibrations which are well separated and occur at $1485\text{-}1400\text{ cm}^{-1}$ and $1110\text{-}1050\text{ cm}^{-1}$, respectively. Nitro-groups in metal coordination complexes may exist as bridging or as end groups. Terminal nitro-groups absorb at $1485\text{-}1370\text{ cm}^{-1}$ and $1340\text{-}1315\text{ cm}^{-1}$ due to the asymmetric and symmetric stretching vibrations of the NO_2 group,

respectively.⁹⁴ Nitrito-complexes do not have a band near 620cm^{-1} which is present for all nitro-complexes. Nitro- groups acting as bridging units (M-ONO-M) between two metal atoms absorb at $1485\text{-}1470\text{ cm}^{-1}$ and at about 1200 cm^{-1} , these bands being broader than those for terminal nitro-groups.^{94,95} The strong absorption peaks at 1446 and 1205 cm^{-1} in the $[\text{Cu}_2([\text{20}]\text{-DCHDC})(\text{O}_2\text{N})_2] \cdot 6\text{H}_2\text{O}$ are assigned to a bidentate nitrito ligand Cu-O₂N. This observation is consistent with the observed X-ray crystal structure of the title complex.



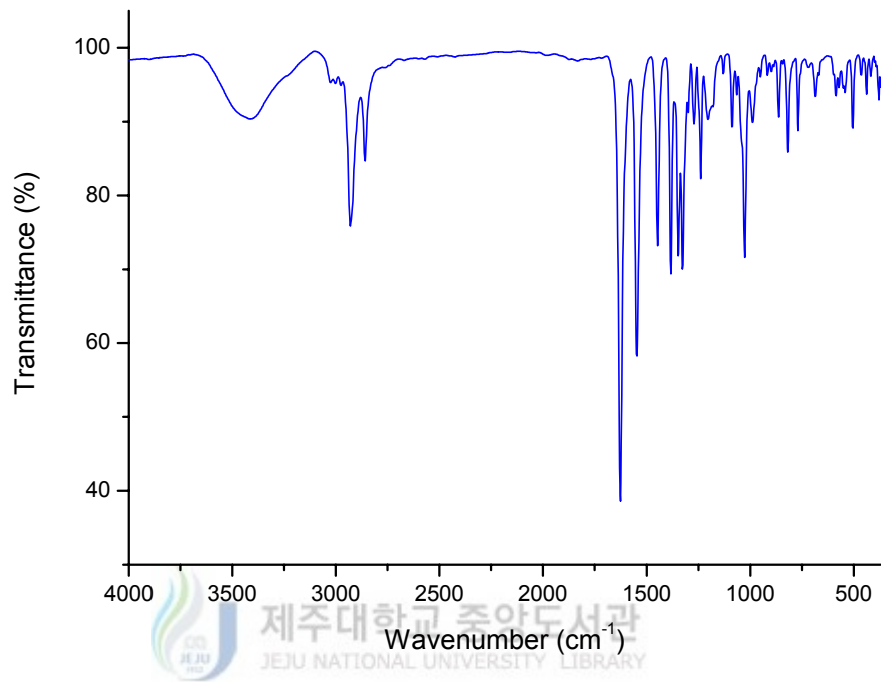
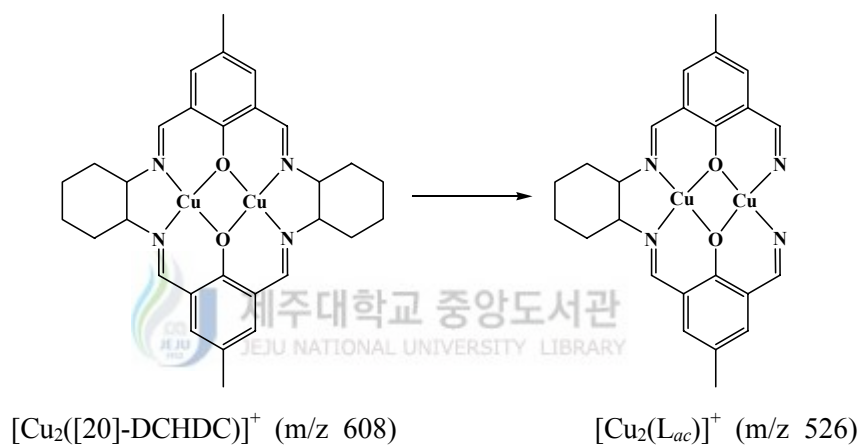


Figure 15. FT-IR spectrum of [Cu₂([20]-DCHDC)(O₂N)₂] · 6H₂O complex.

The FAB mass spectra of the $[\text{Cu}_2([\text{20}]\text{-DCHDC})(\text{O}_2\text{N})_2] \cdot 6\text{H}_2\text{O}$ complex was shown in Figure 16. The molecular ion loses the exocyclic ligands resulting in the formation of the fragment $[\text{Cu}_2([\text{20}]\text{-DCHDC})]^+$. This fragment is well observed in the FAB mass spectra at m/z 608 region. α -Cleavage peak of one cyclohexane from the $[\text{Cu}_2([\text{20}]\text{-DCHDC})]^+$ ion in the formation of the fragment $[\text{Cu}_2(\text{L}_{ac})]^+$ is observed at m/z 526 region.



Removal peak of one copper ion from the $[\text{Cu}_2([\text{20}]\text{-DCHDC})]^+$ ion in the formation of the fragment $[\text{Cu}([\text{20}]\text{-DCHDC})]^+$ is observed at m/z 545. These peaks are associated with peaks of mass one or two greater or less, which are attributed to protonated /deprotonated forms. This also accounts for the slight ambiguities in making assignments. The weak peak corresponding to the $[\text{Cu}_2([\text{20}]\text{-DCHDC})(\text{O}_2\text{N})]^+$ is observed at m/z 655.3.

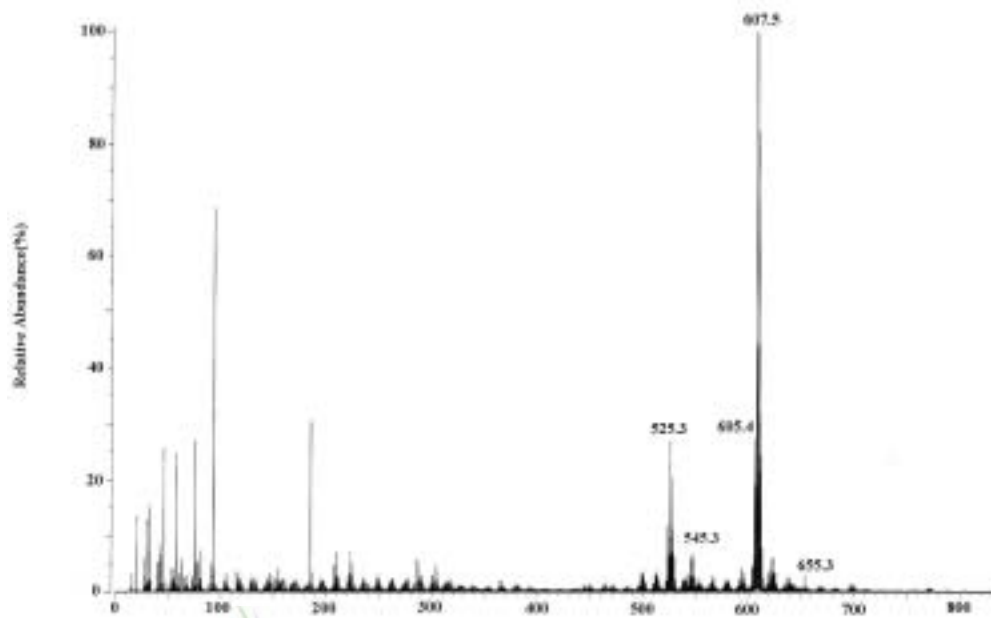
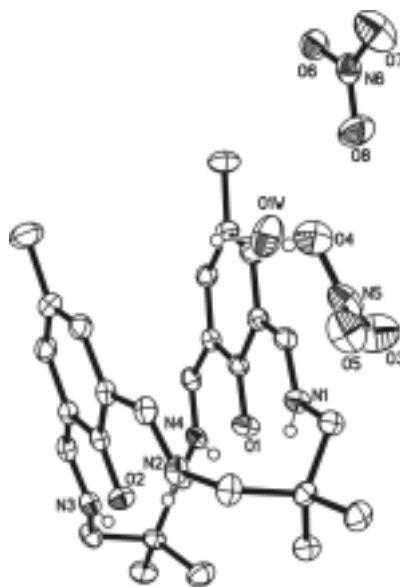
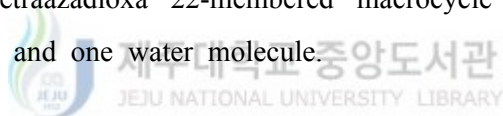


Figure 16. FAB mass spectrum of the $[\text{Cu}_2([\text{20}]\text{-DCHDC})(\text{O}_2\text{N})_2] \cdot 6\text{H}_2\text{O}$.

3. Description of structure and physicochemical properties of Ni(II)-tetraazadioxa 22-membered macrocyclic complexes

1) Structure and physicochemical properties of $[\text{H}_4[22]\text{-HMTADO}](\text{NO}_3)_2 \cdot \text{H}_2\text{O}$ (IV)

Suitable crystals of $[\text{H}_4[22]\text{-HMTADO}](\text{NO}_3)_2 \cdot \text{H}_2\text{O}$ were obtained by slow evaporation of acetonitrile solution of the compound at atmospheric pressure. An ORTEP drawing of core structure (top view) for the complex are given in Figure 17. The crystal structure of this di(hydrionitrate) compound is composed of tetraazadioxa 22-membered macrocycle ($[\text{H}_4[22]\text{-HMTADO}]^{2+}$), two nitrate ions and one water molecule.



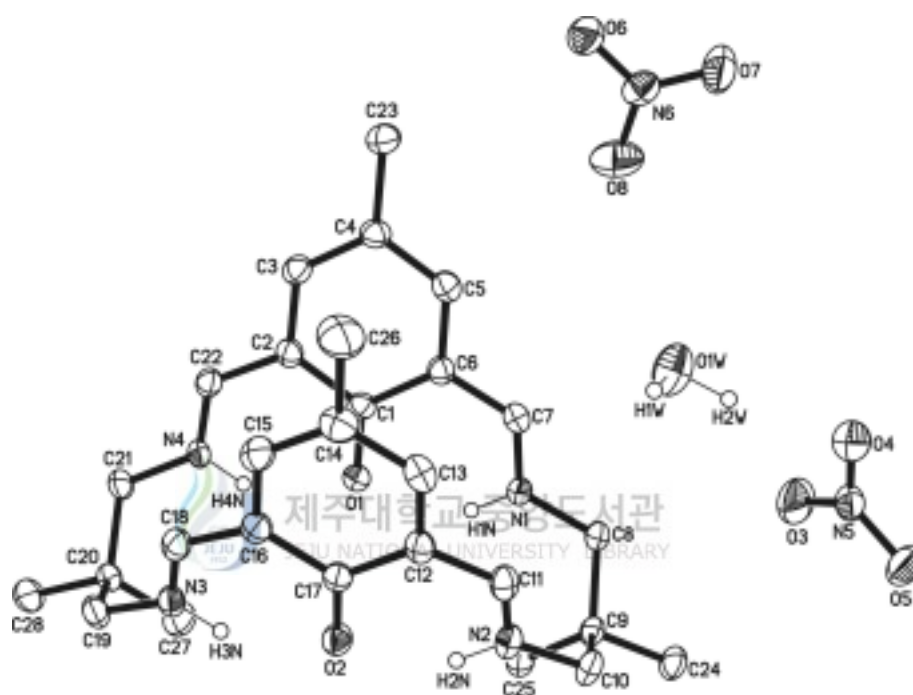
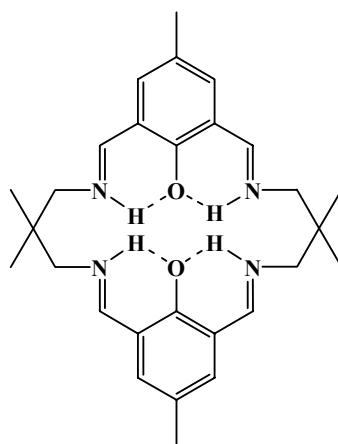


Figure 17. An ORTEP view of core structure (top view) for the $[H_4[22]\text{-HMTADO}](NO_3)_2 \cdot H_2O$ (**IV**) complex showing 50% probability thermal ellipsoids and labels for non-H atoms.

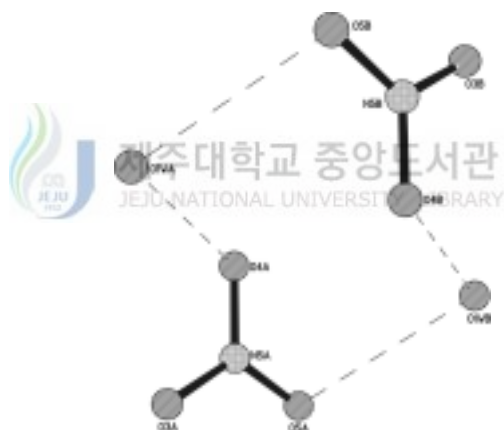
The relevant bond distances and angles are given in Table 35 and 36, respectively. The inner cavity of macrocycle is vacant, and each azomethine nitrogen atoms are protonation. The tetraazadioxa 22-membered macrocycle ($[H_4[22]-HMTADO]^{2+}$) is C_{2v} symmetry. The dihedral angle between the planes defined of two phenoxide is $16.94(9)^\circ$. The overall structure of macrocycle is bent owing to the tetrahedral conformation effect of two dimethyl-propylene at the side. The two dimethyl-propylene are situated eclipsed conformation. In the $[H_4[22]-HMTADO]^{2+}$, two phenoxide planes are close; $N(1)\cdots N(2)$ 3.039 Å, $N(3)\cdots N(4)$ 2.976 Å, $O(1)\cdots O(2)$ 3.275 Å, and $C(23)\cdots C(26)$ 4.829 Å.

As shown in Figure 18 and Table 37, there are two types of hydrogen bonds. The protonated imine and phenoxide oxygen of macrocycle form internal hydrogen bond; $N(1)\cdots O(2)$ 2.659 Å, $N(1)-H(1N)\cdots O(2)$ 133.80° , $N(2)\cdots O(1)$ 2.616 Å, $N(2)-H(2N)\cdots O(1)$ 138.04° , $N(3)\cdots O(2)$ 2.653 Å, $N(3)-H(3N)\cdots O(2)$ 136.85° , $N(4)\cdots O(1)$ 2.605 Å, and $N(4)-H(4N)\cdots O(1)$ 137.03° .



[4]

Under this situation, the self-organization of seems to make the structure **4** more stable by the hydrogen bonding interaction, in which the hydrogens of protonated imine are H-bonded with phenoxide oxygens to form six-membered rings. The nitrate ion form hydrogen bonds of the type Ow-H \cdots O (nitrate) with lattice water; Ow(1) \cdots O(4) 2.868 Å, Ow(1)-H(2w) \cdots O(4) 162.20°, Ow(1) \cdots O(3) 3.312 Å, Ow(1)-H(2w) \cdots O(3) 140.93°, Ow(1) \cdots O(5) (-x+1, -y, -z+1) 2.889 Å, Ow(1)-H(1w) \cdots O(5) (-x+1, -y, -z+1) 162.91°, Ow(1) \cdots O(4) (-x+1, -y, -z+1) 3.271 Å, and Ow(1)-H(1w) \cdots O(4) (-x+1, -y, -z+1) 131.54°.



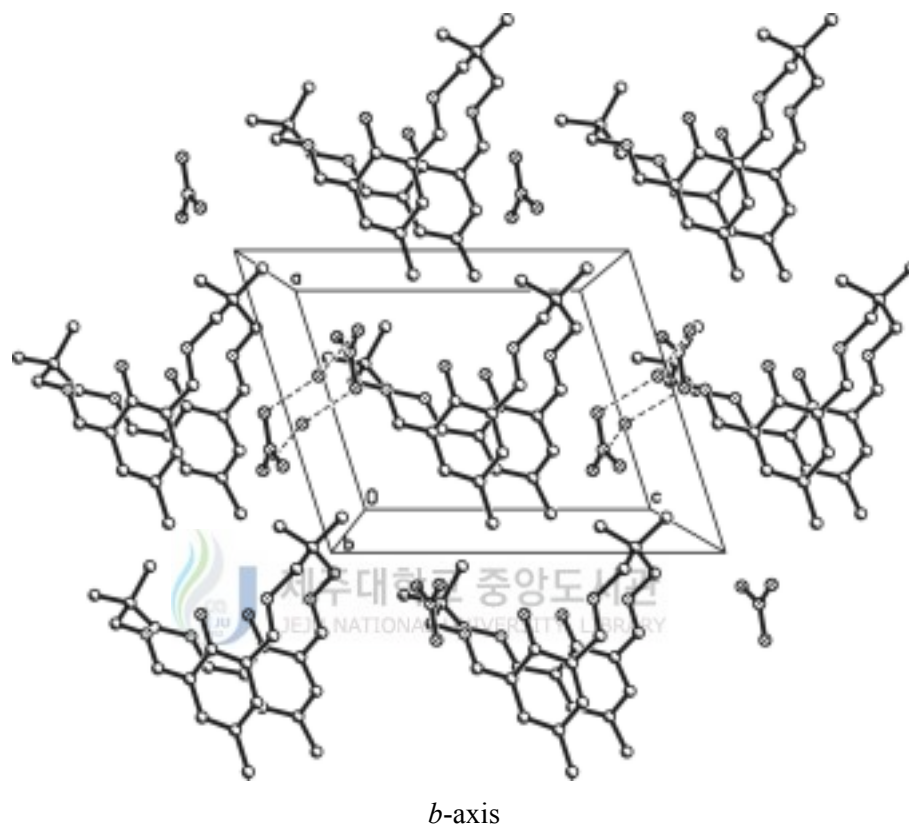


Figure 18. The molecular packing diagram and hydrogen bonding scheme of [H₄[22]-HMTADO](NO₃)₂ · H₂O (**IV**).

Table 35. Bond lengths (Å) for [H₄[22]-HMTADO](NO₃)₂ · H₂O (**IV**)

O(1)-C(1)	1.282(2)	C(9)-C(24)	1.540(3)
O(2)-C(17)	1.277(2)	C(9)-C(10)	1.544(3)
N(1)-C(7)	1.293(3)	C(11)-C(12)	1.427(3)
N(1)-C(8)	1.474(3)	C(12)-C(13)	1.398(3)
N(2)-C(11)	1.291(3)	C(12)-C(17)	1.443(3)
N(2)-C(10)	1.470(3)	C(13)-C(14)	1.387(3)
N(3)-C(18)	1.291(3)	C(14)-C(15)	1.390(3)
N(3)-C(19)	1.464(3)	C(14)-C(26)	1.509(3)
N(4)-C(22)	1.292(3)	C(15)-C(16)	1.404(3)
N(4)-C(21)	1.468(3)	C(16)-C(18)	1.425(3)
C(1)-C(6)	1.439(3)	C(16)-C(17)	1.449(3)
C(1)-C(2)	1.444(3)	C(19)-C(20)	1.533(3)
C(2)-C(3)	1.399(3)	C(20)-C(27)	1.529(3)
C(2)-C(22)	1.427(3)	C(20)-C(21)	1.533(3)
C(3)-C(4)	1.386(3)	C(20)-C(28)	1.538(3)
C(4)-C(5)	1.390(3)	N(5)-O(3)	1.245(3)
C(4)-C(23)	1.517(3)	N(5)-O(5)	1.256(3)
C(5)-C(6)	1.403(3)	N(5)-O(4)	1.256(3)
C(6)-C(7)	1.427(3)	N(6)-O(7)	1.241(3)
C(8)-C(9)	1.536(3)	N(6)-O(6)	1.247(2)
C(9)-C(25)	1.533(3)	N(6)-O(8)	1.254(3)

Table 36. Angles [°] for [H₄[22]-HMTADO](NO₃)₂ · H₂O (**IV**)

C(7)-N(1)-C(8)	123.06(18)	C(25)-C(9)-C(24)	109.90(17)
C(11)-N(2)-C(10)	124.41(19)	C(8)-C(9)-C(24)	105.76(17)
C(18)-N(3)-C(19)	123.43(19)	C(25)-C(9)-C(10)	110.77(18)
C(22)-N(4)-C(21)	124.89(18)	C(8)-C(9)-C(10)	112.97(18)
O(1)-C(1)-C(6)	122.01(18)	C(24)-C(9)-C(10)	106.23(17)
O(1)-C(1)-C(2)	122.51(18)	N(2)-C(10)-C(9)	112.31(17)
C(6)-C(1)-C(2)	115.48(18)	N(2)-C(11)-C(12)	122.7(2)
C(3)-C(2)-C(22)	119.08(19)	C(13)-C(12)-C(11)	118.40(19)
C(3)-C(2)-C(1)	120.87(18)	C(13)-C(12)-C(17)	121.03(19)
C(22)-C(2)-C(1)	120.03(18)	C(11)-C(12)-C(17)	120.33(19)
C(4)-C(3)-C(2)	122.89(19)	C(14)-C(13)-C(12)	123.0(2)
C(3)-C(4)-C(5)	117.09(19)	C(13)-C(14)-C(15)	117.1(2)
C(3)-C(4)-C(23)	121.55(19)	C(13)-C(14)-C(26)	121.4(2)
C(5)-C(4)-C(23)	121.37(19)	C(15)-C(14)-C(26)	121.5(2)
C(4)-C(5)-C(6)	122.85(19)	C(14)-C(15)-C(16)	123.0(2)
C(5)-C(6)-C(7)	118.28(19)	C(15)-C(16)-C(18)	118.5(2)
C(5)-C(6)-C(1)	120.74(19)	C(15)-C(16)-C(17)	120.57(19)
C(7)-C(6)-C(1)	120.98(18)	C(18)-C(16)-C(17)	120.67(19)
N(1)-C(7)-C(6)	124.23(19)	O(2)-C(17)-C(12)	122.37(18)
N(1)-C(8)-C(9)	115.12(17)	O(2)-C(17)-C(16)	122.28(19)
C(25)-C(9)-C(8)	110.95(18)	C(12)-C(17)-C(16)	115.33(18)
N(3)-C(18)-C(16)	123.8(2)	N(4)-C(21)-C(20)	114.11(17)
N(3)-C(19)-C(20)	114.60(17)	N(4)-C(22)-C(2)	122.66(19)
C(27)-C(20)-C(19)	111.68(19)	O(3)-N(5)-O(5)	119.9(2)
C(27)-C(20)-C(21)	110.65(18)	O(3)-N(5)-O(4)	120.2(2)
C(19)-C(20)-C(21)	112.74(18)	O(5)-N(5)-O(4)	119.9(2)
C(27)-C(20)-C(28)	109.83(18)	O(7)-N(6)-O(6)	120.3(2)

C(19)-C(20)-C(28)	105.67(17)	O(7)-N(6)-O(8)	120.6(2)
C(21)-C(20)-C(28)	105.96(18)	O(6)-N(6)-O(8)	119.1(2)

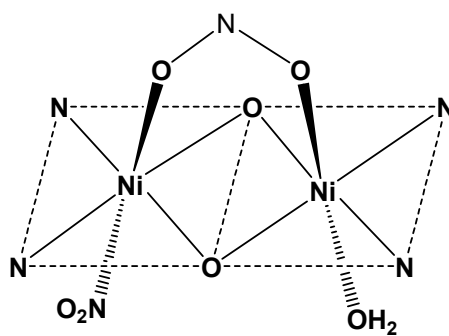
Table 37. Selected bond lengths (Å) and angles(°) for hydrogen bond of [H₄[22]-HMTADO](NO₃)₂ · H₂O (**IV**) complex

D-H···A	d(D-H)	d(H···A)	<DHA	d(D···A)
internal macrocyle ligand (protonation imine NH - phenoxide oxygen)				
N(1)-H(1N)···O(2)	0.913	1.944	133.80	2.659
N(2)-H(2N)···O(1)	0.914	1.864	138.04	2.616
N(3)-H(3N)···O(2)	0.903	1.921	136.85	2.653
N(4)-H(4N)···O(1)	0.885	1.886	137.03	2.605
lattice water - nitrate ions				
Ow(1)-H(2w)···O(4)	0.967	1.931	162.20	2.868
Ow(1)-H(2w)···O(3)	0.967	2.505	140.93	3.312
Ow(1)-H(1w)···O(5) ^{#1}	0.953	1.964	162.91	2.889
Ow(1)-H(1w)···O(4) ^{#1}	0.953	2.560	131.54	3.271

Symmetry transformations used to generate equivalent atoms: #1 ; -x+1, -y, -z+1.

2) Structure and physicochemical properties of $[\text{Ni}_2([\text{22}]\text{-HMTADO})(\mu\text{-O}_2\text{N})(\text{NO}_2)(\text{OH}_2)]$ (**V**)

The green crystals of $[\text{Ni}_2([\text{22}]\text{-HMTADO})(\mu\text{-O}_2\text{N})(\text{NO}_2)(\text{OH}_2)]$ (**V**) suitable for X-ray diffraction study which deposited on standing for *ca.* 1 month were recrystallized from methanol of this complex. An ORTEP view of (**V**) is shown in Figure 19, and bond distances and angles are summarized in Table 38 and 39, respectively. The dinegative $([\text{22}]\text{-HMTADO})^{2-}$ accommodates two Ni(II) ions in its N_4O_2 sites in the Ni(1)···Ni(2) separation of 3.013 Å. The structure of title complex shows that the two metal centers are bridged by the two phenoxide oxygens as well as by two oxygens of the coordinated nitrite (O-bonding) ([5]). Both the metal centers are six-coordinated with irregular octahedral geometry and have N_2O_2 equatorial donors provided by the macrocyclic ligand. The remaining apical position of the Ni(1) center is occupied by a water molecule, while that of another Ni(2) by a nitrite nitrogen (N-bonding) ([5]).



[5]

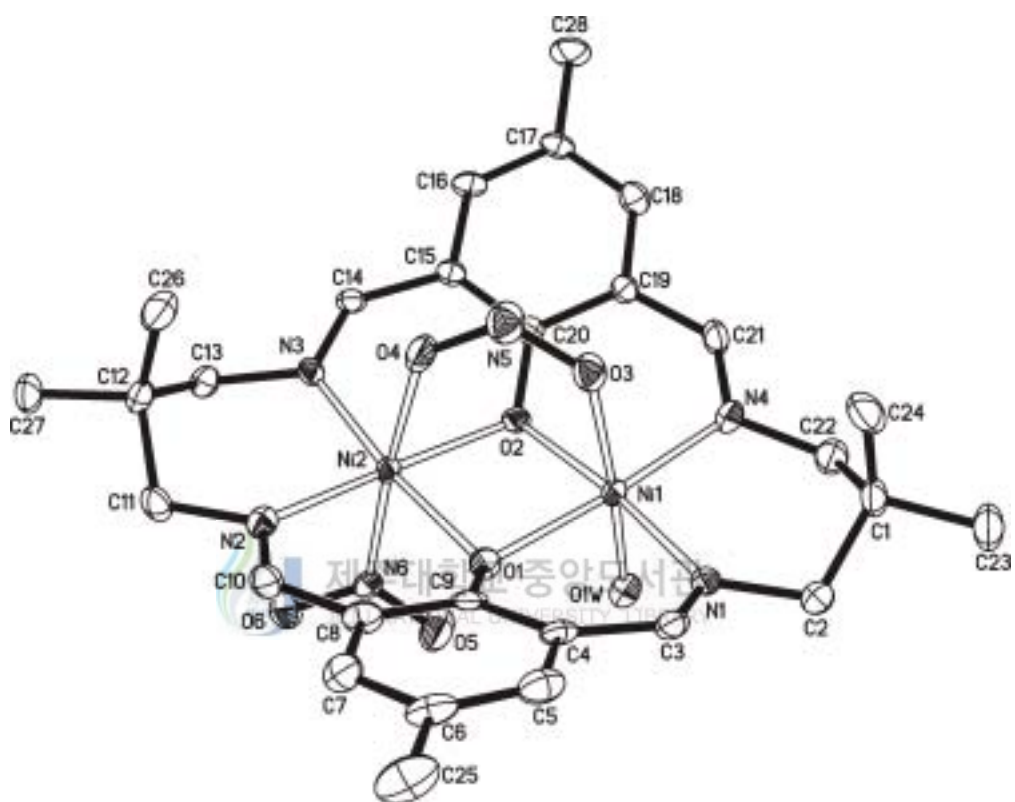
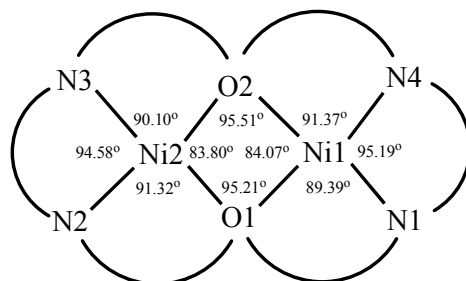


Figure 19. An ORTEP view of core structure (top view) for the $[\text{Ni}_2([\text{22}]\text{-HMTADO})(\mu\text{-O}_2\text{N})(\text{NO}_2)(\text{OH}_2)]$ complex showing 50% probability thermal ellipsoids and labels for non-H atoms.



[6]

The macrocyclic complex adopts a non-flat structure ($\text{Ni}_2\text{N}_4\text{O}_2$) with two octahedral nickel centers bridged by the two phenoxide oxygen atoms; the dihedral angle between the plane defined by N(3), O(2), and O(1) and the plane defined by Ni(1), O(2), and O(1) is 166.29° , and the dihedral angle between the plane defined by N(4), O(2), and O(1) and the plane defined by Ni(2), O(2), and O(1) is 167.08° .

The Ni_2O_2 plane adopts a flat structure with Ni-O-Ni angles ($95.21(13)^\circ$ and $95.51(13)^\circ$) ([6]). The sum of angles 358.59° at the phenoxide oxygens is almost 360° , indicating no square oxygen distortion.

The sum of angles 360.02° at the octahedral Ni(1) basal planes (NiN_2O_2) is exactly 360° , indicating no plane distortion. The Ni(1)-N (imines) bond distances are in the range of 2.027(4) and 2.038(4) Å, and Ni(1)-O (phenoxide) are 2.028(3) and 2.042(3) Å. The Ni(1)-O(3) (nitrito) and Ni(1)-Ow(1) (aqua) bond distances are in the range of 2.118(3) and 2.104(4) Å, respectively. The bond angles of Ni(2)-Ni(1)-O(3) (nitrito), Ni(2)-Ni(1)-Ow(1) (aqua) and O(3)-Ni(1)-Ow(1) are 80.05° , 94.83° and 171.97° , respectively. In this complex Ni(1)-N (imines) and Ni(1)-O (phenolic)

distances are shorter than Ni(1)-O(3) (nitrito) and Ni(1)-Ow(1) (aqua) distances and the angle of Ni(2)-Ni(1)-O(3) (nitrito) is smaller than the ideal value of 90°, indicating that the donor atoms are not able to achieve the apical positions of a perfect octahedron.

The sum of angles 359.80° at the octahedral Ni(2) basal planes (NiN₂O₂) is exactly 360°, indicating no plane distortion. The Ni(2)-N (imines) bond distances are in the range of 2.029(4) and 2.040(4) Å, and Ni(2)-O (phenoxide) are 2.038(3) and 2.043(3) Å. The Ni(2)-O(4) (nitrito) and Ni(2)-N(6) (nitro) bond distances are in the range of 2.164(3) and 2.141(4) Å, respectively. The bond angles of Ni(1)-Ni(2)-O(4) (nitrito), Ni(1)-Ni(2)-N(6) (nitro) and O(4)-Ni(2)-N(6) are 77.15°, 98.70° and 174.68°, respectively. In this complex Ni(2)-N (imines) and Ni(2)-O (phenolic) distances are shorter than Ni(2)-O(4) (nitrito) and Ni(2)-N(6) (nitro) distances and the angle of Ni(1)-Ni(2)-O(4) (nitrito) is smaller than the ideal value of 90°, indicating that the donor atoms are not able to achieve the apical positions of a perfect octahedron. The O(1) and O(2)-phenolic group mean planes of macrocycle are bent 26.52° and 27.11° toward bridged nitrito ligand, respectively, with the basal Ni₂O₂ least-squares plane.

As shown in Figure 20 and Table 40, there are two types of intermolecular hydrogen bonds. The coordinated nitrite molecule form hydrogen bonds of the type Ow-H...O (nitrito) with coordinated water {Ow(1)...O(5); 2.734 Å and Ow(1)-Hw(1B)...O(5); 178.16°}. And the structure of the compound is further consolidated by another hydrogen bond of the type Ow-H...O between the coordinated water molecule and nitrite of neighbor complex {Ow(1)...O(6) (x, y-1/2, -z+1/2); 2.879 Å, Ow(1)-Hw(1

A)⋯O) ($x, y-1/2, -z+1/2$; 159.98°). These interactions result in a formation of polymeric chains and in the packing of the title compound (Figure 20). This chain forms a related layer structure, but within the layers arrange zig-zag configurations.



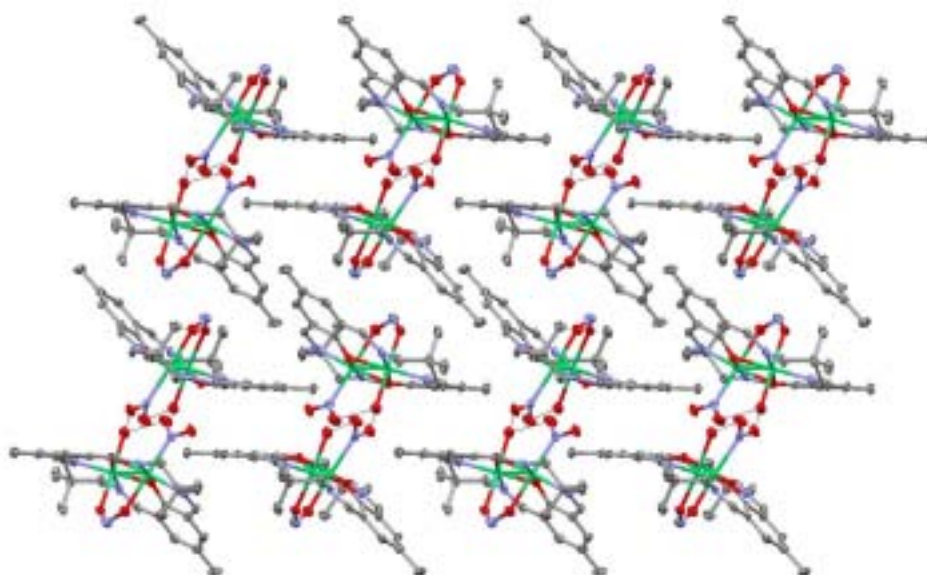


Figure 20. The molecular packing diagram and hydrogen bonding scheme of $[\text{Ni}_2([\text{22}]\text{-HMTADO})(\mu\text{-O}_2\text{N})(\text{NO}_2)(\text{OH}_2)]$.

Table 38. Bond lengths (Å) for [Ni₂([22]-HMTADO)(μ -O₂N)(NO₂)(OH₂)]

Ni(1)-N(4)	2.027(4)	N(2)-C(11)	1.487(6)
Ni(1)-O(2)	2.028(3)	N(3)-C(14)	1.273(6)
Ni(1)-N(1)	2.038(4)	N(3)-C(13)	1.476(6)
Ni(1)-O(1)	2.042(3)	N(4)-C(21)	1.283(6)
Ni(1)-O(1W)	2.104(4)	N(4)-C(22)	1.465(6)
Ni(1)-O(3)	2.118(3)	C(1)-C(23)	1.533(7)
Ni(2)-N(3)	2.029(4)	C(1)-C(24)	1.535(8)
Ni(2)-O(1)	2.038(3)	C(1)-C(2)	1.537(7)
Ni(2)-N(2)	2.040(4)	C(1)-C(22)	1.538(7)
Ni(2)-O(2)	2.043(3)	C(3)-C(4)	1.452(7)
Ni(2)-N(6)	2.141(4)	C(4)-C(5)	1.408(7)
Ni(2)-O(4)	2.164(3)	C(4)-C(9)	1.429(6)
O(1)-C(9)	1.314(6)	C(5)-C(6)	1.382(7)
O(2)-C(20)	1.322(5)	C(6)-C(7)	1.389(7)
O(3)-N(5)	1.269(5)	C(6)-C(25)	1.513(7)
O(4)-N(5)	1.269(5)	C(7)-C(8)	1.403(7)
O(5)-N(6)	1.252(5)	C(8)-C(9)	1.421(7)
O(6)-N(6)	1.248(5)	C(8)-C(10)	1.455(7)
N(1)-C(3)	1.268(6)	C(11)-C(12)	1.532(7)
N(1)-C(2)	1.470(6)	C(12)-C(13)	1.533(7)
N(2)-C(10)	1.281(6)	C(12)-C(27)	1.537(6)
C(12)-C(26)	1.538(7)	C(17)-C(18)	1.386(7)
C(14)-C(15)	1.445(6)	C(17)-C(28)	1.510(6)
C(15)-C(16)	1.405(6)	C(18)-C(19)	1.416(6)
C(15)-C(20)	1.433(6)	C(19)-C(20)	1.428(6)
C(16)-C(17)	1.368(7)	C(19)-C(21)	1.449(7)

Table 39. Angles [°] for [Ni₂([22]-HMTADO)(μ -O₂N)(NO₂)(OH₂)]

N(4)-Ni(1)-O(2)	91.37(14)	N(3)-Ni(2)-N(6)	93.57(14)
N(4)-Ni(1)-N(1)	95.19(16)	O(1)-Ni(2)-N(6)	89.28(13)
O(2)-Ni(1)-N(1)	173.41(14)	N(2)-Ni(2)-N(6)	89.22(15)
N(4)-Ni(1)-O(1)	175.29(15)	O(2)-Ni(2)-N(6)	94.72(14)
O(2)-Ni(1)-O(1)	84.07(13)	N(3)-Ni(2)-O(4)	91.68(14)
N(1)-Ni(1)-O(1)	89.39(14)	O(1)-Ni(2)-O(4)	85.41(13)
N(4)-Ni(1)-O(1W)	87.63(15)	N(2)-Ni(2)-O(4)	91.21(14)
O(2)-Ni(1)-O(1W)	85.10(13)	O(2)-Ni(2)-O(4)	84.41(13)
N(1)-Ni(1)-O(1W)	94.50(15)	N(6)-Ni(2)-O(4)	174.68(13)
O(1)-Ni(1)-O(1W)	93.14(14)	C(9)-O(1)-Ni(2)	124.4(3)
N(4)-Ni(1)-O(3)	91.37(15)	C(9)-O(1)-Ni(1)	125.3(3)
O(2)-Ni(1)-O(3)	86.96(13)	Ni(2)-O(1)-Ni(1)	95.21(13)
N(1)-Ni(1)-O(3)	93.52(15)	C(20)-O(2)-Ni(1)	123.1(3)
O(1)-Ni(1)-O(3)	87.22(13)	C(20)-O(2)-Ni(2)	124.9(3)
O(1W)-Ni(1)-O(3)	171.97(14)	Ni(1)-O(2)-Ni(2)	95.51(13)
N(3)-Ni(2)-O(1)	173.47(14)	N(5)-O(3)-Ni(1)	132.0(3)
N(3)-Ni(2)-N(2)	94.58(15)	N(5)-O(4)-Ni(2)	133.7(3)
O(1)-Ni(2)-N(2)	91.32(14)	C(3)-N(1)-C(2)	116.5(4)
N(3)-Ni(2)-O(2)	90.10(14)	C(3)-N(1)-Ni(1)	122.4(3)
O(1)-Ni(2)-O(2)	83.80(12)	C(2)-N(1)-Ni(1)	121.0(3)
N(2)-Ni(2)-O(2)	173.68(14)	C(10)-N(2)-C(11)	114.9(4)
C(10)-N(2)-Ni(2)	122.7(3)	C(5)-C(4)-C(3)	115.7(4)
C(11)-N(2)-Ni(2)	122.4(3)	C(9)-C(4)-C(3)	124.0(4)
C(14)-N(3)-C(13)	115.9(4)	C(6)-C(5)-C(4)	123.5(5)
C(14)-N(3)-Ni(2)	122.9(3)	C(5)-C(6)-C(7)	116.2(5)
C(13)-N(3)-Ni(2)	121.2(3)	C(5)-C(6)-C(25)	122.8(5)
C(21)-N(4)-C(22)	116.6(4)	C(7)-C(6)-C(25)	120.9(5)

C(21)-N(4)-Ni(1)	122.5(3)	C(6)-C(7)-C(8)	123.0(5)
C(22)-N(4)-Ni(1)	120.8(3)	C(7)-C(8)-C(9)	120.9(5)
O(4)-N(5)-O(3)	117.1(4)	C(7)-C(8)-C(10)	114.7(4)
O(6)-N(6)-O(5)	116.0(4)	C(9)-C(8)-C(10)	124.4(4)
O(6)-N(6)-Ni(2)	121.4(3)	O(1)-C(9)-C(8)	122.4(4)
O(5)-N(6)-Ni(2)	122.4(3)	O(1)-C(9)-C(4)	121.4(4)
C(23)-C(1)-C(24)	110.9(4)	C(8)-C(9)-C(4)	116.1(4)
C(23)-C(1)-C(2)	106.7(4)	N(2)-C(10)-C(8)	128.5(5)
C(24)-C(1)-C(2)	109.9(4)	N(2)-C(11)-C(12)	114.7(4)
C(23)-C(1)-C(22)	106.5(4)	C(11)-C(12)-C(13)	110.8(4)
C(24)-C(1)-C(22)	111.2(4)	C(11)-C(12)-C(27)	105.8(4)
C(2)-C(1)-C(22)	111.5(4)	C(13)-C(12)-C(27)	107.8(4)
N(1)-C(2)-C(1)	113.7(4)	C(11)-C(12)-C(26)	111.3(4)
N(1)-C(3)-C(4)	128.8(5)	C(13)-C(12)-C(26)	111.3(4)
C(5)-C(4)-C(9)	120.1(5)	C(27)-C(12)-C(26)	109.5(4)
N(3)-C(13)-C(12)	114.1(4)	C(17)-C(18)-C(19)	122.6(4)
N(3)-C(14)-C(15)	129.2(4)	C(18)-C(19)-C(20)	120.5(4)
C(16)-C(15)-C(20)	119.6(4)	C(18)-C(19)-C(21)	115.1(4)
C(16)-C(15)-C(14)	116.3(4)	C(20)-C(19)-C(21)	124.3(4)
C(20)-C(15)-C(14)	124.0(4)	O(2)-C(20)-C(19)	122.7(4)
C(17)-C(16)-C(15)	124.4(5)	O(2)-C(20)-C(15)	121.0(4)
C(16)-C(17)-C(18)	116.6(4)	C(19)-C(20)-C(15)	116.3(4)
C(16)-C(17)-C(28)	121.9(5)	N(4)-C(21)-C(19)	127.7(5)
C(18)-C(17)-C(28)	121.5(5)	N(4)-C(22)-C(1)	114.8(4)

Table 40. Selected bond lengths (Å) and angles(°) for hydrogen bond of [Ni₂([22]-HMTADO)(μ-O₂N)(NO₂)(OH₂)] complex

D-H···A	d(D-H)	d(H···A)	<DHA	d(D···A)
coordinated water - coordinated nitrite				
Ow(1)-Hw(1B)···O(5)	0.850	1.884	178.16	2.734
coordinated water - neighbor coordinated nitrite				
Ow(1)-Hw(1A)···O(6) ^{#1}	0.848	2.068	159.98	2.879

Symmetry transformations used to generate equivalent atoms: #1 ; -x, y-1/2, -z+1/2.

The electronic absorption spectrum of [Ni₂([22]-HMTADO)(μ-O₂N)(NO₂)(OH₂)] complex at room temperature were represented in Figure 21. The electronic absorption spectrum of methanol solution is typical of six-coordinate nickel(II) complex indicating that species existing in solution is [Ni₂([22]-HMTADO)(μ-O₂N)(NO₂)(OH₂)]. Two weaker bands are found at 574 nm ($\epsilon = 27.2 \text{ M}^{-1}\text{cm}^{-1}$) and 763 nm ($\epsilon = 8.4 \text{ M}^{-1}\text{cm}^{-1}$), associated with *d-d* transitions. However, strong absorption at 300 - 450 nm is clearly associated with ligand to metal charge transfer transitions, which reflect the presence of highly delocalized π macrocyclic framework. The ground state of *d*⁸ in an octahedral coordination is ³A_{2g}. Two *d-d* bands observed for the complex at 13,106 cm⁻¹ and 17,422 cm⁻¹ can be attributed to the transition in an octahedral model. Thus, these bands may be assigned to the spin allowed transitions ³A_{2g} → ³T_{2g}(F) and ³A_{2g} → ³T_{1g}(F), respectively. ³A_{2g} → ³T_{1g}(P)

transition is not separated by the transfer effect to visible range of charge transfer transitions and absorptions of macrocycle ligand.

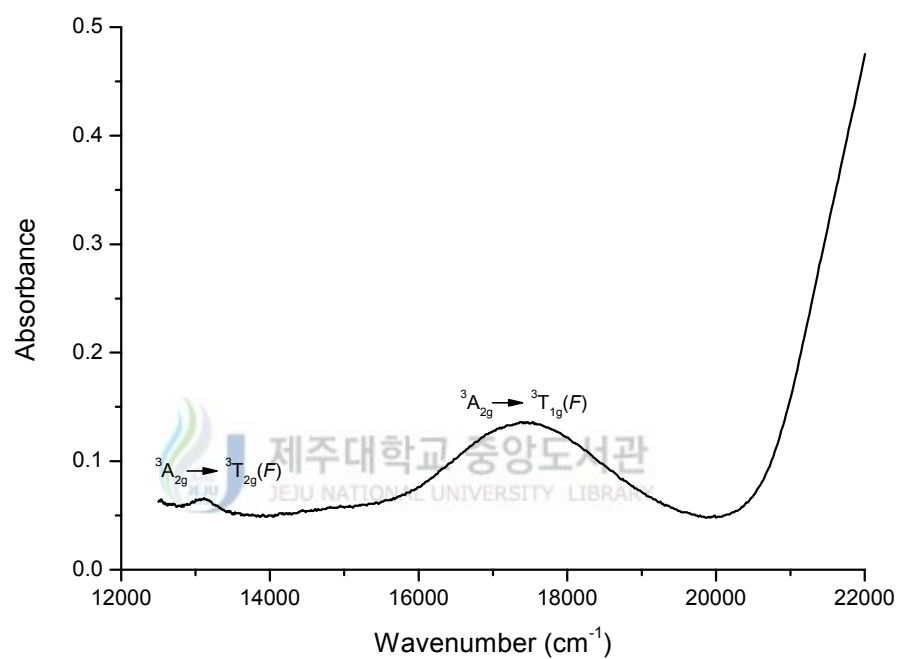


Figure 21. Electronic absorption spectrum of $[\text{Ni}_2([\text{22}]\text{-HMTADO})(\mu\text{-O}_2\text{N})(\text{NO}_2)(\text{OH}_2)]$ in methanol (5.0×10^{-3} M).

IR spectrum of the $[\text{Ni}_2([\text{22}]\text{-HMTADO})(\mu\text{-O}_2\text{N})(\text{NO}_2)(\text{OH}_2)]$ complex was presented Figure 22. The strong and sharp absorption band occurring at 1641 cm^{-1} in the IR spectrum of title complex is attributed to $\nu(\text{C}=\text{N})$ of the coordinated [22]-HMTADO ligand, and the absence of any carbonyl bands associated with the diformyl-phenol starting materials or nonmacrocyclic intermediates.^{92,93} The IR spectra displayed C-H stretching vibrations at 2960 and 2868 cm^{-1} . The absorption band occurring in the IR spectra of the complex in the 3516 cm^{-1} regions may be due to the $\nu(\text{OH})$ vibration of the coordinated water.

Linkage isomerism is possible in the case of metal complexes containing the unit NO_2 . Coordination to the metal atom may occur through the nitrogen atom, resulting in a nitro-complex, or through an oxygen atom, resulting in a nitrito-complex. Nitro-complexes exhibit bands due to asymmetric and symmetric $-\text{NO}_2$ stretching vibration and, in addition, one due to a NO_2 deformation vibration.⁹⁴ The nitrito-complexes exhibit bands due to asymmetric and symmetric $-\text{ONO}$ stretching vibrations which are well separated and occur at $1485\text{-}1400\text{ cm}^{-1}$ and $1110\text{-}1050\text{ cm}^{-1}$, respectively. Nitro-groups in metal coordination complexes may exist as bridging or as end groups. Terminal nitro-groups absorb at $1485\text{-}1370\text{ cm}^{-1}$ and $1340\text{-}1315\text{ cm}^{-1}$ due to the asymmetric and symmetric stretching vibrations of the NO_2 group, respectively.⁹⁴ Nitrito-complexes do not have a band near 620 cm^{-1} which is present for all nitro-complexes. Nitro-groups acting as bridging units (M-ONO-M) between two metal atoms absorb at $1485\text{-}1470\text{ cm}^{-1}$ and at about 1200 cm^{-1} , these bands being broader than those for terminal nitro-groups.^{94,95} The absorption peaks at 1471 and 1217 cm^{-1} in title complex are

assigned to the antisymmetric and symmetric stretching band of bridged nitrite Ni-ONO-Ni, respectively. The stretching band of N-bonded NO₂ are observed at 1404 and 1332 cm⁻¹. The weak absorption band at 617 cm⁻¹ is characteristic of deformation band of N-bonded NO₂. This observation is consistent with the observed X-ray crystal structure of the title complex.



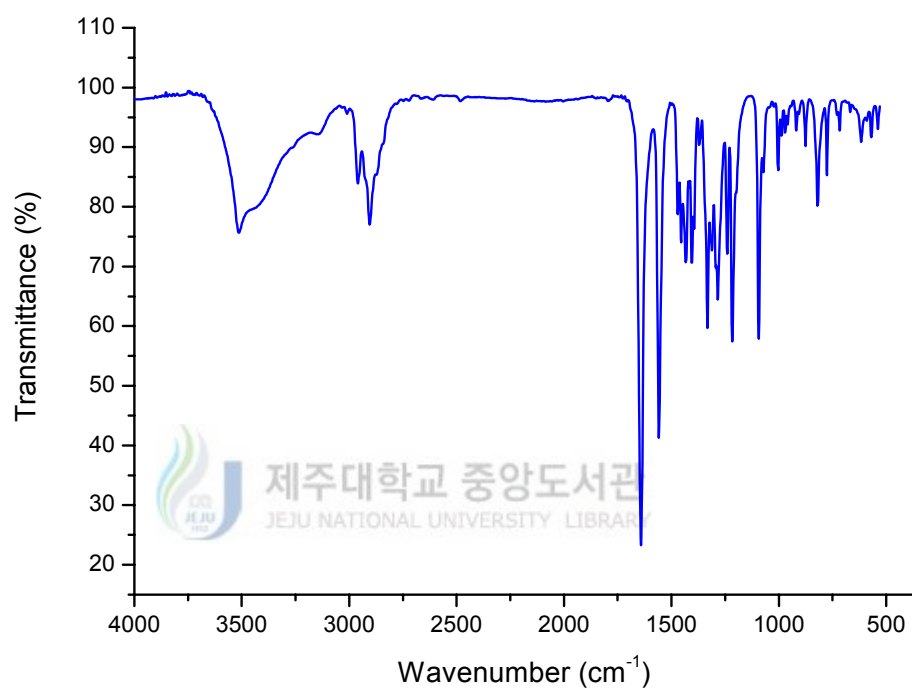


Figure 22. FT-IR spectrum of $[\text{Ni}_2([\text{22}]\text{-HMTADO})(\mu\text{-O}_2\text{N})(\text{NO}_2)(\text{OH}_2)]$ complex.

The FAB mass spectrum of the binuclear $[\text{Ni}_2(\text{[22]-HMTADO})(\mu\text{-O}_2\text{N})(\text{NO}_2)(\text{OH}_2)]$ complex was shown in Figure 23. The FAB mass spectra of title complex contain peaks corresponding to the $[\text{Ni}_2(\text{[22]-HMTADO})]^+$ and $[\text{Ni}(\text{[22]-HMTADO})]^+$ ions at m/z 575 and 517, respectively. These major peaks are associated with peaks of mass one or two greater or less, which are attributed to protonated/deprotonated forms. This also accounts for the slight ambiguities in making assignments. The $[\text{Ni}_2(\text{[22]-HMTADO})\text{NO}_2]^+$ peak is observed at m/z 618.5.



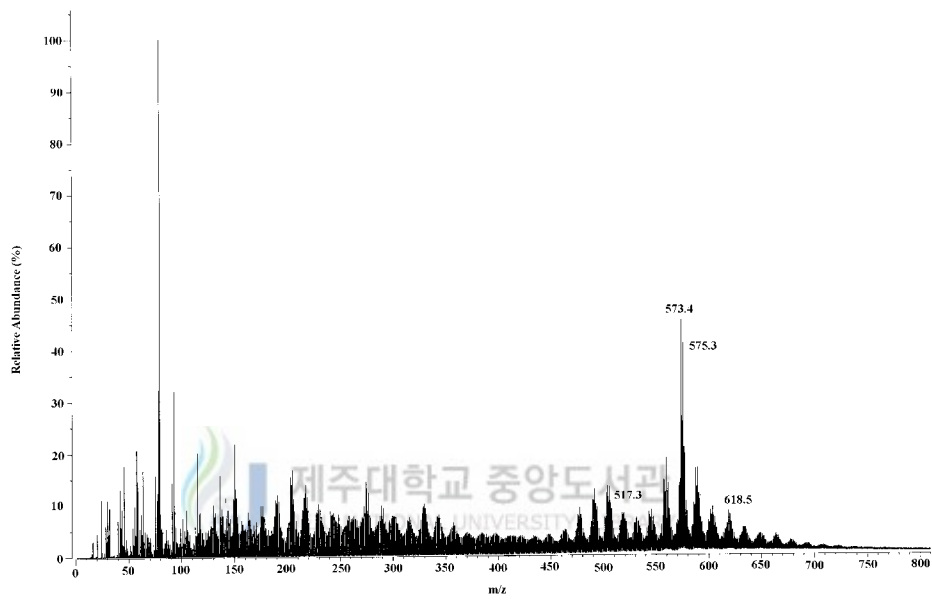


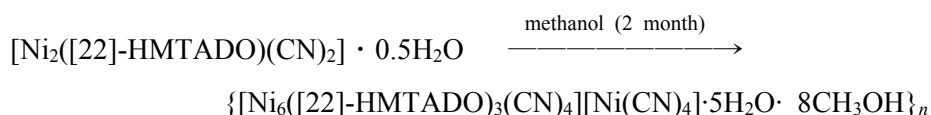
Figure 23. FAB mass spectrum of the $[\text{Ni}_2([\text{22}]\text{-HMTADO})(\mu\text{-O}_2\text{N})(\text{NO}_2)(\text{OH}_2)]$.

3) Structure and physicochemical properties of $\{[\text{Ni}_6([\text{22}]\text{-HMTADO})_3(\text{CN})_4][\text{Ni}(\text{CN})_4]\cdot 5\text{H}_2\text{O}\cdot 8\text{CH}_3\text{OH}\}_n$ (**VI**)

Linkage isomerism is a special case of ambidentate behavior in ligands. The cyanide ion provides good examples of such behavior. In discrete complexes it almost always bonds through the carbon atom because of the stronger π bonding in that mode.⁹⁶ It has also been reported to form a few linkage isomers such as *cis*- $[\text{Co}(\text{trien})(\text{CN})_2]^+$ and *cis*- $[\text{Co}(\text{trien})(\text{NC})_2]^+$.⁹⁶

A large number of polymeric complexes is known containing ambidentate cyanide bridging groups ($\text{M}-\text{C}\equiv\text{N}-\text{M}'$).⁹⁷⁻¹⁰⁰ The 'free' (or co-ordinated by weaker ligands as N-end of the cyano group) sites are then used for polymerisation of the structure by bridging cyano groups.¹⁰¹ The nickel(II) ion in the role of the cationic central atom in the cyano-complexes usually adopts the coordination number six and it is high-spin ($S=1$); four vertices around the central atom need to be saturated by terminating ligands whereas two remaining positions are ready for making a chain structure.⁹⁸

The green polymer crystals of $\{[\text{Ni}_6([\text{22}]\text{-HMTADO})_3(\text{CN})_4][\text{Ni}(\text{CN})_4]\cdot 5\text{H}_2\text{O}\cdot 8\text{CH}_3\text{OH}\}_n$ (**VI**) suitable for X-ray diffraction study which deposited on standing for *ca.* 2 month were crystallized from methanol solution of $[\text{Ni}_2([\text{22}]\text{-HMTADO})(\text{CN})_2] \cdot 0.5\text{H}_2\text{O}$ complex.



An ORTEP view of asymmetric unit with numbering scheme is shown in

Figure 24, and bond distances and angles are summarized in Table 41 and 42, respectively. The structure of compound (VI) is ionic. The unit of title complex contains the polymer $[\text{Ni}_6([\text{22}]\text{-HMTADO})_3(\text{CN})_4]^{2+}$ cations, $[\text{Ni}(\text{CN})_4]^{2-}$ anions, five water molecules, and eight methanol molecules (Figure 25).

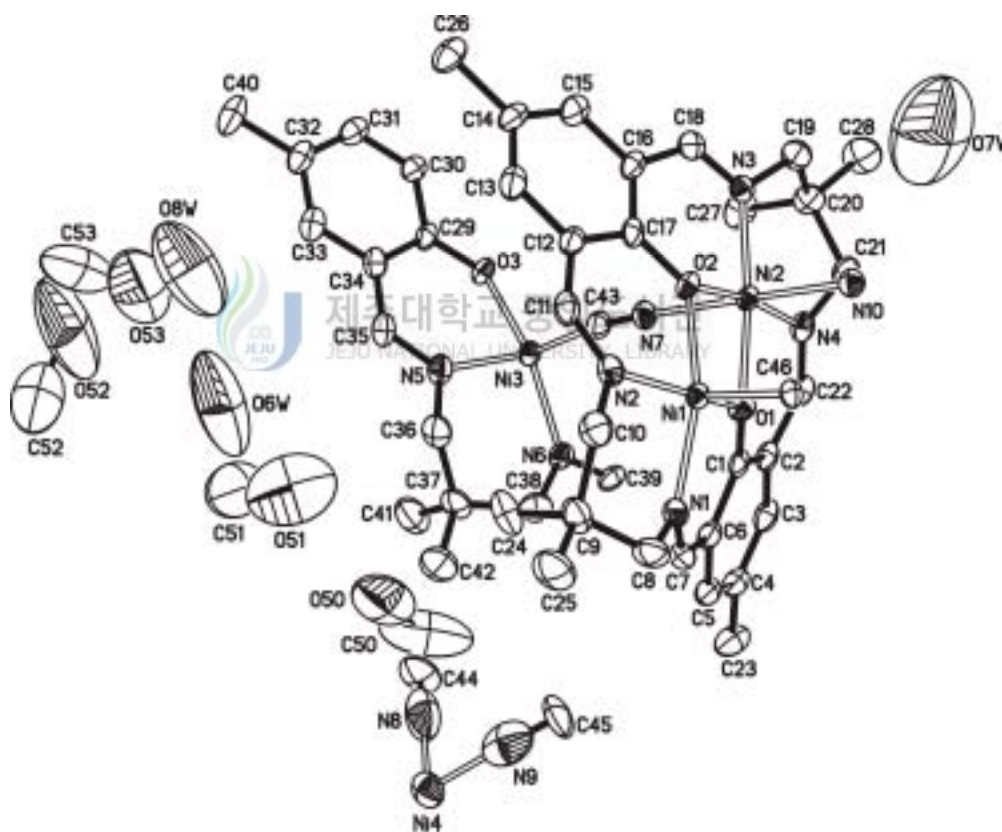


Figure 24. Structural representation of asymmetric unit of $\{[\text{Ni}_6([\text{22}]\text{-HMTADO})_3(\text{CN})_4][\text{Ni}(\text{CN})_4] \cdot 5\text{H}_2\text{O} \cdot 8\text{CH}_3\text{OH}\}_n$ (VI) complex.

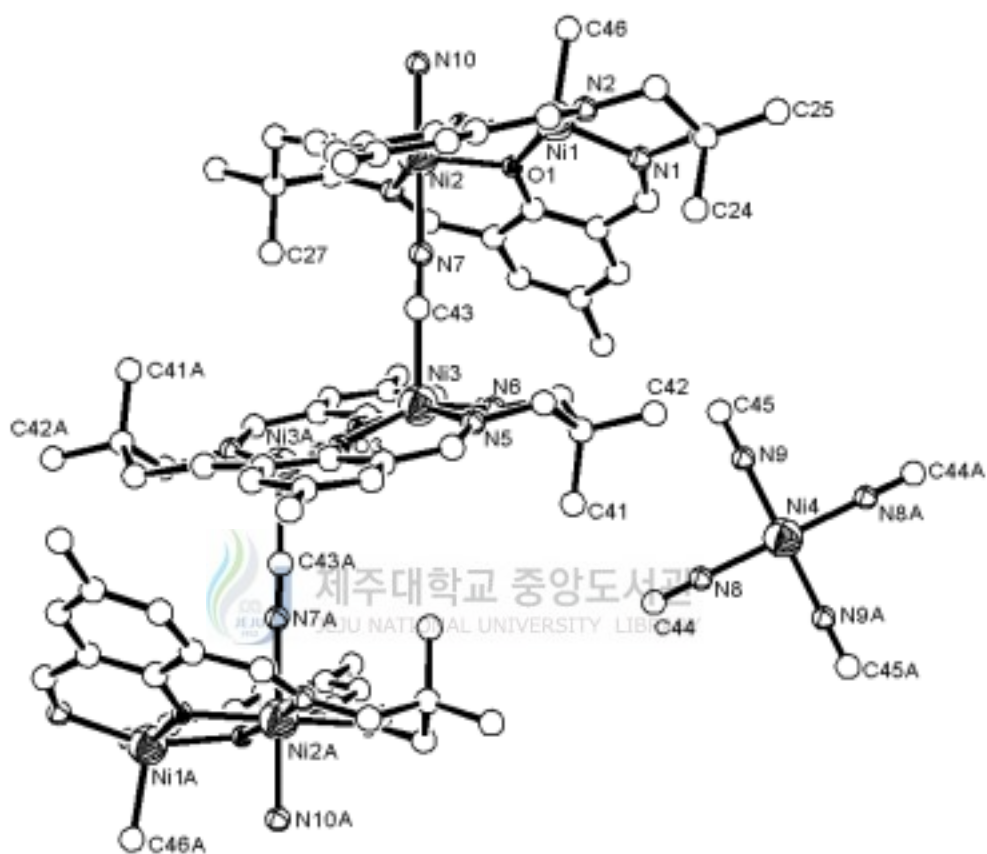
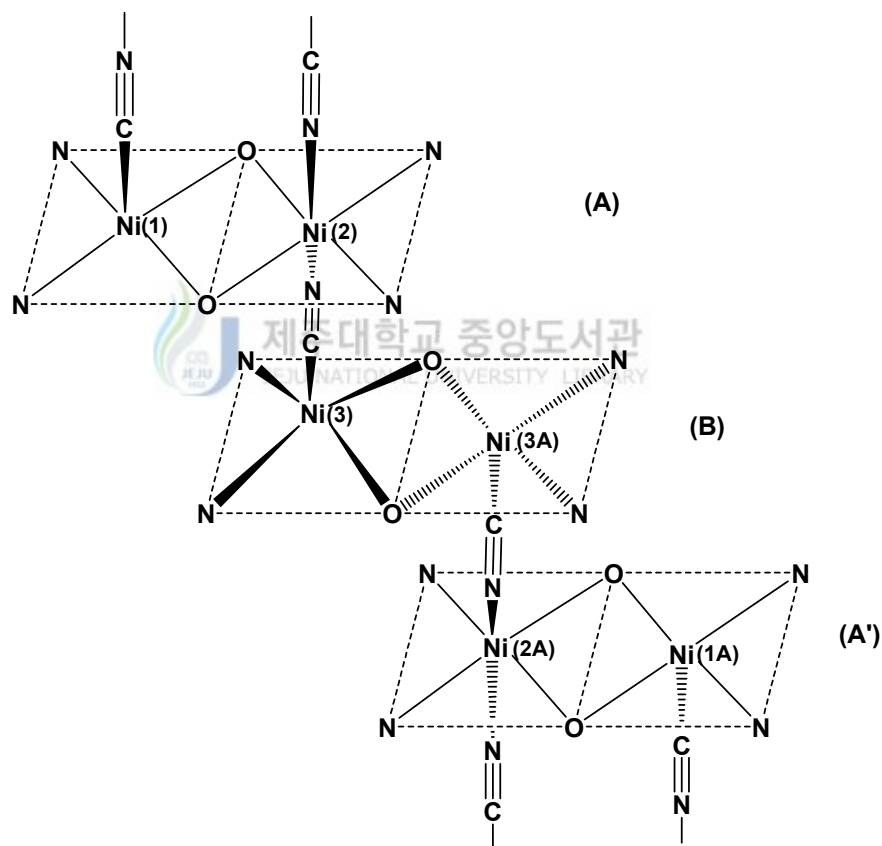


Figure 25. An ORTEP view of core structure (top view) for the $[\text{Ni}_6([\text{22}]\text{-HMTADO})_3(\text{CN})_4][\text{Ni}(\text{CN})_4]$ unit showing 50% probability thermal ellipsoids and labels for non-H atoms.



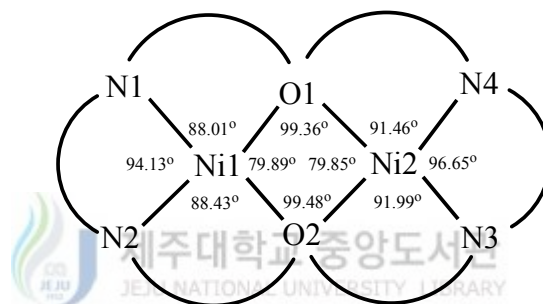
Figure 26. 1D chain structure for $[\text{Ni}_6([\text{22}]\text{-HMTADO})_3(\text{CN})_4]_n$ cation.

A novel one-dimensional chain coordination polymer $[\text{Ni}_6([\text{22}]\text{-HMTADO})_3(\text{CN})_4]_n$ exhibits a novel $-(\text{A-B-A}')-(\text{A-B-A}')-$ chain array, namely the infinite chain is propagated via alternately five and six-coordinate (A), two five coordinate (B), and five and six-coordinate (A'; centro symmetry of A) sites of bivalent Ni ions ([7] and Figure 26).



[7]

The dinegative ([22]-HMTADO)²⁻ in (A) site accommodates two Ni(II) ions with the Ni(1)···Ni(2) separation of 3.097 Å in its N₄O₂ sites. The geometry about Ni(1) in the N₂O₂ site is a square-pyramid with a carbon atom of a bridged cyanide at opposite of (B) site. And the geometry about Ni(2) in another N₂O₂ site is a octahedron with a nitrogen atoms of two bridged cyanide at the trans positions. The two methyl groups (C(24) and C(27)) attached to the dimethyl-propylene are situated *cis* conformation.



[8]

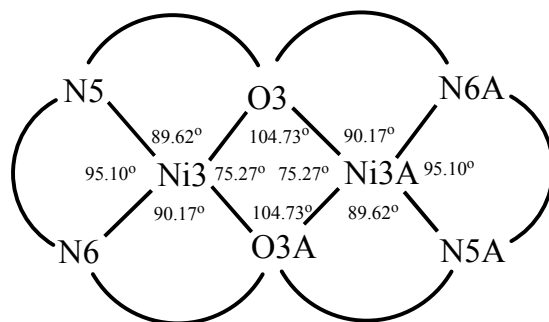
The macrocyclic complex (A) adopts a non-flat structure (Ni₂N₄O₂) with two octahedral nickel centers bridged by the two phenoxide oxygen atoms; the dihedral angle between the plane defined by N(3), O(2), and O(1) and the plane defined by Ni(1), O(2), and O(1) is 169.76°, and the dihedral angle between the plane defined by N(2), O(2), and O(1) and the plane defined by Ni(2), O(2), and O(1) is 176.48°. The bridging angles Ni-O(phenoxide)-Ni within the binuclear cation are equal to 99.36° (Ni(1)-O(1)-Ni(2)) and 99.48° (Ni(1)-O(2)-Ni(2)) ([8]).

The sum of angles (350.46°) at the square-pyramidal Ni(1) basal planes

(NiN₂O₂) is smaller than the ideal value of 360°, indicating plane distortion. The Ni-N (imines) bond distances are in the range of 2.029(4) Å (Ni(1)-N(1)) and 2.014(4) Å (Ni(1)-N(2)), and Ni-O (phenoxide) bond distances are 2.028(3) Å (Ni(1)-O(1)) and 2.032(3) Å (Ni(1)-O(2)). The Ni(1)-C(46) (cyanide) bond distance is 1.989(5) Å. the dihedral angle between the plane defined by N(1), N(2), and O(1) and the plane defined by Ni(1), N(1), and N(2) is 16.29°. Result, the Ni(1) is displaced by 0.569 Å from the basal N₂O₂ least-squares plane towards C(46) (cyanide).

The sum of angles (359.95°) at the octahedral Ni(2) basal planes (NiN₂O₂) is exactly the ideal value of 360°, indicating no plane distortion. The Ni-N (imines) bond distances are in the range of 1.997(4) Å (Ni(2)-N(3)) and 2.017(4) Å (Ni(2)-N(4)), and Ni-O (phenoxide) bond distances are 2.034(3) Å (Ni(2)-O(1)) and 2.027(3) Å (Ni(2)-O(2)). The Ni-N (cyanide) bond distances are in the range of 2.079(4) Å (Ni(2)-N(10)) and 2.147(4) Å (Ni(2)-N(7)).

The dinegative ([22]-HMTADO)²⁻ in (B) site accommodates two Ni(II) ions with the Ni(3)···Ni(3A) (-x+1, -y+1, -z+1) separation of 3.220 Å in its N₄O₂ sites. The binuclear core structures are centrosymmetry with each Ni(II) ion in the N₂O₂ sites being five-coordinate by square-pyramidal geometry of interactions with two nitrogen and two oxygen atoms of the binucleating ligand [22]-HMTADO and two carbon atoms each from the bridged cyanide ligands at an apical site. The two methyl groups (C(41) and C(41) (-x+1, -y+1, -z+1) attached to the dimethyl-propylene are situated *trans* conformation.



[9]

The macrocyclic complex (B) adopts a non-flat structure ($\text{Ni}_2\text{N}_4\text{O}_2$) with two octahedral nickel centers bridged by the two phenoxide oxygen atoms; the dihedral angle between the plane defined by N(5), O(3), and O(3A) and the plane defined by Ni(3A), O(3), and O(3A) is 166.48° . The bridging angles Ni-O(phenoxide)-Ni within the binuclear cation are equal to 104.73° ([9]).

The sum of angles (350.66°) at the square-pyramidal Ni(3) basal planes (NiN_2O_2) is smaller than the ideal value of 360° , indicating plane distortion. The Ni-N (imines) bond distances are in the range of $2.002(4) \text{ \AA}$ (Ni(3)-N(2)) and $2.028(4) \text{ \AA}$ (Ni(3)-N(6)), and Ni-O (phenoxide) bond distance is $2.033(3) \text{ \AA}$ (Ni(3)-O(3)). The Ni(3)-C(43) (cyanide) bond distance is $2.004(5) \text{ \AA}$. the dihedral angle between the plane defined by N(6), N(5), and O(3) and the plane defined by Ni(3), N(5), and N(6) is 19.26° . Result, the Ni(3) is displaced by 0.660 \AA from the basal N_2O_2 least-squares plane towards C(46) (cyanide).

There are four crystallographically independent tetracyanonickellate anions $\{\text{Ni}(\text{CN})_4^{2-}\}$ in the unit cell. The $\{\text{Ni}(\text{CN})_4^{2-}\}$ are exactly planar as required

by symmetry. All cyano groups are terminal.

The lattice water molecules form hydrogen bonds of the type Ow-H \cdots O with another lattice water and lattice methanol molecules {Ow(1) \cdots Ow(3); 2.727 Å, Ow(2) \cdots Ow(3) (x, 1+y, 1+z); 2.445 Å, and Ow(3) \cdots O(50) (1+x, y, z, methanol); 2.892 Å}.

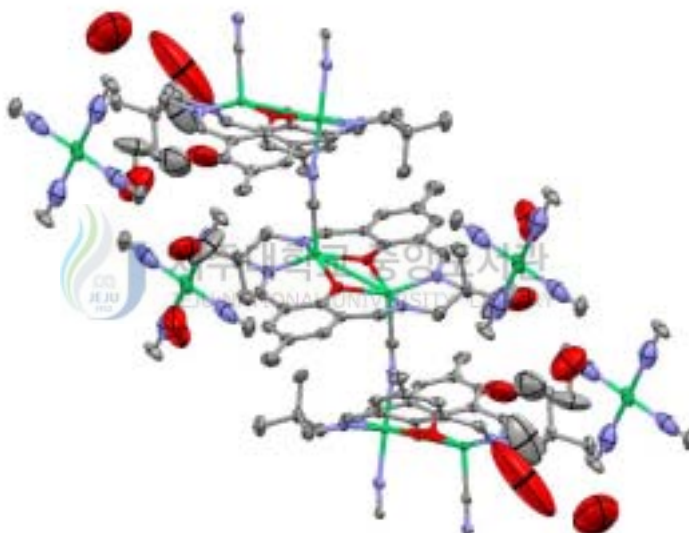


Figure 27. The graph of the independent part of $\{[\text{Ni}_6([\text{22}]\text{-HMTADO})_3(\text{CN})_4] \cdot [\text{Ni}(\text{CN})_4] \cdot 5\text{H}_2\text{O} \cdot 8\text{CH}_3\text{OH}\}_n$.

Table 41. Bond lengths (Å) for $\{[\text{Ni}_6([\text{22}]\text{-HMTADO})_3(\text{CN})_4][\text{Ni}(\text{CN})_4]\cdot 5\text{H}_2\text{O}\cdot 8\text{CH}_3\text{OH}\}_n$

Ni(1)-C(46)	1.989(5)	C(14)-C(15)	1.387(8)
N(8)-C(44)	1.118(10)	C(14)-C(26)	1.508(7)
N(9)-C(45)	1.144(9)	C(15)-C(16)	1.399(7)
N(10)-C(46)#3	1.156(6)	C(16)-C(17)	1.417(7)
C(1)-C(6)	1.419(7)	C(16)-C(18)	1.458(7)
C(1)-C(2)	1.437(7)	C(19)-C(20)	1.545(8)
C(2)-C(3)	1.393(7)	C(20)-C(27)	1.511(8)
C(2)-C(22)	1.453(7)	C(20)-C(28)	1.531(8)
C(3)-C(4)	1.394(8)	C(20)-C(21)	1.539(8)
C(4)-C(5)	1.373(8)	C(29)-C(34)	1.403(7)
C(4)-C(23)	1.519(7)	C(29)-C(30)	1.427(7)
C(5)-C(6)	1.407(7)	C(30)-C(31)	1.388(7)
C(6)-C(7)	1.457(7)	C(30)-C(39)#1	1.454(7)
C(8)-C(9)	1.526(8)	C(31)-C(32)	1.370(8)
C(9)-C(24)	1.534(8)	C(32)-C(33)	1.393(8)
C(9)-C(25)	1.540(8)	Ni(1)-N(2)	2.014(4)
C(9)-C(10)	1.542(8)	Ni(1)-O(1)	2.028(3)
C(11)-C(12)	1.455(7)	Ni(1)-N(1)	2.029(4)
C(12)-C(13)	1.398(7)	Ni(1)-O(2)	2.032(3)
C(12)-C(17)	1.417(7)	Ni(2)-N(3)	1.997(4)
C(13)-C(14)	1.384(8)	Ni(2)-N(4)	2.017(4)
Ni(2)-O(2)	2.027(3)	N(3)-C(18)	1.287(7)
Ni(2)-O(1)	2.034(3)	N(3)-C(19)	1.461(7)
Ni(2)-N(10)	2.079(4)	N(4)-C(22)	1.271(7)
Ni(2)-N(7)	2.147(4)	N(4)-C(21)	1.458(7)
Ni(3)-N(5)	2.002(4)	N(5)-C(35)	1.284(7)

Ni(3)-C(43)	2.004(5)	N(5)-C(36)	1.471(7)
Ni(3)-N(6)	2.028(4)	N(6)-C(39)	1.277(7)
Ni(3)-O(3)#1	2.032(3)	N(6)-C(38)	1.483(7)
Ni(3)-O(3)	2.033(3)	C(32)-C(40)	1.510(8)
Ni(4)-N(9)	1.898(9)	C(33)-C(34)	1.395(8)
Ni(4)-N(9)#2	1.898(9)	C(34)-C(35)	1.440(8)
Ni(4)-N(8)#2	1.940(10)	C(36)-C(37)	1.520(8)
Ni(4)-N(8)	1.940(10)	C(37)-C(38)	1.509(8)
O(1)-C(1)	1.300(6)	C(37)-C(41)	1.523(8)
O(2)-C(17)	1.314(6)	C(37)-C(42)	1.537(8)
O(3)-C(29)	1.313(6)	C(39)-C(30)#1	1.454(7)
O(3)-Ni(3)#1	2.032(3)	C(46)-N(10)#3	1.156(6)
N(1)-C(7)	1.272(7)	O(50)-C(50)	1.47(2)
N(1)-C(8)	1.465(7)	O(51)-C(51)	1.407(8)
N(2)-C(11)	1.266(7)	O(52)-C(52)	1.52(2)
N(2)-C(10)	1.472(7)	O(53)-C(53)	1.54(4)

Symmetry transformations used to generate equivalent atoms:

#1; -x+1, -y+1, -z+1, #2; -x, -y+1, -z, #3; -x+2, -y+2, -z+1.

Table 42. Angles [°] for $\{[\text{Ni}_6([\text{22}]\text{-HMTADO})_3(\text{CN})_4][\text{Ni}(\text{CN})_4]\cdot 5\text{H}_2\text{O}\cdot 8\text{CH}_3\text{OH}\}_n$

C(46)-Ni(1)-N(2)	97.50(18)	N(5)-Ni(3)-C(43)	100.1(2)
C(46)-Ni(1)-O(1)	106.19(17)	N(5)-Ni(3)-N(6)	95.10(18)
N(2)-Ni(1)-O(1)	155.59(15)	C(43)-Ni(3)-N(6)	92.68(19)
C(46)-Ni(1)-N(1)	98.97(18)	N(5)-Ni(3)-O(3)#1	155.67(16)
N(2)-Ni(1)-N(1)	94.13(17)	C(43)-Ni(3)-O(3)#1	103.38(18)
O(1)-Ni(1)-N(1)	88.01(16)	N(6)-Ni(3)-O(3)#1	90.17(16)
C(46)-Ni(1)-O(2)	105.18(17)	N(5)-Ni(3)-O(3)	89.62(16)
N(2)-Ni(1)-O(2)	88.43(16)	C(43)-Ni(3)-O(3)	113.43(18)
O(1)-Ni(1)-O(2)	79.89(13)	N(6)-Ni(3)-O(3)	152.24(16)
N(1)-Ni(1)-O(2)	155.17(15)	O(3)#1-Ni(3)-O(3)	75.27(15)
N(3)-Ni(2)-N(4)	96.65(17)	N(9)-Ni(4)-N(9)#2	180.000(1)
N(3)-Ni(2)-O(2)	91.99(16)	N(9)-Ni(4)-N(8)#2	89.8(3)
N(4)-Ni(2)-O(2)	171.25(16)	N(9)#2-Ni(4)-N(8)#2	90.2(3)
N(3)-Ni(2)-O(1)	171.57(16)	N(9)-Ni(4)-N(8)	90.2(3)
N(4)-Ni(2)-O(1)	91.46(16)	N(9)#2-Ni(4)-N(8)	89.8(3)
O(2)-Ni(2)-O(1)	79.85(14)	N(8)#2-Ni(4)-N(8)	180.000(1)
N(3)-Ni(2)-N(10)	91.28(17)	C(1)-O(1)-Ni(1)	131.6(3)
N(4)-Ni(2)-N(10)	90.99(17)	C(1)-O(1)-Ni(2)	124.2(3)
O(2)-Ni(2)-N(10)	90.15(15)	Ni(1)-O(1)-Ni(2)	99.36(14)
O(1)-Ni(2)-N(10)	90.85(15)	C(17)-O(2)-Ni(2)	123.6(3)
N(3)-Ni(2)-N(7)	89.78(17)	C(17)-O(2)-Ni(1)	130.8(3)
N(4)-Ni(2)-N(7)	90.01(17)	Ni(2)-O(2)-Ni(1)	99.48(14)
O(2)-Ni(2)-N(7)	88.68(15)	C(29)-O(3)-Ni(3)#1	127.2(3)
O(1)-Ni(2)-N(7)	87.95(15)	C(29)-O(3)-Ni(3)	128.0(3)
N(10)-Ni(2)-N(7)	178.46(16)	Ni(3)#1-O(3)-Ni(3)	104.73(15)

C(7)-N(1)-C(8)	115.8(5)	C(3)-C(2)-C(1)	119.5(5)
C(7)-N(1)-Ni(1)	126.5(4)	C(3)-C(2)-C(22)	116.2(5)
C(8)-N(1)-Ni(1)	117.7(3)	C(1)-C(2)-C(22)	124.2(5)
C(11)-N(2)-C(10)	116.6(5)	C(2)-C(3)-C(4)	124.0(5)
C(11)-N(2)-Ni(1)	125.9(4)	C(5)-C(4)-C(3)	116.1(5)
C(10)-N(2)-Ni(1)	117.5(4)	C(5)-C(4)-C(23)	122.4(5)
C(18)-N(3)-C(19)	117.5(4)	C(3)-C(4)-C(23)	121.5(5)
C(18)-N(3)-Ni(2)	121.6(4)	C(4)-C(5)-C(6)	123.1(5)
C(19)-N(3)-Ni(2)	120.8(3)	C(5)-C(6)-C(1)	120.6(5)
C(22)-N(4)-C(21)	118.8(5)	C(5)-C(6)-C(7)	115.8(5)
C(22)-N(4)-Ni(2)	122.0(4)	C(1)-C(6)-C(7)	123.5(5)
C(21)-N(4)-Ni(2)	119.1(4)	N(1)-C(7)-C(6)	127.8(5)
C(35)-N(5)-C(36)	115.9(5)	N(1)-C(8)-C(9)	114.6(5)
C(35)-N(5)-Ni(3)	125.4(4)	C(8)-C(9)-C(24)	110.8(5)
C(36)-N(5)-Ni(3)	118.6(4)	C(8)-C(9)-C(25)	107.2(5)
C(39)-N(6)-C(38)	114.7(5)	C(24)-C(9)-C(25)	109.9(5)
C(39)-N(6)-Ni(3)	123.0(4)	C(8)-C(9)-C(10)	111.2(5)
C(38)-N(6)-Ni(3)	121.2(4)	C(24)-C(9)-C(10)	111.4(5)
C(43)-N(7)-Ni(2)	168.5(4)	C(25)-C(9)-C(10)	106.1(5)
C(44)-N(8)-Ni(4)	178.8(8)	N(2)-C(10)-C(9)	113.1(5)
C(45)-N(9)-Ni(4)	177.4(7)	N(2)-C(11)-C(12)	128.7(5)
C(46)#3-N(10)-Ni(2)	172.1(4)	C(13)-C(12)-C(17)	120.1(5)
O(1)-C(1)-C(6)	121.4(5)	C(13)-C(12)-C(11)	116.4(5)
O(1)-C(1)-C(2)	122.1(5)	C(17)-C(12)-C(11)	123.4(5)
C(6)-C(1)-C(2)	116.5(5)	C(14)-C(13)-C(12)	122.9(5)
C(13)-C(14)-C(15)	116.3(5)	C(31)-C(30)-C(29)	120.0(5)
C(13)-C(14)-C(26)	120.8(5)	C(31)-C(30)-C(39)#1	115.7(5)
C(15)-C(14)-C(26)	122.8(5)	C(29)-C(30)-C(39)#1	124.2(5)

C(14)-C(15)-C(16)	123.6(5)	C(32)-C(31)-C(30)	123.5(5)
C(15)-C(16)-C(17)	119.3(5)	C(31)-C(32)-C(33)	116.3(5)
C(15)-C(16)-C(18)	115.4(5)	C(31)-C(32)-C(40)	121.4(5)
C(17)-C(16)-C(18)	125.1(5)	C(33)-C(32)-C(40)	122.3(6)
O(2)-C(17)-C(12)	120.9(5)	C(32)-C(33)-C(34)	122.6(5)
O(2)-C(17)-C(16)	121.4(5)	C(33)-C(34)-C(29)	120.7(5)
C(12)-C(17)-C(16)	117.7(5)	C(33)-C(34)-C(35)	115.8(5)
N(3)-C(18)-C(16)	127.5(5)	C(29)-C(34)-C(35)	123.4(5)
N(3)-C(19)-C(20)	114.2(5)	N(5)-C(35)-C(34)	128.3(5)
C(27)-C(20)-C(28)	109.6(5)	N(5)-C(36)-C(37)	115.0(5)
C(27)-C(20)-C(21)	110.7(5)	C(38)-C(37)-C(36)	110.8(5)
C(28)-C(20)-C(21)	106.2(5)	C(38)-C(37)-C(41)	111.7(5)
C(27)-C(20)-C(19)	111.5(5)	C(36)-C(37)-C(41)	110.5(5)
C(28)-C(20)-C(19)	106.3(5)	C(38)-C(37)-C(42)	107.4(5)
C(21)-C(20)-C(19)	112.2(5)	C(36)-C(37)-C(42)	106.6(5)
N(4)-C(21)-C(20)	115.7(5)	C(41)-C(37)-C(42)	109.7(5)
N(4)-C(22)-C(2)	128.5(5)	N(6)-C(38)-C(37)	115.6(5)
O(3)-C(29)-C(34)	122.6(5)	N(6)-C(39)-C(30)#1	129.0(5)
O(3)-C(29)-C(30)	120.7(5)	N(7)-C(43)-Ni(3)	171.6(5)
C(34)-C(29)-C(30)	116.7(5)	N(10)#3-C(46)-Ni(1)	178.1(4)

Symmetry transformations used to generate equivalent atoms:

#1; -x+1, -y+1, -z+1, #2; -x, -y+1, -z, #3; -x+2, -y+2, -z+1.

IV. Conclusion

We prepare and isolate (1) Cr(III)-tetraaza 14-membered macrocyclic complexes; *cis*-[Cr([14]-decane)(*o*-OOC₆H₄OH)₂]ClO₄ (**I**), *cis*-[Cr([14]-decane)(*p*-OC₆H₄NO₂)(OH)]ClO₄·H₂O (**II**), (2) Cu(II)-dioxatetraaza 20-membered macrocyclic complexes; [Cu₂([20]-DCHDC)(O₂N)₂] · 6H₂O (**III**), and (3) Ni(II)-dioxatetraaza 22-membered macrocyclic complexes; [H₄[22]-HMTADO](NO₃)₂ · H₂O (**IV**), [Ni₂([22]-HMTADO)(*μ*-O₂N)(NO₂)(OH)₂] (**V**), and {[Ni₆(C₂₈H₃₄N₄O₂)₃(CN)₄][Ni(CN)₄] · 5H₂O · 8CH₃OH}_{*n*} (**VI**).

The crystal structure of (**I**) complex consists of monomeric cation of the indicated formula and noninteracting perchlorate anion. The monomeric cation, [Cr([14]-decane)(*o*-OOC₆H₄OH)₂]⁺ shows a distorted octahedral environment, where the chromium(III) ion is coordinated by secondary amines of the macrocycle and by the two carboxylate oxygen atoms of the monodentate salicylate ligands in *cis* positions. The *rac*-form, [14]-decane readily folds to give *cis*-chromium(III) complexes with the (*RRRR,SSSS*) *sec*-NH configuration and two equatorial and one axial methyl substituents on each six-membered chelate ring. Therefore, two salicylates are bonded to the chromium(III) by monodentate ligand rather than single salicylate bonding by bidentate, so as to form a sterically stable six-coordinate complex. Here, the salicylate acted as bidentate ligand forms a four-membered ring causing too much strain to the structure, whereas two salicylates functioned as monodentate ligand result more preferable structure. The oxygen atoms from the salicylate ligands and two nitrogen donors (positions of *C-methyl* group) of the [14]-decane define

the equatorial coordination plane (CrN₂O₂ *xy*-plane). Hexa-coordination is accomplished via the remaining two nitrogens of macrocyclic ligand (positions of *C-dimethyl* group). The tetra-aza ligand is folded along the N(1)-Cr-N(3) axis (axial position). This configuration is often referred to as the Bosnich type-V stereochemistry. The uncoordinated carboxylic oxygen atom of salicylate ligand form of the type N-H···O with the secondary amine hydrogen of the macrocycle. Under this situation, the self-organization seems to make the structure **2** more stable by the hydrogen bonding interaction, in which the carboxylate oxygen O(1) of salicylate anion is coordinated to the central Cr(III) and O(2) is H-bonded with H(1) to form six-membered ring. The counter ion ClO₄⁻ form of the type N-H···O with the secondary amine hydrogen of the macrocycle. The uncoordinated carboxylic oxygen atom and hydroxy of salicylate ligand form internal hydrogen bond.

The two *d-d* bands of title complex observed at 18484, 25575 cm⁻¹ can be related to the spin-allowed transitions, ${}^4A_{2g} \rightarrow {}^4T_{2g}$ and ${}^4A_{2g} \rightarrow {}^4T_{1g}$, respectively. The assignment of geometric configuration is confirmed by the *d-d* absorption spectra. The less symmetrical *cis*-isomers have much higher extinction coefficients than those of more symmetrical *trans*-isomers.

The IR spectrum of title complex exhibit characteristic absorption bands for the carbonyls of the salicylate carboxylate ligands in the symmetric and asymmetric vibration regions. Specifically, symmetric stretching vibrations, $\nu_s(\text{COO}^-)$ appear at 1387 cm⁻¹ and asymmetric stretching vibrations, $\nu_{as}(\text{COO}^-)$ are observed at 1620 cm⁻¹. The differences between the symmetric and antisymmetric stretches, $\Delta\nu \{= \nu_{as}(\text{COO}^-) - \nu_s(\text{COO}^-)\}$ are on the order of 241 cm⁻¹, indicating that carboxylate groups are either free or coordinated to the

metal ion in a monodentate fashion. In the FAB mass spectrum of *cis*-[Cr([14]-decane)(*o*-OOC₆H₄OH)₂]ClO₄, this is a peak at *m/z* 610.3 corresponding to the molecular ion *cis*-[Cr([14]-decane)(*o*-OOC₆H₄OH)₂]⁺.

The crystal structure of **(II)** complex consists of monomeric cation of the indicated formula and noninteracting perchlorate anion. The monomeric cation, [Cr([14]-decane)(*p*-OC₆H₄NO₂)(OH)]⁺ shows a distorted octahedral environment, where the chromium(III) ion is coordinated by secondary amines of the macrocycle and by one phenolic oxygen atom of the monodentate *p*-nitrophenolate ligand and one hydroxo oxygen atom in *cis* positions. The *rac*-form, [14]-decane readily folds to give *cis*-chromium(III) complexes with the (*RRRR,SSSS*) *sec*-NH configuration and two equatorial and one axial methyl substituent on each six-membered chelate ring. The oxygen atoms from the *p*-nitrophenolate and hydroxo ligands and two nitrogen donors (positions of *C-methyl* group) of the [14]-decane define the equatorial coordination plane (CrN₂O₂ *xy*-plane). Hexa-coordination is accomplished via the remaining two nitrogens of macrocyclic ligand (positions of *C-dimethyl* group). The tetra-aza ligand is folded along the N(1)-Cr-N(3) axis (axial position). This configuration is often referred to as the Bosnich type-V stereochemistry. The secondary amine hydrogens of the macrocycle as well as hydroxo ligand give rise to hydrogen bonds with uncoordinated lattice waters. These interactions result in a formation of polymeric chains. This chain forms a related layer structure, but within the layers *cis*-[Cr([14]-decane)(*p*-OC₆H₄NO₂)(OH)]⁺ ions arrange zig-zag configurations.

The two *d-d* bands of title complex observed at 17301, 21114 cm⁻¹ (sh) can be related to the spin-allowed transitions, ${}^4A_{2g} \rightarrow {}^4T_{2g}$ and ${}^4A_{2g} \rightarrow {}^4T_{1g}$,

respectively. The assignment of geometric configuration is confirmed by the *d-d* absorption spectra. The less symmetrical *cis*-isomers have much higher extinction coefficients than those of more symmetrical *trans*-isomers.

The very strong infrared bands observed at 1494 and 1302 cm^{-1} can be attributed to $\nu_{\text{as}}(\text{NO}_2)$ and $\nu_{\text{s}}(\text{NO}_2)$, respectively, in good agreement with the values given in the literature. In the *p*-nitrophenol case, the intense infrared absorption bands located at 1286, 1327 and 1344 cm^{-1} are allotted to the vibration modes ν_3 , ν_{11} and to the $\nu_{\text{s}}(\text{NO}_2)$, respectively. In the infrared absorption spectra, the three bands of **(II)** are form a broad band centred at 1302 cm^{-1} . In the FAB mass spectrum of *cis*-[Cr([14]-decane)(*p*-OC₆H₄NO₂)(OH)]ClO₄ · H₂O, this is a peak at *m/z* 491.3 corresponding to the molecular ion *cis*-[Cr([14]-decane)(*p*-OC₆H₄NO₂)(OH)]⁺.

The green crystal of **(III)** suitable for structure determination was acquired from methanol and water (10 : 1 v/v) mixed solvent, by slow evaporation of solvent at room temperature. Four formula units comprise the unit cell with quarter of the binuclear complex in the asymmetric unit. The binuclear core structures are centrosymmetry with each copper(II) ion in the N(imine)₂O₂ sites being six-coordinate by capped square-pyramidal geometry of interactions with two nitrogen and two oxygen atoms of the binucleating ligand [20]-DCHDC and two oxygen atoms each from the bidentated nitrite ligands at an apical site (**[3]**). The copper ions are 0.3288 Å displaced from the basal least-squares plane toward nitrite ions. Two nitrite ions attached to two central metal Cu are situated *trans* to each other with respect to the mean molecular plane (**[3]**). The interatomic Cu···Cu separation is 2.9542(8) Å. The macrocyclic complex adopts a non-flat structure with two

square-pyramidal copper centers bridged by the two phenoxide oxygen atoms. The two phenol mean planes are able to flat. The coordinated nitrite molecule form hydrogen bonds of the type Ow-H...O (nitrite) with lattice water. The structure of the compound is further consolidated by another hydrogen bond of the type Ow-H...Ow between the lattice water molecules.

The electronic absorption spectrum exhibited one band at 530 nm due to the ${}^2E_g \rightarrow {}^2T_{2g}$ (O_h) transitions. The two peak positions calculated at 18,315 and 19,011 cm^{-1} can be assigned to the ${}^2B_{1g} \rightarrow {}^2B_{2g}$ and ${}^2B_{1g} \rightarrow {}^2E_g$, respectively. The ${}^2B_{1g} \rightarrow {}^2A_{1g}$ transition bands have expected at much lower energy. The 24,038 cm^{-1} band are clearly associated with ligand to metal charge transfer transitions.

The strong absorption IR peaks at 1446 and 1205 cm^{-1} in the $[\text{Cu}_2([\text{20}]\text{-DCHDC})(\text{O}_2\text{N})_2] \cdot 6\text{H}_2\text{O}$ are assigned to a bidentate nitrito ligand Cu-O₂N. In the FAB mass spectra of the $[\text{Cu}_2([\text{20}]\text{-DCHDC})(\text{O}_2\text{N})_2] \cdot 6\text{H}_2\text{O}$ complex, the molecular ion loses the exocyclic ligands resulting in the formation of the fragment $[\text{Cu}_2([\text{20}]\text{-DCHDC})]^+$. This fragment is well observed in the FAB mass spectra at m/z 608 region. α -Cleavage peak of one cyclohexane from the $[\text{Cu}_2([\text{20}]\text{-DCHDC})]^+$ ion in the formation of the fragment $[\text{Cu}_2(\text{Lac})]^+$ is observed at m/z 526 region. Removal peak of one copper ion from the $[\text{Cu}_2([\text{20}]\text{-DCHDC})]^+$ ion in the formation of the fragment $[\text{Cu}([\text{20}]\text{-DCHDC})]^+$ is observed at m/z 545.

Suitable crystals of $[\text{H}_4[\text{22}]\text{-HMTADO}](\text{NO}_3)_2 \cdot \text{H}_2\text{O}$ (**IV**) were obtained by slow evaporation of acetonitrile solution of the compound at atmospheric pressure. The crystal structure of this di(hydrionitrate) compound is composed of tetraazadioxa 22-membered macrocycle ($[\text{H}_4[\text{22}]\text{-HMTADO}]^{2+}$), two nitrate

ions and one water molecule. Two N_2O_2 sites are vacant, and each azomethine nitrogen atoms are protonation. The tetraazadioxa 22-membered macrocycle ($[H_4[22]-HMTADO]^{2+}$) is C_{2v} symmetry. The dihedral angle between the planes defined of two phenoxide is $16.94(9)^\circ$. This is bent owing to the tetrahedral conformation effect of two dimethyl-propylene at the side. The two dimethyl-propylene are situated eclipsed conformation. In the $[H_4[22]-HMTADO]^{2+}$, two phenoxide planes are shortly; $N(1)\cdots N(2)$ 3.039 Å, $N(3)\cdots N(4)$ 2.976 Å, $O(1)\cdots O(2)$ 3.275 Å, and $C(23)\cdots C(26)$ 4.829 Å. The protonated imine and phenoxide oxygen of macrocycle form internal hydrogen bond. Under this situation, the self-organization seems to make the structure **4** more stable by the hydrogen bonding interaction, in which the hydrogens of protonated imine are H-bonded with phenoxide oxygens to form six-membered ring. The nitrate ion form hydrogen bonds of the type $Ow-H\cdots O$ (nitrate) with lattice water.

The green crystals of $[Ni_2([22]-HMTADO)(\mu-O_2N)(NO_2)(OH_2)]$ (**V**) suitable for X-ray diffraction study which deposited on standing for *ca.* 1 month were recrystallized from methanol of this complex. The dinegative ($[22]-HMTADO$)²⁻ accommodates two Ni(II) ions in its N_4O_2 sites in the $Ni(1)\cdots Ni(2)$ separation of 3.013 Å. The structure of title complex shows that the two metal centers are bridged by the two phenoxide oxygens as well as by two oxygens of the coordinated nitrite (O-bonding) (**[5]**). Both the metal centers are six-coordinated with irregular octahedral geometry and have N_2O_2 equatorial donors provided by the macrocyclic ligand. The remaining apical position of the $Ni(1)$ center is occupied by a water molecule, while that of another $Ni(2)$ by a nitrite nitrogen (N-bonding) (**[5]**). The macrocyclic complex adopts a

non-flat structure ($\text{Ni}_2\text{N}_4\text{O}_2$) with two octahedral nickel centers bridged by the two phenoxide oxygen atoms. The Ni_2O_2 plane adopts a flat structure with the an octahedral nickel centers bridged by the two phenoxide oxygen atoms. The O(1) and O(2)-phenolic group mean planes of macrocycle are bent 26.52° and 27.11° toward bridged nitrito ligand, respectively, with the basal Ni_2O_2 least-squares plane. The coordinated nitrite molecule form hydrogen bonds of the type $\text{Ow-H}\cdots\text{O}$ (nitrito) with coordinated water. And the structure of the compound is further consolidated by another hydrogen bond of the type $\text{Ow-H}\cdots\text{O}$ between the coordinated water molecule and nitrite of neighbor complex. These interactions result in a formation of polymeric chains and in the packing of the title compound. This chain forms a related layer structure, but within the layers arrange zig-zag configurations.

The electronic absorption spectrum of methanol solution is typical of six-coordinate nickel(II) complex indicating that species existing in solution is $[\text{Ni}_2([\text{22}]\text{-HMTADO})(\mu\text{-O}_2\text{N})(\text{NO}_2)(\text{OH}_2)]$. Two weaker bands are found at 574 nm ($\epsilon = 27.2 \text{ M}^{-1}\text{cm}^{-1}$) and 763 nm ($\epsilon = 8.4 \text{ M}^{-1}\text{cm}^{-1}$), associated with *d-d* transitions. However, strong absorption at 300 - 450 nm is clearly associated with ligand to metal charge transfer transitions, which reflect the presence of highly delocalized π macrocyclic framework. Two *d-d* bands observed for the complex at $13,106 \text{ cm}^{-1}$, $17,422 \text{ cm}^{-1}$ can be attributed to the transition in an octahedral model. Thus, these bands may be assigned to the spin allowed transitions ${}^3\text{A}_{2g} \rightarrow {}^3\text{T}_{2g}(\text{F})$ and ${}^3\text{A}_{2g} \rightarrow {}^3\text{T}_{1g}(\text{F})$, respectively. ${}^3\text{A}_{2g} \rightarrow {}^3\text{T}_{1g}(\text{P})$ transition is not separated by the transfer effect to visible range of charge transfer transitions and absorptions of macrocycle ligand.

The absorption IR peaks at 1471 and 1217 cm^{-1} in (V) complex are assigned to the antisymmetric and symmetric stretching band of bridged nitrite Ni-ONO-Ni, respectively. The stretching band of N-bonded NO_2 are observed at 1404 and 1332 cm^{-1} . The weak absorption band at 617 cm^{-1} is characteristic of deformation band of N-bonded NO_2 . The FAB mass spectra of (V) complex contain peaks corresponding to the $[\text{Ni}_2([\text{22}]\text{-HMTADO})]^+$ and $[\text{Ni}([\text{22}]\text{-HMTADO})]^+$ ions at m/z 575 and 517, respectively. The $[\text{Ni}_2([\text{22}]\text{-HMTADO})\text{NO}_2]^+$ peak is observed at m/z 618.5.

The green polymer crystals of $\{[\text{Ni}_6([\text{22}]\text{-HMTADO})_3(\text{CN})_4][\text{Ni}(\text{CN})_4] \cdot 5\text{H}_2\text{O} \cdot 8\text{CH}_3\text{OH}\}_n$ (VI) suitable for X-ray diffraction study which deposited on standing for *ca.* 2 month were crystallized from methanol solution of $[\text{Ni}_2([\text{22}]\text{-HMTADO})(\text{CN})_2] \cdot 0.5\text{H}_2\text{O}$ complex. The structure of compound (VI) is ionic. The unit of title complex contains the polymer $[\text{Ni}_6([\text{22}]\text{-HMTADO})_3(\text{CN})_4]^{2+}$ cations, $[\text{Ni}(\text{CN})_4]^{2-}$ anions, five water molecules, and eight methanol molecules. A novel one-dimensional chain coordination polymer $[\text{Ni}_6([\text{22}]\text{-HMTADO})_3(\text{CN})_4]_n$ exhibits a novel -(A-B-A')-(A-B-A')- chain array, namely the infinite chain is propagated via alternately five and six-coordinate (A), two five coordinate (B), and five and six-coordinate (A'; centro symmetry of A by B site) sites of bivalent Ni ions ([7]).

The dinegative $([\text{22}]\text{-HMTADO})^{2-}$ in (A) site accommodates two Ni(II) ions in its N_4O_2 sites in the Ni(1)···Ni(2) separation of 3.097 Å. The geometry about Ni(1) in the N_2O_2 site is a square-pyramid with a carbon atom of a bridged cyanide at opposite of (B) site. And the geometry about Ni(2) in another N_2O_2 site is a octahedron with a nitrogen atoms of two bridged

cyanide at the trans positions. The two methyl groups (C(24) and C(27)) attached to the dimethyl-propylene are situated *cis* conformation. The macrocyclic complex (A) adopts a non-flat structure ($\text{Ni}_2\text{N}_4\text{O}_2$) with two octahedral nickel centers bridged by the two phenoxide oxygen atoms. The Ni(1) is displaced by 0.569 Å from the basal N_2O_2 least-squares plane towards C(46) (cyanide).

The dinegative ([22]-HMTADO)²⁻ in (B) site accommodates two Ni(II) ions in its N_4O_2 sites in the Ni(3)···Ni(3A) (-x+1, -y+1, -z+1) separation of 3.220 Å. The binuclear core structures are centrosymmetry with each Ni(II) ion in the N_2O_2 sites being five-coordinate by square-pyramidal geometry of interactions with two nitrogen and two oxygen atoms of the binucleating ligand [22]-HMTADO and two carbon atoms each from the bridged cyanide ligands at an apical site. The two methyl groups (C(41) and C(41) (-x+1, -y+1, -z+1) attached to the dimethyl-propylene are situated *trans* conformation. The macrocyclic complex (B) adopts a non-flat structure ($\text{Ni}_2\text{N}_4\text{O}_2$) with two octahedral nickel centers bridged by the two phenoxide oxygen atoms. The Ni(3) is displaced by 0.660 Å from the basal N_2O_2 least-squares plane towards C(46) (cyanide).

There are four crystallographically independent tetracyanonickellate anions $\{\text{Ni}(\text{CN})_4^{2-}\}$ in the unit cell. The $\{\text{Ni}(\text{CN})_4^{2-}\}$ are exactly planar as required by symmetry. All cyano groups are terminal. The lattice water molecules form hydrogen bonds of the type $\text{Ow-H}\cdots\text{O}$ with another lattice water and lattice methanol molecules.

References

1. (a) N. F. Curtis, *Coord. Chem. Rev.* 3 (1968), 3; (b) D. H. Busch, *Science* 171 (1971), 241; (c) S. M. Nelson, *Pure Appl. Chem.* 52 (1980), 2461.
2. V. Alexander, *Chem. Rev.* 95 (1995), 273.
3. (a) H. Okawa, H. Furutachi, and D. E. Fenton, *Coord. Chem. Rev.* 174 (1998), 51; (b) D. E. Fenton and H. Okawa, *Chem. Ber.* 130 (1997), 433; (c) S. R. Collinson and D. E. Fenton, *Coord. Chem. Rev.* 148 (1996), 19; (d) D. E. Fenton, *Pure Appl. Chem.* 58 (1986), 1437.
4. (a) L. F. Lindoy, *The Chemistry of Macrocyclic Ligand Complexes*, Cambridge University, Cambridge, UK, 1989; (b) L. F. Lindoy, *Pure Appl. Chem.* 61 (1989), 1575; (c) L. F. Lindoy, in: R. M. Izatt and J. J. Christensen (Eds.) *Synthesis of Macrocycle: The Design of Selective Complexing Agents*, Wiley, New York, 1987, p. 53.
5. P. Guerriero, S. Tamburini, and P. A. Vigato, *Coord. Chem. Rev.* 139 (1995), 17.
6. O. Kahn, in: A. G. Sykes (Ed.), *Advances in Inorganic Chemistry*, Academic Press, S. Diego, USA, 1995, p. 179.
7. K. S. Murray, in: A. G. Sikes (Ed.), *Advanced in Inorganic Chemistry*, vol. 43, Academic Press, S. Diego, USA, 1995, p. 261.
8. (a) S. R. Coper (Ed.), *Crown Compounds: Toward Future Applications*, VCH Publisher Inc., New York, 1992; (b) G. A. Melson (Ed.), *Coordination Chemistry of Macrocyclic Compounds*, Plenum Press, New

- York, **1979**; (c) A. Martell, J. Penitka, and D. Kong, *Coord. Chem. Rev.* 216-217 (**2001**) 55.
9. E. Kimura, and T. Koike, *Advances in Inorganic Chemistry*, vol. 44, Academic Press, New York, **1996**.
10. E. Kimura, T. Koike, and M. Shionoya, *Struct. Bond.* 89 (**1997**), 1.
11. E. Kimura and T. Koike, *Chem. commun.* **1998**, 1495.
12. S. Blain, P. Appriou, H. Chaumeil, and H. Handel, *Anal. Chim. Acta* 232 (**1990**), 331.
13. H. Tsubuke, T. Yoden, and M. Zenki, *J. Chem. Soc., Chem. Commun.* **1991**, 1069.
14. E. Kimura and T. Koike, *Chem. Soc. Rev.* 27 (**1998**), 179.
15. A. Bakac and W. Wang, *Inorg. Chim. Acta* 297 (**2000**), 27.
16. A. Arounagiri and B. G. Maiya, *Inorg. Chem.* 35 (**1996**), 4267.
17. A. Parand, A. C. Royer, T. L. Cantrell, and M. W. Crowder, *Inorg. Chim. Acta* 268 (**1998**), 211.
18. (a) P. D. Beer and D. K. Smith, in: K. D. Karlin (Ed.), *Progress in Inorganic Chemistry*, vol. 39, John Wiley & Sons, New York, USA, **1982**, p. 1; (b) P. D. Beer and D. K. Smith, in: K. D. Karlin (Ed.), *Progress in Inorganic Chemistry*, vol. 46, John Wiley & Sons, New York, USA, **1997**, p. 1.
- 19 (a) V. McKee, in: A. G. Sikes (Ed.), *Advanced in Inorganic Chemistry*, vol. 40, Academic Press, S. Diego, USA, **1993**, p. 323; (b) J. Nelson, V. McKee, and G. Morgan, in: K. D. Karlin (Ed.), *Progress in Inorganic Chemistry*, vol. 47, John Wiley & Sons, New York, USA, **1998**, p. 167; (c) S. Brooker, *Coord. Chem. Rev.* 222 (**2001**), 33.

20. (a) Y. Inone, and G. W. Gokel (Eds.), *Cation Binding by Macrocycles*, Marcel Dekker Inc., New York, USA, **1990**; (b) A. Branchi, K. Bowman-James, and E. Garcia-Espana (Eds.), *Supramolecular Chemistry of Anions*, Wiley-VCH, New York, USA, **1997**; (c) V. Amendola, L. Fabbri, C. Mangano, P. Pallavicini, A. Poggi, and A. Taglietti, *Coord. Chem. Rev.* 219-221 (**2001**), 821.
21. (a) J. R. Moran, S. Karbach, and D. J. Cram, *J. Am. Chem. Soc.* 104 (**1982**), 5826; (b) D. J. Cram, G. M. Lein, T. Kaneda, R. C. Helgeson, C. B. Knobler, E. Maverick, and K. N. Trueblood, *J. Am. Chem. Soc.* 103 (**1981**), 6228; (c) G. M. Lein and D. J. Cram, *J. Chem. Soc., Chem. Commun.* (**1982**), 301; (d) A. Jasat and J. C. Sherman, *Chem. Rev.* 99 (**1999**), 931.
22. C. D. Gutsche, *Acc. Chem. Res.* 16 (**1983**), 161.
23. G. D. Andreotti, R. Ungaro, and A. Pochini, *J. Chem. Soc., Chem. Commun.* (**1979**), 1005.
24. M. Coruzzi, G. D. Andreotti, V. Bocchi, A. Pochini, and R. Ungaro, *J. Chem. Soc., Perkin Trans. 2* (**1982**), 1113.
25. G. D. Andreotti, A. Pochini, and R. Ungaro, *J. Chem. Soc., Perkin Trans. 2* (**1983**), 1773.
26. R. Ungaro, A. Pochini, G. D. Andreotti, and P. Domiano, *J. Chem. Soc., Perkin Trans. 2* (**1985**), 197.
27. C. Rizzoli, G. D. Andreotti, R. Ungaro, and A. Pochini, *J. Mol. Struct.* 82 (**1982**), 1.
28. R. Ungaro, A. Pochini, G. D. Andreotti, and V. Sangermano, *J. Chem. Soc., Perkin Trans. 2* (**1984**), 1979.

29. S. Shinkai, S. Mori, H. Koreishi, T. Tsubaki, and O. Manabe, *J. Am. Chem. Soc.* 108 (1986), 2409.
30. S. Shinkai, K. Araki, T. Tsubaki, and O. Manabe, *J. Chem. Soc., Perkin Trans. 1* (1987), 2297.
31. S. Shinkai, K. Araki, S. Shibata, and O. Manabe, *J. Chem. Soc., Perkin Trans.* (1989), 195.
32. C. D. Gutsche and K. C. Nam, *J. Am. Chem. Soc.* 110 (1988), 6153.
33. C. D. Gutsche and I. Alam, *Tetrahedron* 44 (1988), 4689.
34. F. Arnaud-Neu, E. M. Collins, M. Deasy, G. Ferguson, S. J. Harris, B. Kaitner, A. J. Lough, M. A. McKervey, E. Marques, B. H. Ruhl, M. J. Schwing, and E. M. Seward, *J. Am. Chem. Soc.* 111 (1989), 8681.
35. G. Ferguson, B. Kaitner, M. A. McKervey, and E. M. Seward, *J. Chem. Soc., Chem. Commun.* (1987), 587.
36. A. Arduini, E. Ghidini, A. Pochini, R. Ungaro, G. D. Andreetti, G. Calestani, and F. Ugozzoli, *J. Inclusion Phenom.* 6 (1988), 119.
37. (a) C. Alfieri, E. Dradi, A. Pochini, R. Ungaro, and G. D. Andreetti, *J. Chem. Soc., Chem. Commun.* (1983), 1075; (b) D. N. Reinhoudt, D. J. Dijkstra, P. J. A. in't Veld, K. E. Bugge, S. Harkema, R. Ungaro, and E. Ghidini, *J. Am. Chem. Soc.* 109 (1987), 4761.
38. A. Arduini, A. Pochini, S. Reverberi, R. Ungaro, G. D. Andreetti, and F. Ugozzoli, *Tetrahedron* 42 (1986), 2089.
39. G. Calestani, F. Ugozzoli, A. Arduini, E. Ghidini, and R. Ungaro, *J. Chem. Soc., Chem. Commun.* (1987), 344.
40. D. E. Fenton, in: A. G. Sykes (Ed.), *Advanced in Inorganic and Bioinorganic Mechanism*, vol. 2, Academic Press, London, 1983, p. 187.

41. K. D. Karlin and J. Zubieta, *Copper Coordination Chemistry and Biochemistry: Biochemical and Inorganic Perspectives*, vols. 1 and 2, Adenine Press, Guilderland, NY, **1986**.
42. K. D. Karlin and J. Zubieta, *Biological and Inorganic Copper Chemistry*, vols. 1 and 2, Adenine Press, Guilderland, NY, **1986**.
43. (a) D. E. Fenton, U. Casellato, P. A. Vigato, and M. Vidali, *Inorg. Chim. Acta* 95 (**1984**), 187; (b) D. E. Fenton, U. Casellato, P. A. Vigato, and M. Vidali, *Inorg. Chim. Acta* 62 (1982) 57.
44. P. Guerriero, P. A. Vigato, D. E. Fenton, and P. C. Hallier, *Acta Chem. Scand.* 46 (**1992**), 1025.
45. U. Casellato, P. A. Vigato, D. E. Fenton, and M. Vidali, *Chem. Soc. Rev.* 8 (**1979**), 199.
46. P. Zanello, S. Tamburini, P. A. Vigato, and G. A. Mazzochin, *Coord. Chem. Rev.* 77 (**1987**), 165.
47. P. A. Vigato, S. Tamburini, and D. E. Fenton, *Coord. Chem. Rev.* 106 (**1990**), 25.
48. D. E. Fenton and P. A. Vigato, *Chem. Soc. Rev.* 17 (**1988**), 89.
49. T. M. Sorrel, *Tetrahedron* 45 (**1989**), 3.
50. P. A. Vigato and S. Tamburini, *Coord. Chem. Rev.* 248 (**2004**), 1717.
51. D. D. Perrin and W. L. F. Armarego, *Purification of Laboratory Chemicals*, Pergamon, 3rd edn., **1988**.
52. Curtis, N. F. *J. Chem. Soc.* **1964**, 2644.
53. R. W. Hay and N. F. Curtis, *J. Chem. Soc. Perkin I* **1964**, 2644.
54. J. Eriksen, and O. Mønsted, *Acta Chem. Scand.* A37 (**1983**), 579.
55. T. Shozo, *Bull. Chem. Soc. Jpn.* 57 (**1984**), 2683.

56. J. C. Byun, Y. C. Park, and C. H. Han, *J. Kor. Chem. Soc.* 43/3 (1999), 267.
57. Bruker, *SAINTPLUS NT Version 5.0. Software Reference Manual Bruker AXS: Madison, Wisconsin, 1998.*
58. Bruker, *SHELXTL NT Version 5.16. Program for Solution and Refinement of Crystal Structures Bruker AXS: Madison, Wisconsin, 1998.*
59. House, D. A.; Hay, R. W.; Ali, M. A. *Inorg. Chim. Acta* 72 (1983), 239.
60. M. S. El-Shahawi, *Spectrochimica, Acta Part A*, 52 (1996), 139.
61. Noal A. P. Kane-Maguire, Kevin C. Wallace, and David B. Miller, *Inorg. Chem.*, 24 (1985), 597.
62. C. F. C. Wong and A. D. Kirk, *Inorg. Chem.* 17 (1978), 1672.
63. J. Ferguson and M. L. Tobe, *Inorg. Chim. Acta* 4 (1970), 109.
64. J. C. Byun, G. C. Kim, and C. H. Han, *Bull. Korean Chem. Soc.* 25 (2004), 977.
66. J. C. Byun, Y. C. Park, J. S. Youn, C. H. Han, and N. H. Lee *Bull. Korean Chem. Soc.* 26 (2005), 634.
66. J. C. Byun, Y. C. Park, and C. H. Han, *Bull. Korean Chem. Soc.* 26 (2005), 1044.
67. J. C. Byun and C. H. Han, *Bull. Korean Chem. Soc.* 26 (2005), 1395.
68. B. Bosnich, C. K. Poon, and M. L. Tobe, *Inorg. Chem.* 4 (1965), 1102.
69. V. Felix, T. M. Santos, and M. J. Calhorda, *Inor. Chim. Acta* 356 (2003), 335.
70. D. A. House and P. J. Steel,; *Inorg. Chim. Acta* 269 (1998), 229.
71. D. J. Hodgson, E. Pedersen, H. Toftlund, and C. Weiss, *Inorg. Chim. Acta* 120 (1986), 177.
72. C. Glidewell, R. M. Gregson, and A. J. Lough, *Acta cryst. C* 56

- (2000), 174.
74. C. M. Zakaria, G. Ferguson, and C. Glidewell, *Acta cryst. C* 57 (2001), 683.
74. J. C. Kim, and A. J. Lough, *Inorg. Chem. Commun.* 5 (2002), 616.
75. K. V. Domasevitch, V. V. Ponomareva, and E. B. Rusanov, *Inorg. Chim. Acta* 268 (1998), 93.
76. K. Y. Choi, M. J. Kim, and C. P. Hong, *Bull. Korean Chem. Soc.* 23 (2002), 1062.
77. W. J. Geary, *Coord. Chem. Rev.* 7 (1971), 81.
78. L. Dubicki and P. Day, *Inorg. Chem.* 10 (1971), 2043.
79. R. G. Swisher, R. C. Brown, R. C. Smierciak, and E. L. Blinn, *Inorg. Chem.* 20 (1981), 3947.
80. J. H. Choi, *Spectrochim. Acta* 56A (2000), 1653.
81. J. H. Choi, *Chem. Phys.* 256 (2000), 29.
82. K. Nakamoto, *Infrared and Raman Spectra of Inorganic and Coordination*, Part B ; John Wiley & Sons ; New York, 1997.
83. D. Zhang, G. Lan, S. Hu, and H. Wang, *J. Raman. Spectrosc.* 24 (1993), 753.
84. M. Harrand, *J. Raman. Spectrosc.* 4 (1975), 53.
85. M. Joyeux, G. Menard, and N. Quy Dao, *J. Raman. Spectrosc.* 19 (1988), 499.
86. M. Joyeux, and N. Quy Dao, *J. Raman. Spectrosc.* 19 (1988), 441.
87. G. Varsanyi, *Assignments for Vibrational spectra of Seven Hundred Benzene Derivatives*, Adam Hilger, London, 1974.
88. J. H. S. Green and D. J. Harisson, *Spectrochim. Acta* A 26 (1970), 1925.
89. W. A. Bueno and S. Serrano, *Can. J. Appl. Spectrosc.* 38/6 (1993), 170.
90. M. B. Salah, P. Becker, and C. Carabatos-Nédelec, *Vib. Spectrosc.* 26

- (2001), 23.
91. D. Sutton, *Electronic Spectra of Transition Metal Complexes*, McGraw-Hill, London, **1968**.
 92. L. A. Kahwa, J. Selbin, T. C. Y. Hsieh and R. A. Laine, *Inorg. Chim. Acta* 118 (1986), 179.
 93. D. Suresh Kumar and V. Alexander, *Inorg. Chim. Acta* 238 (1995), 63.
 94. G. Socrates, *Infrared and Raman Characteristic Group Frequencies*. 3rd edn., Wiley, New York, **2001**, p. 320.
 95. G. Socrates, *Infrared and Raman Characteristic Group Frequencies*. 3rd edn., Wiley, New York, **2001**, p. 317.
 96. J. E. Huheey, E. A. Keiter, and R. L. Keiter, *Inorganic Chemistry: Principles of Structure and Reactivity* 4ed., HarperCollins College Publishers, **1993**, p 519.
 97. H. J. Buser, D. Schwarzenbach, W. Petter, and A. Ludi, *Inorg. Chem.* 16 (1977), 2704.
 98. J. Paharova, J. Cernak, R. Boca, and Z. Zak, *Inorg. Chim. Acta* 346 (2003), 25.
 99. Clack C. Chang, Brian Pfennig, and Andrew B. Bocarsly, *Coord. Chem. Rev.* 208 (2000), 33.
 100. Jie-Hui Yu, Ji-Qing Xu, Qing-Xin Yang, Ling-Yun Pan, Tie-Gang Wang, Chang-Hai Lu, and Tian-Hui Ma, *J. Mol. Struct.* 658 (2003), 1.
 101. J. Černák, M. Orendáč, I. Potočňák, J. Chomič, A. Orendáčová, J. Skoršepa, and A. Feher, *Coord. Chem. Rev.* 224 (2002), 51.

국문 초록

Cr(III)-tetraaza 14원 거대고리 착물; (1) *cis*-[Cr([14]-decane)(*o*-OOCC₆H₄OH)₂]-ClO₄, (2) *cis*-[Cr([14]-decane)(*p*-OC₆H₄NO₂)(OH)]ClO₄·H₂O, Cu(II)-dioxatetraaza 20원 거대고리 착물; (3) [Cu₂([20]-DCHDC)(O₂N)₂]·6H₂O, Ni(II)-dioxatetraaza 22원 거대고리 리간드 및 착물; (4) [H₄[22]-HMTADO](NO₃)₂·H₂O, (5) [Ni₂([22]-HMTADO)(μ-O₂N)(NO₂)(OH₂)], (6) {[Ni₆(C₂₈H₃₄N₄O₂)₃(CN)₄][Ni(CN)₄]·5H₂O·8CH₃OH}_n 들을 합성하고 구조 분석 및 물성 연구를 하였다. *cis*-[Cr([14]-decane)(*o*-OOCC₆H₄OH)₂]ClO₄ 착물의 결정 구조는 +1가의 착이온과 배위되지 않은 과염소산 음이온으로 구성되어 있다. [Cr([14]-decane)(*o*-OOCC₆H₄OH)₂]⁺ 은 Cr(III) 이온에 배위된 [14]-decane 거대고리 내의 4개의 2차 아민과 한자리 보조 리간드인 2개의 살리실산 이온의 산소 원자에 의해 Bosnich type-V 시스형의 찌그러진 팔면체 배위 환경을 갖고 있다. *cis*-[Cr([14]-decane)(*p*-OC₆H₄NO₂)(OH)]ClO₄·H₂O의 결정 구조도 +1가의 착이온과 배위되지 않은 과염소산 음이온으로 구성되어 있다. [Cr([14]-decane)(*p*-OC₆H₄NO₂)(OH)]⁺ 은 Cr(III) 이온에 배위된 [14]-decane 거대고리 내의 4개의 2차 아민과 한자리 보조 리간드인 1개의 니트로페놀산 이온의 산소 원자와 1개의 하이드록소에 의해 시스형의 찌그러진 팔면체 배위 환경을 가진다. 구리 2핵 착물 [Cu₂([20]-DCHDC)(O₂N)₂]·6H₂O은 [20]-DCHDC 거대고리 리간드의 2개의 질소, 두 개의 산소 그리고 2자리 보조리간드 아질산이온들이 각각의 구리(II) 이온에 6배위된 2개의 사각 피라미드 구조를 가지며, 두 사각 피라미드 구조는 중심 대칭을 이루고 있다. 구리이온들은 아질산이온 꼭지점 쪽으로 0.3288 Å 솟아 있다. 2개의 아질산이온들은 각각의 구리이온에 대해 트랜스 배열을 하고 있으며, 구리이온들 사이의 거리는

2.9542(8) Å이다. N₄O₂ 형 거대고리 리간드 [H₄[22]-HMTADO](NO₃)₂ · H₂O 결정은 2개의 N₂O₂ 자리는 금속이 배워되지 않은 채 비어 있고 각각의 아조메틴 그룹의 질소는 양성자화 되었다. 22원 거대고리 Ni(II) 2핵 착물 [Ni₂([22]-HMTADO)(μ-O₂N)(NO₂)(OH₂)]은 ([22]-HMTADO)²⁻에 2개의 Ni(II) 중심금속에 다리결합한 아질산 분자 한개와 반대편 트랜스 위치에 질소가 결합한 아질산 한 분자와 한개의 물분자가 결합된 두 개의 찌그러진 팔면체 구조를 갖는다. Ni(II) 이온들 사이의 거리는 3.013 Å이다. 녹색의 고분자 결정 {[Ni₆([22]-HMTADO)₃(CN)₄][Ni(CN)₄]·5H₂O·8CH₃OH}_n은 [Ni₆([22]-HMTADO)₃(CN)₄]²⁺ 중합체와 [Ni(CN)₄]²⁻로 이루어진 이온결합 구조를 이루고 있다. 중합체 [Ni₆([22]-HMTADO)₃(CN)₄]_n의 사슬 구조는 두개의 Ni(II) 금속이 5배위와 6배위 구조를 갖는 (A)-형 거대고리와 두 개의 5배위 구조를 갖는 (B)-형 거대고리, 그리고 (A)-형의 중심대칭구조인 (A')-형 거대고리가 -(A-B-A')-(A-B-A')- 배열을 갖는 구조이다. Ni(CN)₄²⁻은 사각 평면체 구조를 형성하고 있다.

감 사 의 글

늦게 시작한 공부가 얼마나 어려운지 절실히 느꼈습니다.

먼저 이 논문을 완성할 수 있도록 한없이 지도와 격려로서 이끌어 주신 변중철 교수님께 말로 다 할 수 없을 만큼의 감사를 드립니다. 그리고 부족하기 이를 데 없는 논문을 자세히 지적해주신 경북대학교 박유철 교수님, 제주대학교 강창희 교수님, 이선주 교수님, 그리고 한양대학교 이학기 술연구소 박기민 교수님! 정말로 고맙습니다.

또한 교과를 지도해 주신 한성빈 교수님, 정덕상 교수님, 김덕수 교수님, 김원형 교수님, 이남호 교수님께 깊은 감사를 드립니다.

논문의 시작에서 마칠 때까지 항상 함께한 문대훈 박사, 김구철 박사, 한충훈 박사, 김기주 군을 비롯한 무기실험실 모든 멤버들과 오늘의 기쁨을 나누고 싶습니다. 제주대학교 중앙도서관

특히 한충훈 박사와 김기주 군에게 다시 한 번 고마움을 표합니다. 주저앉고 싶을 때마다 걱정과 사랑으로 늘 애태우시던 어머니, 장인어른 그리고 장모님, 염려와 격려를 아끼지 않으신 친인척, 동료 교사들께도 무한한 감사를 드립니다.

늘 생사고락을 함께하는 아내와 나의 두 아들, 한길, 한함에겐 무어라 할 말이 없구나.

지금부터는 그동안 저를 사랑하고, 가르치고, 격려하고, 염려해 준 모든 분들께 부끄럽지 않은 행동을 할 것과 연구한 지식을 일선 교육 현장에서 최선을 다하여 적용할 것을 지면을 통해서나마 약속드립니다.